INFORMATION TO USERS

This manuscript has been reproduced from the microfilm master. UMI films the text directly from the original or copy submitted. Thus, some thesis and dissertation copies are in typewriter face, while others may be from any type of computer printer.

The quality of this reproduction is dependent upon the quality of the copy submitted. Broken or indistinct print, colored or poor quality illustrations and photographs, print bleedthrough, substandard margins, and improper alignment can adversely affect reproduction.

In the unlikely event that the author did not send UMI a complete manuscript and there are missing pages, these will be noted. Also, if unauthorized copyright material had to be removed, a note will indicate the deletion.

Oversize materials (e.g., maps, drawings, charts) are reproduced by sectioning the original, beginning at the upper left-hand corner and continuing from left to right in equal sections with small overlaps.

Photographs included in the original manuscript have been reproduced xerographically in this copy. Higher quality 6" x 9" black and white photographic prints are available for any photographs or illustrations appearing in this copy for an additional charge. Contact UMI directly to order.

UMI®

UNIVERSITY OF OKLAHOMA

GRADUATE COLLEGE

THE DIRECT PARTIAL OXIDATION OF METHANE TO ORGANIC
OXYGENATES USING A DIELECTRIC BARRIER DISCHARGE REACTOR

A DISSERTATION

SUBMITTED TO THE GRADUATE FACULTY

in partial fulfillment of the requirements for the

degree of

DOCTOR OF PHILOSOPHY

By

DAVID W. LARKIN
Norman, Oklahoma
2001

UMI Number: 3000736

UMI®

THE DIRECT PARTIAL OXIDATION OF METHANE TO ORGANIC OXYGENATES USING A DIELECTRIC BARRIER DISCHARGE REACTOR

A DISSERTATION
APPROVED FOR THE SCHOOL OF CHEMICAL ENGINEERING
AND MATERIAL SCIENCE

BY

ACKNOWLEDGEMENTS

commitment for his subject material was clearly evident. The knowledge that I acquired from him will serve me well.

Further, Dr. Jeffrey H. Harwell receives my gratitude for allowing me to be a part of this outstanding program and serving on my committee. In addition, I would also like to thank him for his spiritual guidance. His talk on Christianity and evolution was truly inspirational. On so many different levels, I have the utmost respect for Dr. Harwell, and I have learned a great deal about life through his good example.

In addition, I would like to thank Dr. Robert L. White for serving on my committee. He was gracious enough to take time out of his busy schedule to present his perspective as a chemist on my doctoral research, which I greatly appreciated. It is always extremely helpful to have the input of an expert from a related field.

I sincerely would like to thank Dr. Robert Reed for being my Sunday school teacher. He has been a source of inspiration for me, and his teachings on the Bible will forever affect my life. I would also like to thank him for the many times he took me out to lunch and invited me to his house for dinner with his family.

I would also like to share my appreciation for the help provided by everyone in the Lab (Terry, Chris, Tan, Huy, and Duc) as well as Larry Isley. In addition, I

would like to thank the University of Oklahoma for its commitment in hiring excellent faculty. I feel extremely fortunate to have been taught by a gifted group of professors. Oklahoma provides students with the opportunity to become the best they possibly can be in whatever field they choose.

Finally, I would like to thank my family for the guidance and support they have given me for my educational goals. Without their love, encouragement, and assistance, I would have never been able to obtain my career objectives.

TABLE OF CONTENTS

LIST OF FIGURES

LIST OF TABLES

ABSTRACT

Driven by the need to process natural gas economically in remote areas, homogeneous one-step partial oxidation of methane is being investigated actively by many researchers. The present work focuses on the direct homogeneous oxidative conversion of methane to organic oxygenates (methanol, formaldehyde, methyl formate, and formic acid) using a dielectric barrier discharge (DBD) reactor. The DBD reactor (also known as a silent electric discharge reactor) for this work is annular, consisting of two metal electrodes separated by a gas gap and a glass dielectric covering the outer surface of the inner electrode. The reactor operates at kilovolt voltage and 26 to 178 W of AC power. The frequency ranges from 100 to 264 Hz.

This work shows that when changing from a pure methane feed to a 3:1 methane-oxygen feed, the methane conversion rate increased by a factor of three. This is because active oxygen species activate methane, which results in the methane reaction rate being enhanced. In addition, oxygen cannot be replaced with carbon monoxide or carbon dioxide and still have organic oxygenate production. However, the addition of carbon dioxide to a methane-oxygen feed results in carbon dioxide further inhibiting production of carbon dioxide.

The effects of temperature on product selectivity were studied through the use of a water jacket. Lowering the temperature of water within the water jacket from

75 °C to 28 °C resulted in a 54% increase in organic oxygenate selectivity and a 56 % decrease in CO_x selectivity. This is because lowering the system temperature reduced the organic oxygenates' vapor pressures to that of their equilibrium partial pressures, resulting in *in situ* removal of these products from the reaction zone via condensation. Thus, over oxidation of these products was prevented. This work also confirms, through water-carbon monoxide and hydrogen-carbon dioxide feed experiments, that the water-gas shift and reverse water-gas shift reactions take place during the partial oxidation of methane in a DBD reactor. Finally, this work shows that in carbon dioxide reforming of methane, the partial pressures of carbon dioxide and helium in the feed affect product selectivities and methane and carbon dioxide conversions.

In regards to the system's energy usage, methane conversion as a function of energy consumption was investigated. Increases in methane conversion resulted in increases in the system's energy consumption due to limited partial pressures of oxygen within the reaction zone. Experimentally simulating reactors in series with intermediate oxygen addition showed that a high methane conversion (59%) could be obtained without as great an increase in energy usage as a single pass reactor uses for a similar methane conversion. In addition, using a recycle with a low per pass residence time (2.2 seconds), in which organic oxygenates were removed after each pass via a condenser, enhanced the organic oxygenate liquid selectivity by preventing over-oxidation of these products.

The effects of changing the electrical properties within a methane-oxygen DBD system were also investigated. Increasing the gas gap from 4.0 mm to 12.0 mm caused the reduced electric field to decrease from 30 volts/cm/torr to18 volts/cm/torr, which resulted in a shift in the product distribution from organic oxygenate liquids to ethane, ethylene, and acetylene. This is because the energy deposition directed toward oxygen dissociation was decreasing and the energy deposition directed toward methane and oxygen excitation was increasing. Through experiments at different pressures, this work shows that the methane reaction rate could be enhanced when increasing the pressure from one atmosphere to two atmospheres, while still maintaining 46% selectivity in organic liquid oxygenates. This is as a result of operating at a reduced electric field strength with a significant amount of energy directed toward oxygen dissociation. Finally, this work shows, through residence time studies, that methane and oxygen react to form methanol, which further reacts to form formaldehyde, methyl formate, and formic acid.

The Partial Oxidation of Methane to Organic Oxygenate Liquids using a Dielectric Barrier Discharge Reactor

CHAPTER ONE: Introduction and Literature Review

1.1 General Introduction

The real push to discover new sources of energy came in the 1970s, when this country faced an oil crisis. The crisis effectively demonstrated that the world's oil reserves are not infinite and are being gradually depleted. Due to the fact that there is still a strong public resistance to nuclear energy, natural gas appears to be a very desirable energy source. One reason for this, is because of the vast reserves of natural gas around the world, which are estimated to total 10^7 million tons. Natural gas is also a clean burning fuel. It gives more energy per CO_2 molecule created than can oil. It can, therefore, potentially help reduce the problem of global warming.[1,2]

Natural gas is primarily composed of methane. Methane, by volume %, represents 80 to 95% of the composition of the gas. As much as 10% of the gas could be composed of ethane, propane, and butane. Some natural gases, such as Lacq, have a carbon dioxide content greater than 10%.[1]

Presently, natural gas is being used as a combustion fuel in industrialized areas close to large natural gas reserves. However, there is a considerable amount of

natural gas in remote places around the world. To transport adequate amounts of the gas from remote places to industrial processing facilities requires that the gas be compressed to 80 bars or liquefied via refrigeration. Thus, considerable amounts of natural gas reserves are not utilized due to these high transport costs. Potentially, this problem can be solved if natural gas at remote locations can be processed into an organic oxygenate liquid, such as methanol, which does not need refrigeration or compression for transport.[1] Methanol is currently being used as a feed stock, mostly to manufacture formaldehyde and until recently methyl tert-butyl ether. This market, however, needs only 24 million tons per year of methanol, which is far less than the estimated 10^7 million tons of natural gas reserves. For this reason, many industrial groups are doing research on targeting methanol produced from remote natural gas as a transportation fuel or boiler fuel. The current industrial methanol synthesis process is steam reforming to synthesis gas, which then further reacts to form methanol (detailed discussion given is section 1.2). However, this multi-step energy intensive process is too expensive to implement in remote places.[1]

One technique that could prove to be favorable is the direct partial oxidation of methane to methanol. This one-step partial oxidation process might substantially cut down the process operating costs enough to effectively utilize these gas reserves.[2] However, currently there is no one-step partial oxidation process to methanol that is economically feasible. A potential solution for this problem is using a dielectric barrier discharge (DBD) reactor (also called a silent electric discharge reactor) for the

direct partial oxidation of methane to organic oxygenates such as methanol (methanol, formaldehyde, methyl formate, and formic acid). Unlike the current industrial methanol synthesis process, this one-step process allows useful chemistry at room temperature and atmospheric pressure as well as pressures higher than atmospheric (electrons in the discharge initiate the reactions because their kinetic energies are significantly greater than the kinetic energies of ions and neutral species). In addition, because a significant amount of the products are in liquid phase at room temperature and atmospheric pressure, the transportation costs due to compression could be reduced.

1.2 Industrial Methanol Synthesis Process

Methanol, until the early 1900s, was produced by destructive wood distillation. In 1923, BASF came up with a synthetic methanol synthesis process in which synthesis gas flowed over a Zn/Cr_2O_2 catalyst (300-400 °C and around 300 atm). In 1966, ICI came up with a more reactive catalyst, $Cu/ZnO/Al_2O_3$. This new catalyst allowed the methanol synthesis process to have a lower operating temperature range (220-300 °C) and a lower operating pressure range (50 to 100 atms) than BASF's process. However, before either process can be used to produce methanol from synthesis gas, synthesis gas itself has to be generated from steam reforming of methane.[3]

3

Hence, both processes (BASF's high pressure process and ICI's low pressure process) are two-step processes in which the first step is methane steam reforming. The important reactions in this step are shown below:

$$CH_4 + H_2O \leftrightarrow 3H_2 + CO \qquad \Delta H_{298\ K} = 206 \text{ kj/mol (reaction 1)}$$

$$CO + H_2O \leftrightarrow CO_2 + H_2 \qquad \Delta H_{298\ K} = -41 \text{ kj/mol (reaction 2)}$$

The first reaction, which is endothermic, is thermodynamically favored by high temperature and low pressure. On the other hand, the water-gas shift reaction (reaction 2) is not pressure dependent and is favored by low temperature (exothermic reaction). However, heat produced by the second reaction is never able to make up for the heat required for the first reaction as shown by the overall reaction still being endothermic:[4]

$$CH_4 + 2H_2O \leftrightarrow CO_2 + 4H_2O \qquad \Delta H_{298\ K} = 165 \text{ kj/mol (reaction 3)}$$

Thus, furnaces are required for additional heat input. Two-thirds of the operating costs of the overall process come from this first step.[2,4]

A typical steam reforming process might have two reformers in series. The steam-methane feed (typically a 5:1 ratio) will enter the first reformer at 500 °C and flow over a supported nickel catalyst (system pressure = 15 to 30 atm) in which the

4

methane and steam react to form synthesis gas (CO_2 also formed by the water-gas shift reaction). The product stream will then exit the first reformer at 800 to 850 ^{0}C and flow to the second reformer, in which its exiting product stream temperature is 900 to 1100 ^{0}C. Once past the second reformer, the product stream will have only .5 to 1.5% of methane remaining.[3,5]

This product stream will then feed to the synthetic methanol synthesis stage (second step). The two important reactions that occur within this stage, shown below, are exothermic:

$$CO + H_2O \leftrightarrow H_2 + CO_2 \qquad \Delta H_{298\,K} = -41.2 \text{ kj/mol}$$

$$\Delta G_{298\,K} = -28.6 \text{ kj/mol (reaction 4)}$$

$$CO_2 + 3H_2 \leftrightarrow CH_3OH + H_2O \qquad \Delta H_{298\,K} = -49.5 \text{ kj/mol}$$
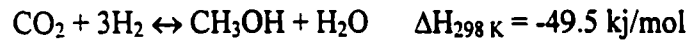
$$\Delta G_{298\,K} = -3.3 \text{ kj/mol (reaction 5)}$$

Thus, the overall reaction, in which for every three moles of feed converted (1 mole $CO + 2$ moles of H_2), one mole of methanol is formed, is also exothermic:

$$CO + 2H_2 \leftrightarrow CH_3OH \qquad \Delta H_{298\,K} = -90.6 \text{ kj/mol}$$

$$\Delta G_{298\,K} = -25.3 \text{ kj/mol (reaction 6)}$$

Table 1.1 shows that as the temperature increases for reaction 6, ΔG also increases (this means the equilibrium constant for reaction 6 decreases with increasing temperature).

Table 1.1: ΔG vs. T for Methanol Synthesis from Synthesis Gas

T (°C)	25	200	225	250	275	300	325
ΔG (kj/mol)	-25.3	13.3	18.7	24.2	29.7	35.2	40.7

Therefore, thermodynamically methanol synthesis from synthesis gas favors low temperature. However, as shown below, undesirable side reactions to hydrocarbons, ethers, and higher alcohols can also take place, which are thermodynamically more favored than the formation of methanol:

$$CO + 3H_2 \leftrightarrow CH_4 + H_2O \qquad \Delta H_{298\ K} = -206.2\ kj/mol$$

$$\Delta G_{298\ K} = -142.3\ kj/mol \text{ (reaction 7)}$$

$$2CO + 4H_2 \leftrightarrow CH_3OCH_3 \qquad \Delta H_{298\ K} = -204.8\ kj/mol$$

$$\Delta G_{298\ K} = -67.2\ kj/mol \text{ (reaction 8)}$$

$$2CO + 4H_2 \leftrightarrow C_2H_5OH + H_2O \qquad \Delta H_{298\ K} = -255.6\ kj/mol$$

$$\Delta G_{298\ K} = -122.6\ kj/mol \text{ (reaction 9)}$$
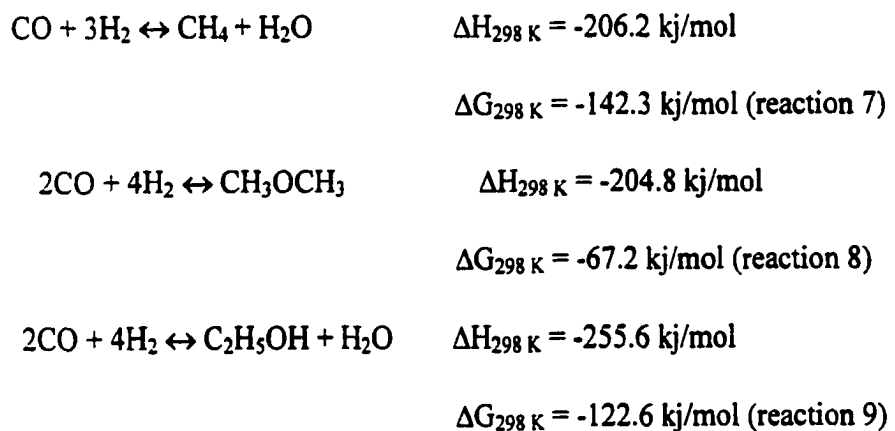
This means the selectivity to methanol is controlled by the catalyst selectivity favoring the methanol pathway.[3,5]

As already stated, the methanol catalysts are Zn/Cr_2O_2 (high pressure methanol synthesis catalyst) and $Cu/ZnO/Al_2O_3$ (low pressure methanol synthesis catalyst). The latter is favored by industry because of reduced compression cost, longer catalyst life, larger capacity, and improvement in productivity from 770 to 1120 tons of methanol per million cubic meters of natural gas. Thus, in 1997, 75% of all the methanol plants worldwide used the low pressure methanol synthesis catalyst.[3]

A typical low pressure methanol synthesis stage is shown in Figure 1.1. As can be seen in the figure, a recycle is used in which 15% of the CO is converted per pass (5% for high pressure process). In addition, crude liquid methanol is condensed in the separator and is sent to a distillation column where the methanol is separated from water and other carbon products. As can be seen in Table 1.2, the low pressure methanol synthesis catalyst does not form as much of the undesirable carbon products as the high pressure methanol synthesis catalyst does. However, Table 1.3 shows that when poisons and contaminants are allowed to be present within the low pressure methanol synthesis process, the selectivity and/or catalyst reactivity are affected detrimentally.[3,5]
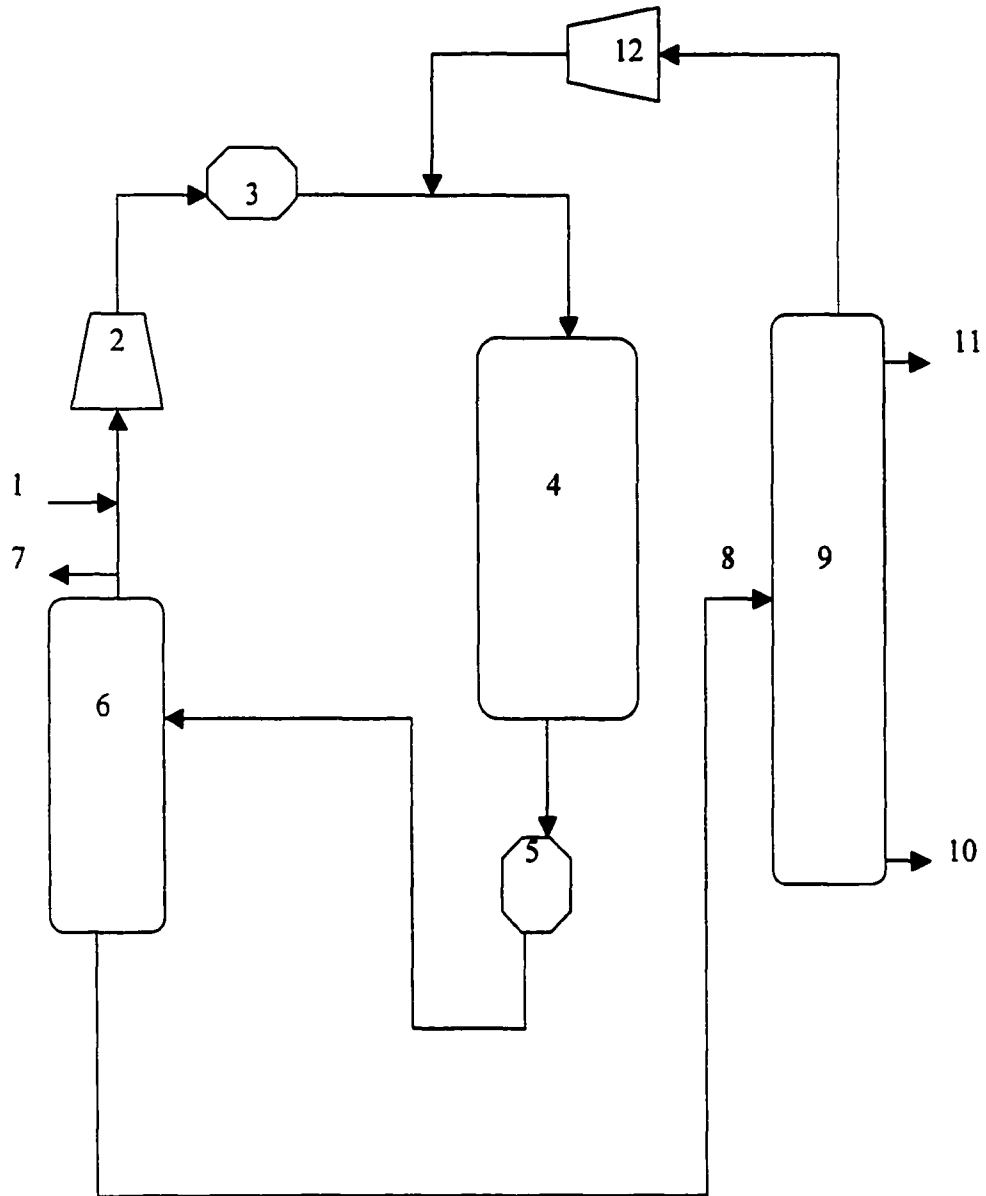
Figure 1.1: Low Pressure Methanol Synthesis Stage [1 = Feed (typical feed: 15% CO, 8% CO$_2$, 74% H$_2$, and 3% CH$_4$), 2 = Recompressor, 3 = Heater, 4 = Methanol Synthesis Reactor, 5 = Cooler, 6 = Condenser Separator, 7 = Purge, 8 = Crude Liquid Methanol, 9 = Distillation Column, 10 = carbon byproducts and water, 11 = Methanol, 12 = Recompressor]

Table 1.2: By-Product Formation

By-Product	High Pressure process	Low Pressure Process
Dimethyl ether	5000-10000 ppm(w/v)	20-150 ppm(w/v)
Carbonyl Compounds	80-220 ppm(w/v)	10-35 ppm(w/v)
Higher Alcohols	3000-5000 ppm(w/v)	100-800 ppm(w/v)
Methane	2% input Carbon	none

Table 1.3: Effects of Contaminants and Poisons on $Cu/ZnO/Al_2O_3$ Catalyst

Contaminant or poison	Possible sources	Effects
Silica, other acidic oxides	Transport in steam in plant gases	Waxes, other by-products formed
γ-Alumina	Catalyst manufacture	Dimethyl ether formed
Alkali	Catalyst manufacture	Decreased activity, higher alcohols formed
Iron	Transport in Plant as $Fe(CO)_5$	Methane, paraffins, waxes formed
Nickel	Transport in Plant as $Ni(CO)_4$	Methane formed, decreased activity
Cobalt	Catalyst manufacture	Methane formed, decreased activity
Lead, heavy metals	Catalyst manufacture	Decreased activity
Chlorine compounds	Transport in plant gases	Permanent decrease in activity
Sulphur compounds	Transport in plant gases	Permanent decrease in activity

Finally, in regards to energy usage, a large-scale industrial methanol plant requires 11 eV per molecule of methanol produced. However, in remote areas, the energy consumption for this process would increase because the process would have to be scaled down due to limited gas reserves.[6] Thus, to utilize gas reserves more economically in remote areas, a new process is needed.

1.3 Discharge Systems

This work uses a dielectric barrier discharge system to partially oxidize methane into organic oxygenates. Therefore, the following section provides a better understanding of discharge systems in general by giving an overview of them (radio frequency discharge system, microwave discharge system, glow discharge system, corona discharge system, and barrier discharge system). However, much of the focus will be directed toward the silent electric discharge system (DBD system), because it is the system used for this work.

The first discharge system to be discussed is the radio frequency discharge system (rf). It operates at high frequencies that can range from 2 to 60 MHz. Radio frequency systems can operate below atmospheric pressure. They can also operate at atmospheric pressure. One major advantage of the rf process is that it has no electrodes. This means that contamination from metal electrodes is completely avoided. The actual discharge is caused by an external induction coil wrapped around the annular system.[7, 8]

Microwave discharge systems operate at high frequencies. The frequency range of the microwave systems are between 2 to 10 GHz. These systems have been known to operate at pressures as high as one atmosphere. Due to the fact that only electrons can follow the oscillations of the electric field, the plasmas generated are far from equilibrium. One type of plasma reactor configuration is a tube with only a few centimeters diameter. The length of the tube, however, can be as long as four meters. Varying the pressure can produce electron densities between 10^8 to 10^{15} cm^{-3}. Microwave discharge is mostly used for elemental analysis.[7, 8]

Glow discharge systems generally operate at pressures smaller than 10 mbar. The typical setup for producing a glow discharge applies a potential difference across two metal electrodes that have low pressure gas between them. The gas and electrodes are contained in a glass tube. The power can come from an AC or DC source. The disadvantage with using a DC source is that reactions tend to be formed in certain zones in the tube. The way to get around this is to switch to a 50 to 60 cycles/s AC source. The electric field generated in a glow discharge is generally around 10 V/cm. The electrons have energies between .5 to 2 eV, and their densities fall within the range of 10^8 to 10^{11} cm^{-3}. Glow discharge methods are not thought able to be industrially applicable because of the low pressures and low mass flow rates at which these systems have to operate.[8]

Glow discharge becomes very unstable when the pressure is increased. Generally, the glow turns into a high current arc discharge. One way to stabilize the discharge at higher pressures is to use inhomogeneous electrode geometries. For example, one electrode might be a point electrode, while the other is a plane electrode (corona discharge system). When this is done properly, a corona discharge is observed between the two electrodes. The corona discharge can be classified as a negative discharge or a positive discharge, depending on the polarity of the field and the exact geometrical setup of the electrodes. For a positive corona discharge, there is an inception voltage that has to be reached before a corona discharge can take place. This inception voltage depends on the gap width between the electrodes and the radius of the point. Once beyond the inception voltage a typical corona discharge can be seen. At voltages just past the inception point, the inhomogeneous streamers are produced and can be seen going from the point to the plane electrode. With a steady increase in voltage, the stream-like filaments turn into a homogeneous glow. If too much voltage is applied, then the glow becomes an arc discharge. In a negative corona discharge, an inception voltage also has to be reached. When it is reached, so-called Trichel pulses are generated between the electrodes. If the voltage is increased steadily, the pulse discharge becomes a pulseless homogeneous glow. Finally, at high enough voltages, the homogeneous discharge breaks down into an arc discharge. In corona discharge, the electron energies and densities can be around 5 eV and 10^{13} cm^{-3}, respectively.[8,9]

The final type of discharge system to be discussed is a silent electric discharge system (DBD system). To create a silent electric discharge, two flat plates are separated by a gap, and one or both of them are covered with a dielectric material such as glass. An AC power source with a transformer is used to create the potential difference in voltage (kV range) across the plates. Thus, the silent electric discharge reactor acts as a capacitor. The effect of the glass dielectric is to distribute the microdischarges across the entire electrode area and to limit the duration of each microdischarge. The gap width, pressure, and composition of the gas are factors that determine the dielectric strength of the system. Two common geometries for the silent electric discharge system are annular and planar, as shown in Figures 1.2 and 1.3.[8,10]

Figure 1.2: Annular Configuration

Outer
Electrode

Gas Gap

Glass
Dielectric

Inner
Electrode
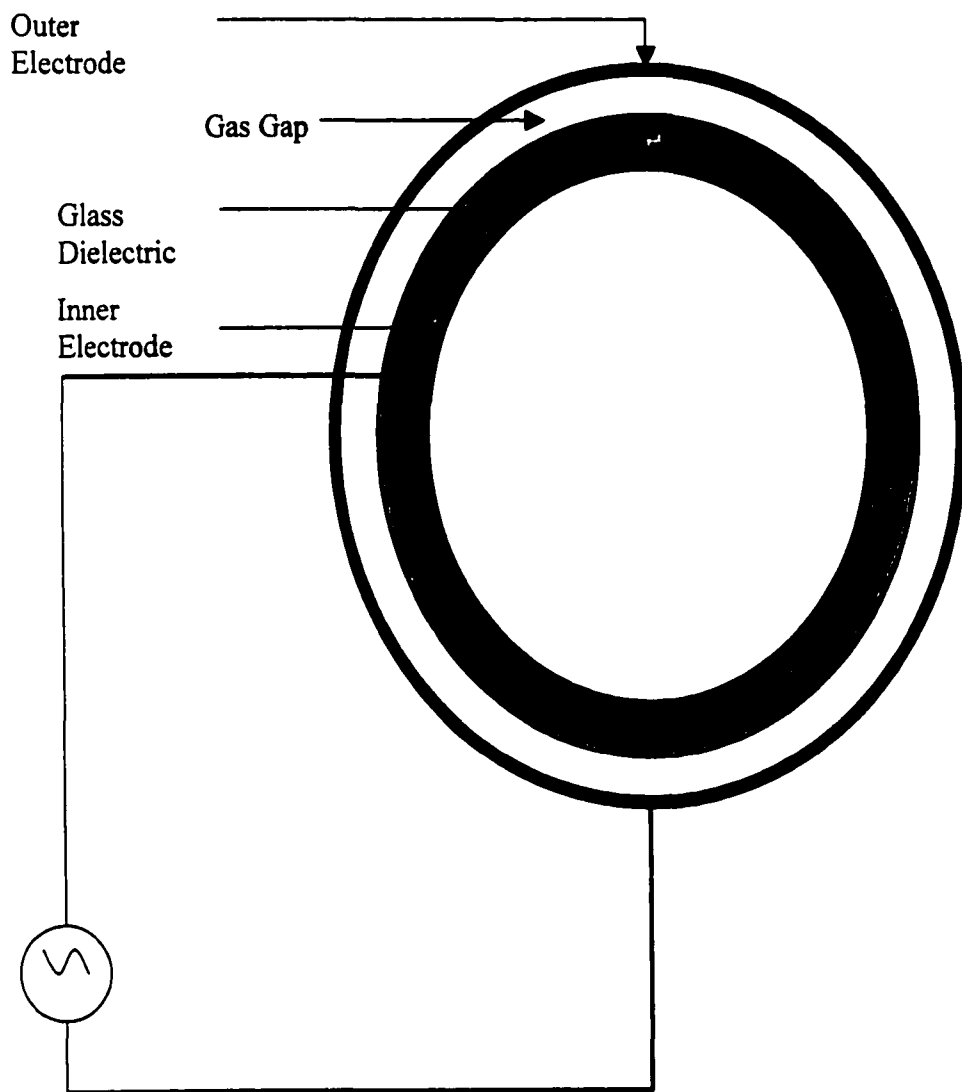
Figure 1.3: Planar Configuration

Top Electrode

Gas Gap

Glass Dielectric

Bottom Electrode
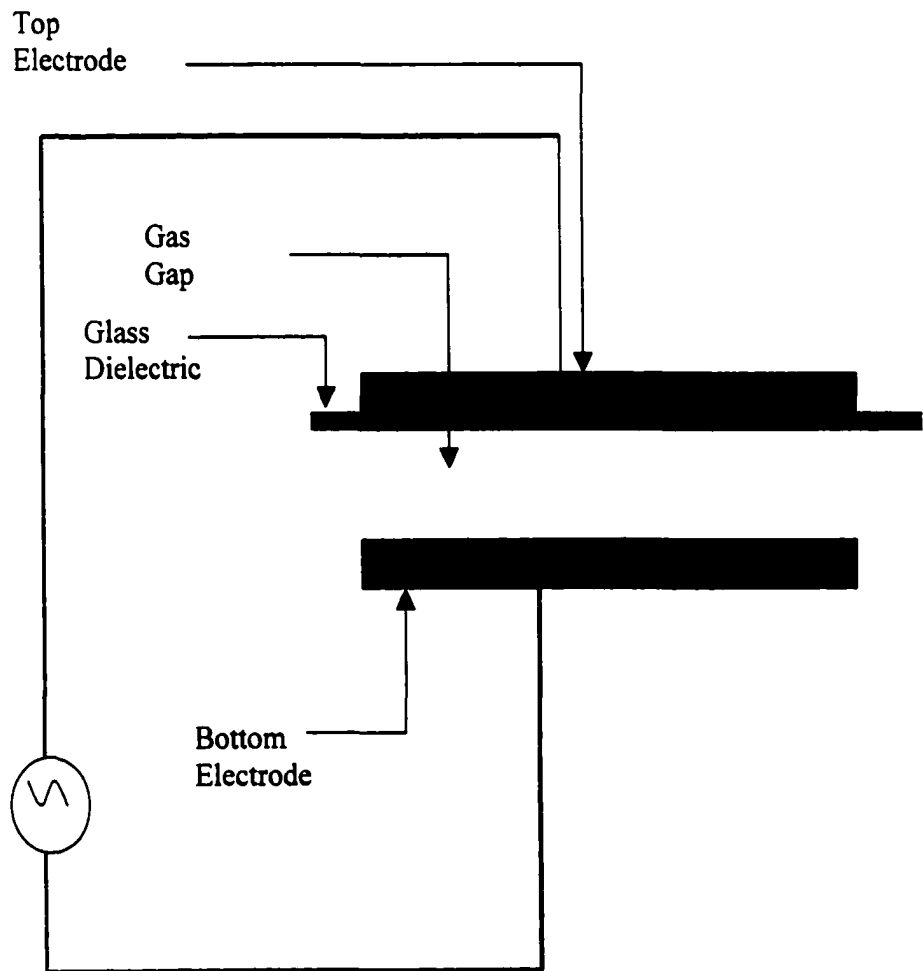
Researchers have also investigated how the discharge is initiated in a silent electric discharge reactor. Initially, some electrons are present in the gas gap due to photons from cosmic rays causing the ionization of some gas species. In addition, electrons can be present as a result of being ejected from the cathode due to, for example, UV illumination. With this in mind, once the electric field strength starts to increase due to increasing potential difference in voltage between the two electrodes, the kinetic energies of these electrons present within the gas gap will also increase as they accelerate toward the anode. Some of the electrons will have high enough kinetic energies that when they undergo inelastic collisions with neutral gas molecules, the molecules will go to higher vibrational or electronic states. When an electron's kinetic energy is higher than the ionization energy of a given gas molecule, ionization (electron ejected from a neutral molecule leaving an positive ion behind) can take place. Thus, an ejected electron in conjunction with the original electron can then repeat the process such that ultimately an avalanche of electrons will reach the anode, as shown in Figure 1.4. In addition, some of the excited molecules may emit photons when they return to the ground state. These photons may cause photo-emission of electrons at the cathode that can, therefore, start additional electron avalanches. Once the microdischarge filament forms across the gas gap due to electron avalanche, a conductive channel is established between the electrode and the glass dielectric. The life span of this conductive channel is on the order of a few nanoseconds due to local charge accumulation on the dielectric. This is because the charge accumulation reduces the electric field strength locally within the conductive

16

channel to the point at which ionization of gas species can no longer take place (locally reduces electric field strength). Finally, the system voltage at which microdischarges start occurring is called the breakdown voltage. A further increase of voltage on the primary side of the transformer (low voltage side) does not increase the breakdown voltage (it's constant), as shown Figure 1.5. However, the increase in primary voltage does increase the power input into the system by increasing the number of microdischarges occurring within it.[11, 12]

Figure 1.4: Electron Avalanche

Anode

Glass Dielectric

Electron Avalanche

Cathode
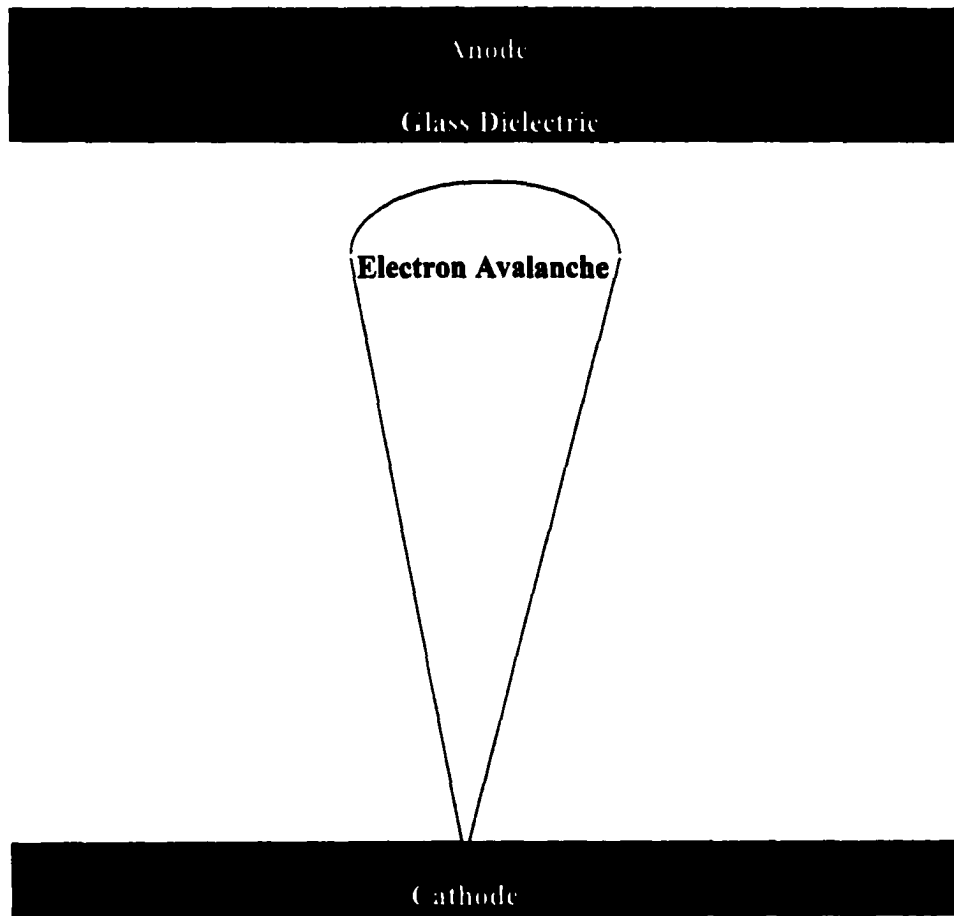
Figure 1.5: Secondary Voltage vs. Time
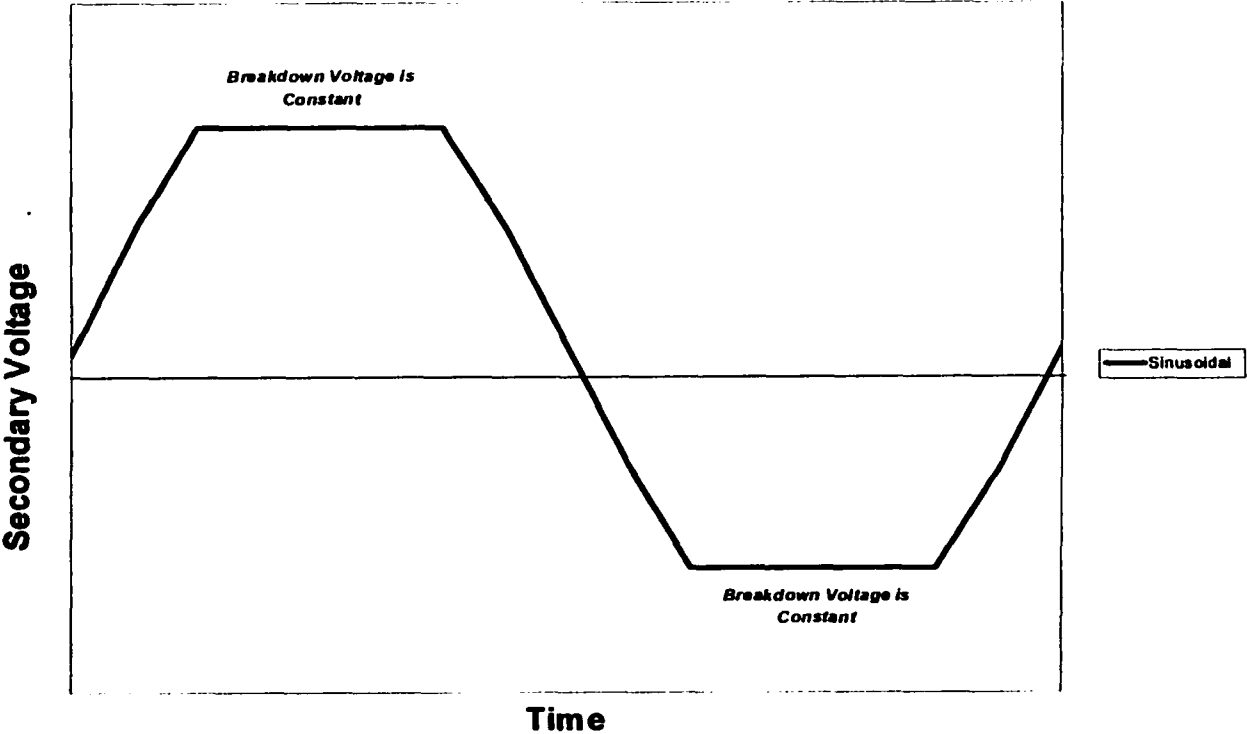
Some of the physical properties just described can actually be observed through the use of an oscilloscope. When the current of this system is measured as a function of time through an oscilloscope, spiked hairs are observed, as seen in Figure 1.6. These spiked hairs represent the discharges taking place within the system. It has been shown that the sum of the lengths of the hairs is linearly dependent on the total amount of charge being transferred between the plates. Thus, an increase in voltage beyond the breakdown potential increases the number of microdischarge filaments which can be observed in an oscilloscope by the increase in the hair lengths' sum.[13]

Figure 1.6: Current vs. Time

Current

Sinusoidal

Time
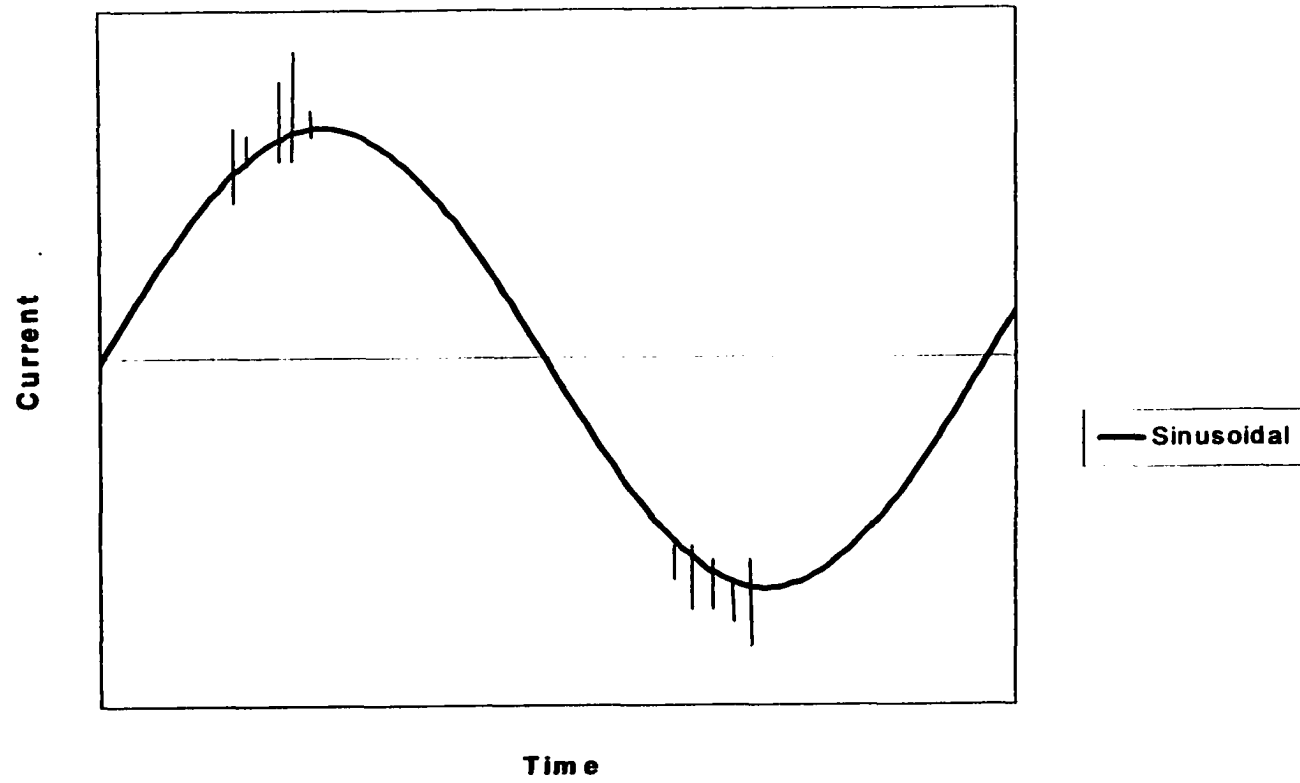
1.4 Plasma Chemistry

In order to understand what might be occurring within the reaction zone of a silent electric discharge reactor, it is important to understand the fundamentals of plasma chemistry. Thus, the following section discusses these fundamentals and gives several examples of applications for which plasma reactors might be used. In addition, ozone generation, a current industrial plasma reactor application, is also described.

A plasma is a gas that is partially ionized, in which the overall charge of the system is quasi-neutral. The two branches of plasma chemistry are surface chemistry and volume chemistry. Examples of surface chemistry are etching, deposition, and surface modification. Ozone production in a silent electric discharge reactor would be an example of volume chemistry. The following discussion will be restricted to volume chemistry, which is the type of plasma chemistry that is occurring in the homogeneous partial oxidation of methane.[8,14]

Plasma volume chemistry can be created in an apparatus that consists of electrodes and a discharge volume in which discharges take place. In this discharge volume, interactions between accelerated particles and other chemical species occur. The accelerated particles consist of ions and electrons. The other chemical species consist of atoms, molecules, and radicals. The externally induced electric field acts upon the ions and electrons without directly affecting the neutral species.[8]

The two types of plasmas that can be created in this discharge volume are equilibrium plasmas and nonequilibrium plasmas. A plasma is in equilibrium when the kinetic energies of the charge particles and neutral species are the same. This can be accomplished by using very high temperatures. High temperatures increase the number of collisions of all particles to such an extent that the energy is equally distributed among all the particles. Nonequilibrium plasmas are plasmas in which the electrons have a much higher kinetic energy than the ions and neutral species have. For example, applying strong electric fields at reduced pressures can generate electron energies in the range of 1 to 10 eV while the remaining particles energies are a few hundredths eV. These nonequilibrium plasmas can be created at room temperature by discharge systems, such as the silent electric discharge that has already been discussed in the previous section. Thus, equilibrium and nonequilibrium plasmas are also referred to as hot and cold plasmas due to the temperature environments in which these plasmas exist. Finally, both types of plasmas are considered quasi-neutral, because the total density of positive charge carriers is roughly equal to the total density of negative charge carriers.[8, 14]

In cold plasmas, the reactions first are initiated by the electrons. This occurs through the collision of electrons with atomic/molecular gas species within the system. These collisions might be elastic, but they can also be inelastic, ionization, and attachment collisions. Once the electron collisions with gas species have taken place, other reactions, such as atomic/molecular reactions, can also occur.[8]

There has been considerable research done on plasma chemistry using discharge reactors.[8, 15-18] For example, research has been done on hydrogen peroxide generation in a silent electric discharge reactor (hydrogen peroxide is an important industrial product in terms of bleaching and disinfecting). In this study, hydrogen and oxygen gas (4.5 % vol. O_2) were fed to the reactor at 253 K. After passing through the reactor, hydrogen peroxide and water were caught by using a condensation trap. It was found that increasing the gap width while maintaining the same residence time resulted in an increase in the hydrogen peroxide concentration. On the other hand, for the same gap width, when the residence time increased, the hydrogen peroxide concentration decreased. For both these cases, the pulse current pure unit discharge area was kept constant.[15, 16]

There has also been research in several other areas with discharge reactors.[8] For example, N_2H_4 (hydrazine), a component in rocket fuel, has been made from NH_3 or N_2 and H_2 in a silent electric discharge reactor. In addition, research has been done on NO_x and SO_x removal. For example, a flue gas with NO_x and SO_2 was sent through a corona discharge in which HNO_3 and H_2SO_4 were the products. Next, these products were reacted with NH_3 to form ammonium salts (($NH_4)_2SO_4$ and NH_4NO_3). Removal of toxic organic substances using a silent electric discharge reactor also has been explored. Toxic compounds have been decomposed using a thermal plasma at high temperature. This, however, requires a large amount of energy to raise the gas temperature several thousand degrees. Thus, using a silent electric discharge reactor might be more economically desirable, because it can

24

operate at room temperature. Conceivably, a silent electric discharge reactor might be used to remove PCBs, dioxins, solvent vapors, nerve gas, and pesticides.[8] Finally, research with discharge reactors has been done in the area of natural gas processing (discussed in section 1.5)

Silent electric discharge reactors also have been used on an industrial basis in the area of ozone production. Ozone production occurs by feeding oxygen to an ozone generator (DBD reactor). The ozone generator generally operates at atmospheric pressure and is able to take room temperature oxygen and convert some of it to ozone by passing high energy electrons, 1 to 10 eV, through the gas stream. The electron densities can be as high as 10^{14} cm^{-3}.[8]

A research group from Japan has conducted ozone studies with a silent electric discharge reactor (DBD reactor). An AC power source was used in conjunction with a transformer, and this allowed the voltage to range from 2 kV to 10 kV. In addition, the frequency was varied from 50 to 2000 Hz. The results show that an increase in pulse current (current traveling across the gas gap) from 10 to 200 μamps linearly increases ozone production. From 200 to 1000 μamps the ozone production levels off. Past 1000 μamps, ozone production is constant. Thus, from 10 to 1000 μamps, as the number of electrons crossing the gap increases, the chances of ozone formation also increases. However, at a certain point (beyond a 1000 μamps), the net rate of destruction of ozone equals the net rate of creation of ozone and, thus, additional pulse current does not lead to an increase in ozone production. The width

of the gas gap also has an effect on ozone production. For the same pulse current, an increase in width from 1 to 3 mm results in an increase in ozone production.[17, 18]

1.5 Homogeneous Partial Oxidation of Methane to Methanol using Thermal and DBD Reactors

Many researchers have studied the homogeneous partial oxidation of methane using thermal and dielectric barrier discharge reactors.[19-47, 50-54] The former uses high temperatures to initiate reactions while the latter uses high energy electrons to do so. The following section gives an overview of the research conducted in both areas (thermal and DBD processes). In addition, attempts to produce methanol from other feeds (CH_4-CO_2, CH_4-H_2O, H_2-CO_2), as opposed to the traditional methane-oxygen or methane-air feeds, will also be covered.

1.5.1 Partial Oxidation of Methane (POM) through Thermal Means

The partial oxidation of methane to methanol is an exothermic reaction, as shown below:

$$CH_4 + .5\ O_2 \rightarrow CH_3OH \qquad \Delta H_{298\ K} = -126.2\ kj/mol$$

Table 1.4 shows that ΔG increases with increasing temperature and, therefore, thermodynamically POM to methanol favors low temperature

Table 1.4: ΔG as a Function of T for POM to Methanol

T (°C)	25	400	450	500	550	600
ΔG (kj/mol)	-111.5	-93.1	-90.7	-88.2	-85.8	-83.3

However, energy has to be input into the system in order to initiate the reaction. One way of inputting energy into the system is through thermal means, and much research has been done in this area.[19-42] Typically, the partial oxidation of methane (POM) has been conducted at temperatures within the range of 400 to 600 °C and pressures within the range of 5 to 65 atms. In addition, the mole percent of oxygen in the feed has not exceeded 10% within this pressure range (A methane-oxygen-ozone study has had up to 15% oxygen in the feed, however, the pressure was 1.5 atm).[19-34]

In regards to economics, several studies have compared the thermal POM with the commercial methanol synthesis process.[36-40] The studies show that methane conversions of 7.5% to 10.0% with 70% selectivity toward methanol would be required in order to compete with the commercial methanol synthesis process. However, roughly only 20% to 30% selectivity toward methanol has been obtained in this methane conversion range (7.5% to 10.0%) for the homogeneous partial oxidation of methane using thermal means.[19-34]

A research group in Germany has completed a study on the homogeneous partial oxidation of methane in a thermal reactor.[41] However, they passed oxygen

through an ozone generator (DBD reactor) before the stream was mixed with methane. Hence, a methane-oxygen-ozone stream was fed to a 1 mm diameter alumina flow tube (thermal reactor). The temperature in the tube was varied between 480 to 830 K. The products detected from the reaction were H_2O, H_2O_2, CH_2O, CH_3OH, CO, and CO_2. Trace amounts of C_2H_6 and CH_3OOH were also detected. The results show that when the ozone concentration in the feed is increased while maintaining a constant methane-oxygen feed, the product concentrations increase. The authors believe, however, that it is atomic oxygen instead of ozone(O_3) that is causing this, because thermal decomposition of ozone is 23 kcal/mole while the theoretical activation energy required for ozone to react with methane is 27 kcal/mole.[41]

A Canadian research group has also passed an oxygen stream through an ozone generator (DBD reactor) and then mixed it with a methane stream before sending the stream (methane-oxygen-ozone feed) to a thermal reactor.[42] The oxygen composition in the feed, depending on the experiment, was in the range of 4.4 mole percent to 15.0 mole percent. The composition of ozone in oxygen was 8 wt. %. In addition, they have also done experiments that fed only a methane-oxygen stream (no ozone in the feed) to the thermal reactor. The results show, that at 401 °C, considerable amounts of methanol, formaldehyde, carbon monoxide, and carbon dioxide are formed when ozone is in the feed. Trace amounts of ethane can also be seen. When oxygen was not fed to the silent electric discharge reactor first, no reaction occurred in the thermal reactor at 401 °C. Thus, without ozone in the feed, it

was only at 434 °C that traces of methanol could be detected. Therefore, their study suggests atomic oxygen might be initiating the reaction at 401 °C. Finally, for a methane conversion of 7%, their process showed only 9% selectivity toward methanol.[42]

1.5.2 Partial Oxidation of Methane using a Dielectric Barrier Discharge Reactor

As already mentioned, the homogeneous partial oxidation of methane can also be accomplished using a dielectric barrier discharge (DBD) reactor. There have been several studies in this area in which various parameters have been adjusted to determine their effects on the overall process.[43-47, 50-54] For example, research has been completed using a DBD reactor (gap distance = 1.9 mm, 110°C) with 13:1 methane-oxygen feed.[43] In the study, it was found that when the voltage was increased, and, hence, the transported charge across the gas gap increased, the oxygen conversion was enhanced. In addition, a decrease in the methanol and formaldehyde selectivities were also seen with an increase in voltage. This was a result of over-oxidation of these organic oxygenates, as shown by the increase in CO_x selectivity. In this same study, when the residence time was increased, the oxygen conversion increased. In addition, for the residence time experiments, similar trends were seen in organic oxygenate and CO_x selectivities as demonstrated in the voltage experiments.[43]

The methane-oxygen feed ratio in a DBD reactor has also been studied.[44] The results show that when reducing a 20:1 methane-oxygen feed ratio to a 3:1 methane-

oxygen feed ratio the methane conversion rate increases by 42%. This suggests active oxygen species within the reaction zone activate methane molecules, which results in the enhancement of the methane reaction rate. In addition, when the methane-oxygen feed ratio changed from 20:1 to 3:1, the ethane production rate decreased and the methanol production rate increased. These production rate results are caused by the decreasing probability of methane coupling reactions due to the increased partial pressure of oxygen in the feed. In addition, increasing the partial pressure of oxygen in the feed promotes partial oxidation of methane to methanol.[44]

Research has also completed in this area from Switzerland.[45] They show that when mole% of air is increased from 0 to 70% in a methane-air stream being fed to a DBD reactor, the percent yield in methanol increases from 0 to about 2.5. However, they found that higher percent yields in methanol occur in methane-oxygen feed experiments (e.g., 2.3:1 methane-oxygen feed gave 3% yield to methanol). In addition, their study shows that when the methane conversion increases, the energy consumption of the system also increases.[45] This is most likely due to the fact that oxygen conversion also increases as methane conversion increases, which means the partial pressure of oxygen down the length of the reactor is decreasing (This work does not give its results in oxygen conversion however, another study does show that as methane conversion increases, oxygen conversion also increases for a methane-oxygen system within a DBD reactor[44]). Hence, a decrease in active oxygen species down the length of the reactor causes a decrease in the methane reaction rate.

In addition, studies have been conducted on the partial oxidation of methane to methanol using pulsed DBD reactors.[46, 47] For example, a pulse generator has been used in which the voltage rise time is about 15 ns.[47] Their results show that when they decrease the methane-oxygen ratio from 49:1 to 1.5:1 in methane-oxygen-argon feeds (80 % of feed composition is argon), the methanol and CO_x selectivities increase and the C_2H_x selectivities decrease. Hence, increased oxygen partial pressure in the feed promotes methanol and CO_x pathways. In addition, when the argon mole% in the feed was increased form 0 to 80 in a methane-oxygen-argon feed (1.5:1 methane-oxygen ratio), the methanol yield went from .6% to about 6%. The study also shows that when increasing the partial pressure of argon in a methane-oxygen-argon feed, the current across the gas gap increases, which offers a possible explanation for the increase in methanol yield. In other words, the presence of argon increases the number of free electrons in the gas gap, which, therefore, might enhance the number of reactions taking place within the reaction zone.[47]

Researchers have also tried to use CO_2 and H_2O in place of oxygen in a DBD reactor. However, the yields to methanol have been at best very low. For example, a 6:1 methane-water feed resulted in .5% yield in methanol.[48] Futher, when using methane-carbon dioxide feeds, methanol was not detected.[46] Finally, a 3:1 hydrogen–carbon dioxide stream has also been fed to a DBD reactor. The yield in methanol for this system was also low (.1%).[49]

1.6 Present Work and Dissertation Objectives

The present work studies the direct partial oxidation of methane using a DBD reactor. The objective of the study is to gain a better understanding of process parameters that positively influence methane conversion, desired product selectivities, and energy consumption of the system, as well as to obtain a better understanding of what is occurring within the reaction zone of the DBD reactor. The former is accomplished through process development experiments, while the latter is explored through carbon pathway experiments and computer simulations (Bolsig: an electron Boltzmann solver by Kinema Software and CPAT). The computer simulations give a better understanding of species that might be responsible for initiating the reactions taking place within the system at various conditions.

Chapter Two covers the experimental procedure and design for this study. In addition, definitions of the various terminology used (conversion, product selectivities, and energy consumption) are given.

Some natural gas reserves have CO_2 present within them. Therefore, Chapter Three discusses the influence carbon dioxide has on the system when added to a methane-oxygen feed. Methane-oxygen-carbon monoxide systems are also discussed in this chapter. Finally, methane-carbon monoxide and methane-carbon dioxide systems are covered in this chapter regarding the question as to whether oxygen can

be replaced with carbon monoxide or carbon dioxide and still form organic oxygenate products.

In the partial oxidation of methane in a DBD reactor, the probability that organic oxygenates will be further oxidized to CO_x increases the longer they stay within the reaction zone. Chapter Four, therefore, discusses how organic oxygenate and CO_x selectivities are affected when *in situ* removal of organic oxygenates in the reaction zone via condensation occurs. Chapter Four also discusses whether reactor geometry (annular vs. planar) affects product selectivities and methane and oxygen conversions. In addition, hydrogen-carbon dioxide systems and a water-carbon monoxide system are explored in regards to whether the water-gas shift and reverse water-gas shift pathways are possible in a methane-oxygen system within a DBD reactor. The chapter ends with a discussion on carbon dioxide reforming of methane in regards to the effects that the partial pressure of carbon dioxide and helium have on product selectivities and methane and carbon dioxide conversions (methane-carbon dioxide-helium system).

Having a low energy usage per molecule of methane converted is desirable for a process implementing the partial oxidation of methane. Thus, Chapter Five examines the effects on energy consumption when the methane conversion increases for a methane-oxygen system within a DBD reactor. Chapter Five also reviews process development experiments to gain a better understanding of how methane conversion and organic oxygenate selectivities can be enhanced. In addition, other

process development experiments are conducted to determine how energy consumption and product selectivities change when oxygen in a methane-oxygen system is replaced with oxygen enriched air. Finally, because natural gas contains ethane, the effects ethane has in a methane-ethane-oxygen system are explored.

Chapter Six discusses how changes in the reduced electric field strength affects methane and oxygen conversion, product selectivities, and energy consumption for a methane-oxygen system within a DBD reactor (reduced electric field is changed by altering the system's gas gap distance or the system's pressure). This is accomplished through experiments and the use of the Bolsig simulator (an electron Boltzmann solver by Kinema Software and CPAT), which is able to determine the average electron energies and the energy depositions directed toward the various collision processes in a methane-oxygen system within a DBD reactor. In addition, the effects pressure has on a methane-oxygen system in terms of feed concentration is also discussed. Finally, residence time experiments with a methane-oxygen system are conducted to better determine the carbon pathways that are occurring within the system.

Chapter Seven gives the overall conclusions for this work as well as recommendations for further study on the homogeneous partial oxidation of methane in a DBD reactor.

Literature Cited

(1) Crabtree, Robert H. Aspects of Methane Chemistry. Chem. Rev. 1995, 95, 987-1007

(2) Lange, Jean-Paul Perspectives for Manufacturing Methanol at Fuel Value. Ind. Eng. Chem. Res. 1997, 36, 4282-4290

(3) Farrauto, R. J, Bartholomew, C. H.;

Fundamentals of Industrial Catalytic Processes Blackie Academic & Professional, 1997

(4) Barbieri, Giuseppe, P. Di Maio, Francesco; " Simulation of the Methane Steam Re-forming Process in a Catalytic Pd-Membrane Reactor," Ind. Eng. Chem. Res., Vol 36, 1997, 2121-2127

(5) Wolfe, Martin Twigg; Catalyst Handbook, 2nd Edition Publishing, Ltd., 1989

(6) Rostrup-Nielson, Jens R. Catalysis and Large-Scale Conversion of Natural Gas. Catalysis Today, Vol. 21, 1994, 257-267

(7) McTaggart, F. K. Plasma Chemistry In Electrical Discharges. Elsevier Publishing Company, New York, 1967

(8)   Eliasson, Baldur; Kogelschatz, Ulrich   Nonequilibrium Volume Plasma Chemical Processing. IEEE Transactions On Plasma Science Vol. 19, No 6, December 1991

(9) Chang, Jen-Shih; Lawless, Phil A.; Yamamoto, Toshiaki Corona Discharge Processes. IEEE Transactions on Plasma Science Vol. 19, No 6. December 1991

(10)   Kogelschatz, Ulrich; Eliasson, Baldur; Egli, Walter   Dielectric-Barrier Discharges Principle and Applications.   J. PHYS IV France 7 , Colloque C4, 1997, 47-64

(11) Alston, L.L.; High-Voltage Technology, Oxford University Press, 1968

(12) Dr Li-Ming Zhou; "Non-Thermal Plasma Features in Dielectric Barrier Discharges" Written report to Institute for Gas Utiliaztion Technologies at the University of Oklahoma, November of 1998

(13) Suzuki, Momotario; Naito, Yoshihide. On the Nature of the Chemical Reaction In Silent Electrical Discharge. II. Proc. Japan Acad., 1950, 26, 20

(14)   Bruno, Giovanni; Capezzuto, Pio; Cicala, Grazia   Chemistry of Amorphous Silicon Deposition Processes: Fundamentals and Controversial Aspects. Academic Press, Boston, 1995

(15)   Morinaga, Kihei   The Reaction of Hydrogen and Oxygen through a Silent Electric Discharge I. This Bulletin, 35, 345, 1962.

(16)   Morinaga, Kihei   The Reaction of Hydrogen and Oxygen through a Silent Electric Discharge II. This Bulletin, 35, 625, 1962.

(17)   Morinaga, K.; Suzuki, M.   The Chemical Reaction in Silent Electric Discharge I. This Bulletin, 34, 157, 1961

(18)   Morinaga, K.; Suzuki, M.; The Chemical Reaction in Silent Electric Discharge II. The Frequency Effect on Ozone Formation. Bull. Chem. Soc. of Japan, 35, 204, 1962

(19)   Foulds, G.A., Gray, B.F.; "Homogeneous Gas-Phase Partial Oxidation of Methane to Methanol and Formaldehyde," Fuel Processing Technology, Vol. 42, 1995, 129-150

(20) Foulds, G.A., Gray, B.F., Miller, S.A. and Walker, G.S.; "Homogeneous Gas Phase Oxidation of Methane using Oxygen as Oxidant in an Annullar Reactor," Ind. Eng. Chem. Res., Vol. 32, 1993, 780-787

(21) Foulds, G.A., Miller, S.A., Walker, G.S.; "Gas-Phase Partial Oxidation of Methane," Symposium on Natrual Gas Upgrading II, Presented before the Division of Petroleum Chemistry, Inc., American Chemical Society, San Francisco Meeting, 5-10 April, 1992, 26-33

(22) Foulds, G.A., Gray, B.F., Griffens, J.F., Miller, S.A., Walker, G.F.; "Direct Partial Oxidation of Methane to Methanol," CHEMICAL 92, Proceedings of the Twentieth Australian Chemical Engineering Conference, Vol. 1, Canbera, Australia, 27-30 September, 1992, 67-73

(23) Foulds G.A., Miller, S.A., Walker, G.S.; "Homogeneous Direct Partial Oxidation of Methane to Methanol" CHEMICA 91, Proceedings of the Nineteenth Australian Chemical Engineering Conference, Vol. 1, Newcastle, Australia, 18-20 September, 1991, 566-573

(24) Chun, J.W. Anthony, R.G.; "Partial Oxidation of Methane, Methanol and Mixtures of Methane and Methanol, Methane and Ethane, and Methane, Carbon Dioxide, and Carbon Monoxide," Ind. Eng. Chem. Res., Vol. 30, 1991, 2287-2292

38

(25) Chun, J.W. Anthony, R.G.; "Free-radical Kinetic Model for the Homogeneous Oxidation of Methane to Methanol," Ind. Chem. Res., Vol. 32, 1993, 796-799

(26) Thomas, D.J., Willi, R., Bailker, A.; "artial Oxidation of Methane: The Role of Surface Reactions;" Ind. Eng. Chem. Res., Vol. 31, 1992, 2272-2278

(27) Walsh, D.E., Martenak, D.J., Han, S., Palermo, R.E.; "Direct Oxidative Methane Conversion at Elevated Temperatures and Moderate Pressures," Ind. Eng. Chem. Res., Vol. 31, 1992, 1259-1262

(28) Rytz, D.W., Baiker, A.; "Partial Oxidation of Methane to Methanol in a Flow Reactor at Elevated Pressure," Ind. Eng. Chem. Res.,Vol. 30, 1991, 2287-2292

(29) Gesser, H.D., Hunter, N.R., Morton, L.; "Direct Conversion of Methane to Methanol," Symposium of Methane Upgrading. Presented Before the Division of Petroleum Chemsitry, Inc., American Chemical Society, Atlanta Meeting, 14-19 April, 1991, 160-165

(30) Gesser, H.D., Hunter, N.R., Morton, L.; Yarlagadda, P.S., Fung, D.P.C.; "The Direct Conversion of Methane to Methanol by a High Pressure Partial Oxidation Reaction," National Meeting of the American Chemical Society, Vol. 32, 255-259

(31)   Gesser, H.D., Hunter, N.R., Morton, L.; "Direct Conversion of Natural Gas to Methanol by Controlled Oxidation," United State Patent 4,618,732

(32)   Burch, R., Squire, G.D., Tsang, S.C.; "Direct Conversion of Methane to Methanol," J. Chem. Soc. Faraday Trans. 1, 85, 1989, 3561-3568

(33)   Fukuoka, N, Omata, K, Fujimoto, K; "Effect of Additives on the Partial Oxidation of Methane," Pacifichem '89, Abstract, Conference Proceedings , Vol. 135, 1989, 106-107

(34)   Charlton, B.G., Foulds, G.A., Walker, G.S., Jones, J.C., Gray, B.F.; " The Gas-phase Partial Oxidation of Methane to Methanol in a CSTR," CHEMICAL 92, Proceedings of the Twentieth Australian Chemical Engineering Conference, Vol. 1, Canbera, Australia, 27-30 September, 1992, 67-73

(35)   Sinev, M. Yu; Korshak, V.N.; Krylov, O.V.; "The Mechanism of the Partial Oxidation of Methane," Uspekhi Khimii. 58, 38-57, 1989

(36)   Dautzenburg, F.M.; "The characteristics and Challenges of New Natural Gas Technologies," Eurogas 90, Proceedings from the European Applied Research Conference on Natural Gas, Trondheim, Norway, 28-30 May, 1990, 179-194

(37)   Edwards, J.H., Foster, N.R.; "The Potential of Methanol Production from Natural Gas by Direct Catalytic Partial Oxidation," Fuel Sci. Technol., Vol. 4, 1986, 365-390

(38)   Geerts, J.W.M.H., Hoebink, J.H.B.J., Van der Wiele, K; "Methanol from Natural Gas. Proven and New Technologies," Catal. Today, Vol. 6, 1990, 613-620

(39)   Kuo, J.C.W., Kresge, C.T. and Palermo, R.E.; "Evaluation of Direct Methane Conversion to Higher Hydrocarbons and Oxygenates," Catal. Today, Vol. 4, 1989, 463-470

(40)   Jackson, P.J., Ravarapu, V.N., White, N., Whitehead, R.J.; "A Comparative Assessment of the Production of Ethylene and Methanol by the Direct Partial Oxidation of Natural Gas," CHEMECA 92, Proceedings of the Twentieth Australian Chemical Engineering Conference, Vol. 1, Canbera, Australia, 27-30 September, 1992, 145-152

(41)   Rotzoll, G.; "Mass Spectrometric Investigation and Computer Modeling of the $CH_4-O_2-O_3$ Reaction from 480 to 830 K,". J. Phys. Chem., Vol. 90, 1986, 677-683

(42)   Gesser, H.D.; Hunter, N.R.; Das, P.A.   The Ozone Sensitized Oxidation Conversion of Methane to Methanol. C. L., 16: 217-221, 1992

(43)   Shepelev, S.S., Gesser, H.D., Hunter, N.R.; "Light Paraffin Oxidative Conversion in a Silent Electric Discharge Reactor," Plasma Chemistry and Plasma Processing, Vol. 13, No. 3, 1993, 479-488

(44)   Bhatnagar, Rajat, Mallinson, R.G.; "Methane Conversion in AC Electric Discharges at Ambient Conditions," Methane and Alkane Conversion Chemistry, Plenium Press, 1995, 249-264

(45)   Zhou, L.M., Xue, B., Kogelschatz; U., Eliasson, B.; "Partial Oxidation of Methane to Methanol with Oxygen or Air in a Nonequilibrium Discharge Plasma," Plasma Chemistry and Plasma Processing, Vol. 18, No. 3 , 1998, 375-393

(46)   O-okayama, Merguro-ku; "Application of Plasma Chemistry to the Highly Efficient Utilization of Energy," Proc. of the Int. Symp. on CO_2 Fixation & Efficient Utilization of Energy, Tokyo, Japan, 1993, 37-42

(47)   Okumoto, M., Takshima, K., Katsura, S., Mizuno, A.; "Direct Synthesis of Methanol from Methane using Non-thermal Plasma," The Asia-Pacific Workshop on Water and Air Treatment by Advanced Oxidation Treatments, 1998

(48) Okazaki, Ken, Ogawa, Kuniyasu, Yamada, Nobuhide, Kishida, Takuya; "Direct Synthesis of Methanol from Methane and Water-vapor Mixtures using Plasma Chemical Reaction," Principle of Energy Production, Reports of Project Research (No. 256) Supported by Grant-in Aid on Priority Areas, Ministry of Japan Education, Nov, 1998

(49) Eliasson, Baldur, Kogelschatz, Ulrich, Xue, Bingzhang, Zhou, Li-Ming; "Hydrogenation of Carbon Dioxide to Methanol with a Discharge Activated Catalyst," Ind. Eng. Chem. Res., Vol. 37, 1998, 3350-3357

(50) Okumoto, Mamoru, Rajanikanth, Katsura, Shinji, Mizuno, Akira; "Nonthermal Plasma Approach in Direct Methanol Synthesis from Methane," IEEE Transactions on Industry Applications, Vol. 34, No. 5, 1998, 940-944

(51) Larkin, D.W., Caldwell, T.A., Lobban, L.L., Mallinson, R.G.; "Oxygen Pathways and Carbon Dioxide Utilization in Methane Partial Oxidation in Ambient Temperature Electric Discharges," Energy & Fuels, Vol. 12, No. 4, 1998, 740-744

(52) Larkin, D.W., Leethochawalit, S., Caldwell, T.A., Lobban, L.L., Mallinson, R.G.; "Carbon Pathways, CO_2 Utilizaton, and *In Situ* Product Removal in Low Temperature Plasma Methane Conversion to Methanol," Greenhouse Gas Control Technologies, Elsevier Science Ltd., 1999, 397-402

(53)   Larkin, D.W., Lobban, L.L., Mallinson, R.G.; "Production of Organic Oxygenates in the Partial Oxidation of Methane in a Silent Electric Discharge Reactor," Ind. Eng. Chem. Res., Web Release Date: February 28th, 2001

(54)   Larkin, D.W., Lobban, L.L., Mallinson, R.G.; "Organic Oxygenate Pathways from Partial Oxidation of Methane in a Silent Electric Discharge Reactor," publication pending

CHAPTER TWO: Experimental Section

2.1 Experimental Design and Procedures

The overall experimental setup is shown in Figure 2.1. With this setup in mind, mass flow controllers (Porter Instrument Company) regulate the flow of feed gases (supplied by gas cylinders from Sooner Air Gas) to an annular reactor as shown in Figure 2.2. The feed gas enters the reactor from the top and flows down axially through the gap between the two concentric cylinders. Inside the inner glass cylinder is a metal foil that acts as one electrode, while the stainless steel wall of the outer cylinder acts as the other electrode. Thus, the reactor acts as a capacitor with a glass dielectric in which uniformly distributed "micro-discharge" streams disperse throughout the volume of the reactor. The product stream exits the annular reactor from the bottom. The outer reactor shell is surrounded by a water cooling jacket.

The reaction products are fed to a liquid trap cooled by dry ice and acetone, which maintain the trap temperature at around –55 °C. The primary products collected in the trap are water, methanol, formaldehyde, methyl formate, ethanol, and formic acid. Depending on the reactor temperature, some of these products may be condensed in the reactor and then carried out by the gas stream. Past the liquid trap, the effluent gas stream flows to an EG&G Carle Series 400 AGC gas chromatograph with a hydrogen analysis system. In the recycle experiments (Recycle Diagram shown in Figure 2.3), once the gas passes through the liquid trap, most of the remaining gas is fed back to the reactor; however, a small fraction exits through a purge stream that flows to the EG&G Carle Series 400 AGC gas chromatograph.
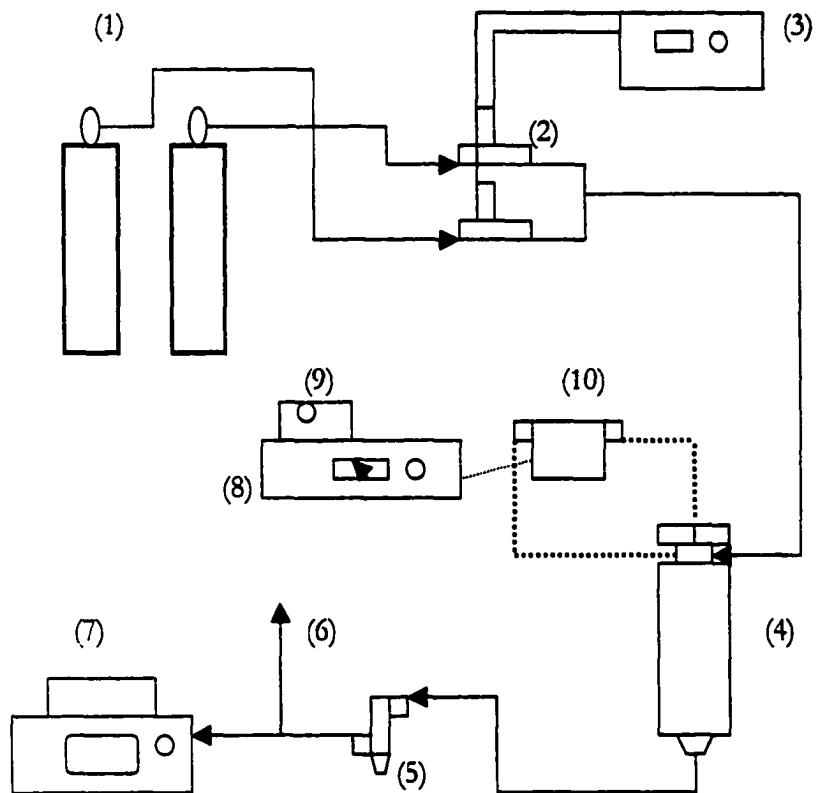
Figure 2.1: Experimental Setup : (1) CH4 & O2 Gas cylinders, (2) Mass flow
Controllers, (Porter Instrument Company), (3) Porter flow module, (4) Silent Electric
Discharge Reactor, (5)Liquid trap, (6) Gas stream to vent, (7) EG&G Carle Series
400 AGC, (8) Elgar Model 501 SL AC power supply, (9) CBK precision function
generator, (10) 15060 P Franceformer transformer

Figure 2.2: Annular Reactor

Water outlet

Water Jacket

Water Inlet

Feed Gas Inlet

Inner electrode (metal foil)

Gas Gap

To Transformer

Glass dielectric

Outer electrode

Gas Outlet
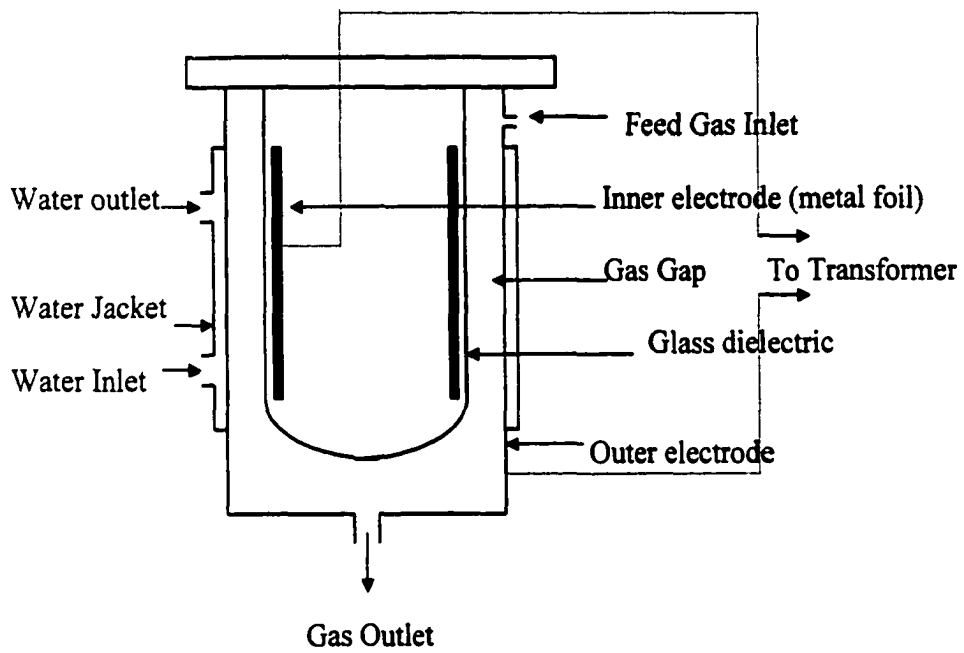
Figure 2.3: Recycle Diagram

Recycle Loop

CH$_4$ & O$_2$
Input

Feed

DBD Reactor

Vacuum Pump
(MB-21)

Liquid
Trap

Purge
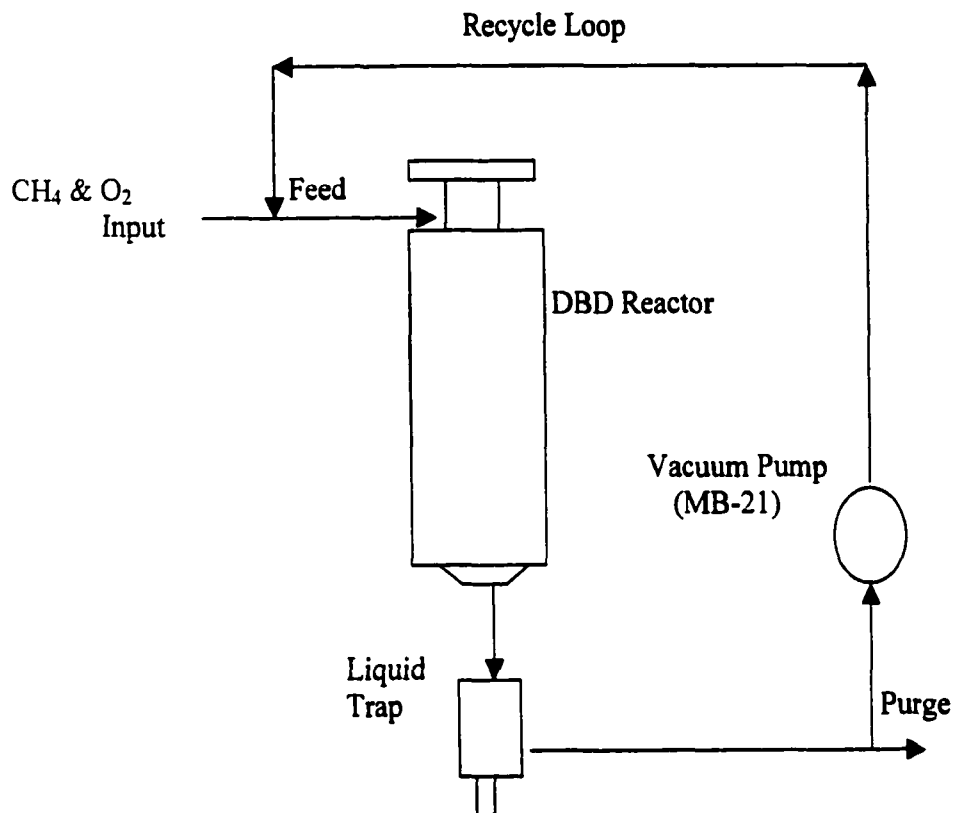
The flow rates of the feed gas stream and the product gas stream are determined by using a soap bubble meter and stopwatch after they leave the condenser. The organic oxygenate liquid products are collected after the experiment and analyzed with a Varian 3300 GC on a Porapak Q column with TCD.

An Elgar model 501 SL is the AC power supply to the reactor. It has a maximum power output of 500 watts, a voltage range of 0 to 130 V, and a current range of 0 to 5.8 A. The frequency range for the power supply is from 45 to 5000 Hz. The Elgar is used in conjunction with a CBK precision function generator that allows a sinusoidal waveform to be generated at the desired frequency. The voltage is stepped up (kV range for high voltage side) through the use of a 15060 P Franceformer transformer and is applied to the reactor. Power is measured on the primary side using a Microvip 1.2 Energy Analyzer.

2.2 Calibrations

In conjunction with a Porter flow module, the mass flow controllers (Porter Instrument Company) were calibrated for the feed and product gases (methane, ethane, ethylene, acetylene, oxygen, nitrogen, hydrogen, carbon monoxide, and carbon dioxide) of this work. The procedure for doing these calibrations is as follows. A gas (e.g. CH_4) is flowed through a mass flow controller over a range of Porter flow module set points (10%, 30%, 50%, 70%, 90%), and the flow rate of the gas at each set point is measured using a bubble meter and a stopwatch. The relationship between the gas flow rate and the Porter flow module set point is linear

and, hence, a linear regression is used to determine the gas flow rate as a function of the Porter flow module set point (gas flow rate = m*set point + b where m and b are the slope and y intercept, respectively).

In addition, the EG&G Carle Series 400 AGC gas chromatograph (Carle GC) was also calibrated for the feed and product gases of this work. This was accomplished by using the following procedure. A gas of known composition (e.g., 25 mole percent oxygen and 75 mole percent methane) is sent to the Carle GC, which gives the corresponding TCD GC area counts for the components in the gas. Several TCD GC area counts are obtained for each component at a given composition in order to obtain the component composition's average TCD GC area count. The relationship between a component's TCD GC area count and its composition in the gas is linear. Thus, gas streams with different compositions are flowed to the Carle GC such that a TCD GC area count is determined for each composition of a component. This, therefore, allows utilization of a linear regression to obtain the composition of each gas component as a function of its TCD GC area count (mole percent of a gas = m*TCD area count + b).

As for the Varian 3300 GC, it is calibrated for organic liquid oxygenates (methanol, methyl formate, formic acid, and formaldehyde). Each organic liquid oxygenate is calibrated as follows. First, a water-organic liquid oxygenate solution of known composition is made. A Hamilton 7000 series syringe then injects 1 µl of this solution into the Varian 3300 GC, which gives the corresponding TCD GC area count of the organic liquid oxygenate (water TCD GC area count is also given). This is

repeated several times to get an average TCD GC area count for the organic liquid oxygenate's composition. Again, the relationship between the TCD GC area count of a component and its composition is linear. Thus, several different compositions of an organic liquid oxygenate and their corresponding TCD area counts are obtained in order to use a linear regression to determine the organic liquid oxygenate's composition as a function of its TCD GC area count (wt. % of organic liquid oxygenate = m*TCD GC area count + b).

2.3 Gas and Organic Liquid Oxygenate Analysis

A gas stream (containing some or all of the following: methane, ethane, ethylene, acetylene, oxygen, nitrogen, hydrogen, carbon monoxide, carbon dioxide) is analyzed as follows. Its flow rate, as already mentioned, is determined with a bubble meter and a stopwatch. The composition of the gas stream is determined by the components' calibration equations from the Carle GC in conjunction with the components' TCD area counts. With the gas stream flow rate and composition determined, the component flow rates within the gas stream can be obtained (all component volumetric flow rates converted to molar flow rates).

As for the liquid product composed of organic oxygenates and water, the amount of time that is used to collect it (collection time) within the trap is recorded. In addition, the overall weight of the liquid product is also taken, which, in conjunction with the collection time, allows its mass flow rate to be determined (weight of liquid sample/collection time). By using the Varian 3300 GC composition

calibration equations in conjunction with their TCD GC area counts the composition of the liquid product (wt%) is determined. TCD area counts are obtained by injecting a 1 μl liquid sample, produced from an experiment, into the Varian 3300 GC via a Hamilton 7000 series syringe. With the liquid product's mass flow rate and composition (wt%) determined, component mass flow rates can be obtained (all component mass flow rates converted to molar flow rates).

2.4 Assumptions and Definitions for Experiments

The following assumptions were made for the experimental calculations:

1. The behavior of the gases is ideal.
2. The flow rates are determined at room temperature and atmospheric pressure.

The following definitions were used for the calculations (Note: Definitions 1-6 apply when a feed component's net rate of destruction in the reaction zone is greater than its net rate of creation. Definition 8b applies when a feed component's net rate of creation in the reaction zone is greater than its net rate of destruction):

1. % CH_4 conversion = [(molar flow rate of CH_4 entering reactor – molar flow rate of CH_4 exiting reactor)/(molar flow rate of CH_4 entering reactor)]*100

2. % O_2 conversion = [(molar flow rate of O_2 entering reactor – molar flow rate of O_2 exiting reactor)/(molar flow rate of O_2 entering reactor)]*100

3. % CO conversion = [(molar flow rate of CO entering reactor – molar flow rate of CO exiting reactor)/(molar flow rate of CO entering reactor)]*100

4. % CO_2 conversion = [(molar flow rate of CO_2 entering reactor – molar flow rate of CO_2 exiting reactor)/(molar flow rate of CO_2 entering reactor)]*100

5. % C_2H_6 conversion = [(molar flow rate of C_2H_6 entering reactor – molar flow rate of C_2H_6 exiting reactor)/(molar flow rate of C_2H_6 entering reactor)]*100

6. % H_2 conversion = [(molar flow rate of H_2 entering reactor – molar flow rate of H_2 exiting reactor)/(molar flow rate of H_2 entering reactor)]*100

7a. reacted carbon = total carbon molar flow rate within feed components entering the reactor - total carbon molar flow rate within feed components exiting the reactor

Note: If the net rate of creation is greater than the net rate of destruction for a feed component containing carbon, its entering and exiting molar flow rates are not used to determine the reacted carbon. Instead, the component is defined as a product (see 8b).

7b. reacted CH_4 = CH_4 molar flow rate entering the reactor – methane molar flow rate exiting reactor

8a. % Product Selectivity = (carbon molar flow rate of a product (e.g. methanol) exiting reactor)/(reacted carbon) * 100

8b. If a gas component formed within the reaction zone is also used as a feed component, the following definition for % product selectivity applies for the component:

% Product Selectivity = [(carbon molar flow rate of the component exiting the reactor – carbon molar flow rate of the component entering reactor)/reacted carbon]*100

9a. % H_2 selectivity = [(molar flow rate of H_2 leaving reactor)/(reacted CH_4*2)]*100

9b. If hydrogen is also a feed component, the following definition applies:

% H_2 selectivity =[(molar flow rate of H_2 exiting reactor – molar flow rate of H_2 entering reactor)/(reacted CH_4*2)]*100

10. Energy consumption is on an eV per molecule of converted methane basis

CHAPTER THREE: Oxygen Pathways And Carbon Dioxide Utilization in Methane Partial Oxidation in Ambient Temperature Electric Discharges

Abstract:

This methane conversion work studies a plasma reaction system for the production of organic oxygenates. The reactor consists of a glass dielectric interposed between the metal electrodes and a flowing gas stream through which kilovolt AC power with frequencies in the range of one to two hundred Hertz is applied. The geometry for this amounts to an annular system in which gas flows axially between the electrodes, with one electrode covered by a glass plate. The effect of the glass dielectric is to distribute the microdischarges across the entire electrode area and limit the duration of each microdischarge. The partial oxidation studies in this configuration produce methanol and other oxygenates (formaldehyde, formic acid, methyl formate). Selectivities for these products combined amount to 50-65 percent. These are the primary products when oxygen is included in the feed to the reactor. By-products here include significant levels of CO and CO_2, but it has been determined that CO_2 in the feed inhibits further production of CO_2 thereby eliminating net CO_2 production while increasing CO selectivity. These results show that oxygen appears to be needed in order to obtain higher methane conversions and significant oxygenated liquid organic products. CO or CO_2 do not appear to be substitutes for oxygen when trying to generate these desired oxygenated products.

3.1 Introduction

The relatively abundant resource of natural gas and its low cost and lower environmental impacts make this the carbon based fuel of choice well into the twenty-first century. Additionally these same factors make it a desirable feedstock for production of a number of commodity chemicals [1]. There is additional need for new technologies which can also allow recovery of the many remote gas resources which are presently burned with no economic value and with significant negative environmental impact. Present technology uses steam reforming to produce synthesis gas which is converted to methanol and other chemicals. Substantial research is being conducted on more efficient direct routes to oxygenates through direct partial oxidation chemistry. None of the direct partial oxidation routes has achieved the breakthroughs needed in order to be competitive, although new methods using non-equilibrium plasmas and plasma promoted catalysis appear to offer significant potential. [2, 3, 4, 5] Additional research into enhancement of the carbon balance of methane conversion by reforming with CO_2 in order to "recycle" existing fully oxidized carbon is also being conducted. A significant additional motivation for this is the fact that much of the methane resource base occurs with significant CO_2 (natural gas, landfill gas, etc.) which must be removed at considerable expense before the methane is usable. Conversion processes which reduce or eliminate this requirement offer a significant economic advantage as well as environmental benefit.

Plasma reactors may provide a useful technology for this problem. These types of reactors are already being used to study possible applications in the control of NO_x, SO_x, CO_x, toxic gases, volatile organic compounds, hazardous emissions, and for ozone synthesis [6].

This study uses a silent electric discharge to cause the reaction of methane to form oxygenated products. This discharge is created with an ozone type barrier discharge reactor connected to an AC power source. A Non-spark high energy environment is created that allows low gas temperatures to exist in a high electron temperature environment [6]. The purpose of this study is to determine the effect of CO_2 and CO on the partial oxidation of methane in a non-equilibrium plasma environment as well as studying the oxygen pathways involved in this system. This research is an extension of Bhatnagar and Mallinson's work [3]. Due to enhanced analysis capabilities there is improvement in the speciation of the oxygenated liquid products. The general trends from the previous study still hold to be true, however, through GC/MS analysis the significant liquid oxygenate products are found to be methanol, methyl formate, formaldehyde, and formic acid and ethanol is produced only in small amounts.

3.2 Experimental Section

To conduct the partial oxidation experiments, a silent electric discharge reactor (DBD reactor) is used, as shown in Figure 2.2. The gap the gas flows through is 0.5 mm wide. The active reaction area is 920 cm^2. The effective annular volume of the reactor is then 225 milliliters. The experimental design and procedures are discussed in section 2.1 and the overall experimental setup is shown in Figure 2.1.

Four types of experiments are conducted in this study. The first two involve using a stream of methane, oxygen, and carbon monoxide or methane, oxygen, and carbon dioxide. The CO_x flow rate is varied between 0 and 60 cc/min. All of these experiments have a 200 cc/min total flow rate. The methane to oxygen ratio is kept constant at 3:1. The frequency and voltage are set at 100 Hz and 8.5 kV. The third type of experiment feeds methane, oxygen, carbon monoxide, and carbon dioxide to the plasma reactor. The methane to oxygen ratio ranges from 2.65:1 to 3:1. The frequency and voltage are kept at 100 Hz and 8.5 kV for these experiments. The last type of experiment involves feeding pure methane or streams of methane with carbon dioxide, or with carbon monoxide, or with helium, or with carbon dioxide and carbon monoxide to the reactor. The frequency and voltage for all of these experiments are 200 Hz and 16 kV.

For all of the experiments, the carbon selectivity is defined as the total number of moles of carbon formed of a particular product divided by the total number of

58

moles of carbon reacted(calculated from molar flow rates). If the only carbon source is methane the calculation is straightforward. Moles of methane fed to the reactor minus the moles of methane leaving the reactor gives the total number of moles of carbon that have reacted. The calculation becomes a little more complicated if carbon monoxide or carbon dioxide are added to the feed stream. If there is a net loss in carbon monoxide or carbon dioxide, then the moles of carbon that have reacted from these compounds are added to the moles of carbon from the methane reacted which gives the total moles of carbon reacted. The conversion is simply defined as the difference between moles of a feed component in and moles of that feed component out divided by moles of the feed component in. Thus, any feed component which has a net loss in moles during the reaction will have its conversion calculated.

3.3 Results and Discussion

The base experiment for this study is with methane and oxygen only. This follows the work of Mallinson et al. (1987) and Bhatnagen and Mallinson (1995).[3, 7] In this study the product analysis, as already mentioned, has been refined and use has been made of the variables studied in the previous work in order to determine optimum conditions for liquids production.

Frequency has been found to be a significant variable affecting the performance of the reactor system. Table 3.1 compares the results at 100 Hz and 200 Hz for the methane oxygen system. The two significant differences in these

experiments are the methane and oxygen conversions. At 200 Hz the conversion for methane is 14 % while conversion for oxygen is 48 %. When frequency is decreased to 100 Hz the methane and oxygen conversion increase to 20% and 67%, respectively. The product selectivities, on the other hand, do not significantly change. A more detailed study has been made using a pure hydrocarbon reactant, Caldwell et al (2001).[8]

Table 3.1: Frequency/Voltage experimental results (200 cc/min flow rate & 3:1 $CH_4:O_2$)

Freq. (Hz)	Voltage (kV)	Mole % CH_4 Conv.	Mole % O_2 Conv.	% CO Select.	% CO_2 Select.	% Methan -ol Select.	% Methyl-formate Select.	%. Formic Acid Select.	% Formal-dehyde Select.	Org. Liq. Sum	% Ethane Select.
100	8.5	20	67	15	12	15	10	16	12	53	4
200	16.0	14	48	18	15	13	9	16	12	50	5

The next set of experiments varies the flow rate of CO in a 3 to 1 methane and oxygen stream. The results can be seen in Table 3.2. As the CO flow rate increases, the net selectivity for CO decreases from 15% to 0% while the selectivity for CO_2 increases from 12% to 37%. With a flow rate of 20 cc/min or greater of CO, the rate of its destruction is greater than the rate of its creation and, thus, produces a net selectivity of zero. When comparing the results with the results of the experiment which had no CO in the feed, it is apparent that the liquid product selectivities are unaltered. The one exception to this is when the CO feed flow rate is 60 cc/min. At this point the liquid product selectivities decrease. This occurs because, as the CO flow rate is increased, the oxygen feed flow rate decreases. As oxygen becomes sufficiently limited the production of the oxygenated liquid products decreases. These results show that the contribution from CO to the formation of liquid products is evidently negligible and that CO is not an intermediate product leading to liquids production, but on the contrary appears to be a precursor to CO_2. Another result of the increase in CO is the increase in the selectivity for ethane. Without CO, ethane's selectivity is 4% while at a 60 cc/min CO flow rate its selectivity increases to 8%. Thus, the effect on the activation of methane is less than on oxygenate production as methane conversion drops only a few percent from its original value. The limited oxygen environment increases the probability of coupling of activated methane.

Table 3.2: CO Experimental results (3:1 CH$_4$:O$_2$, 8.5 kV, 100 Hz, 200 cc/min flow rate)

CO Flow Rate (cc/min)	Mole % CH$_4$ Conv.	Mole % CO Conv.	Mole % O$_2$ Conv.	% CO Select.	% CO$_2$ Select.	% Methan -ol Select.	% Methyl- formate Select.	%. Formic Acid Select.	% Formal- dehyde Select.	Org. Liq. Sum	% Ethane Select.
0	20	-	67	15	12	15	10	16	12	53	4
10	17	-	63	7	21	17	15	13	12	57	5
20	19	5	66	0	24	17	12	14	12	55	5
40	20	8	78	0	31	16	12	13	10	51	7
60	18	7	74	0	37	12	12	4	6	34	8

The next set of experiments is run with CO_2 present instead of CO in the feed stream. The CO_2 experimental results can be seen in Table 3.3. In these experiments, as the CO_2 feed flow rate increases, the CO_2 selectivities decrease while the CO selectivities increase. The liquid selectivities, as is the case in the CO experiments, are unaffected when CO_2 is fed into the feed stream until the CO_2 flow rate is raised to 60 cc/min. At this flow rate, the liquid oxygenates selectivities start to decrease because of the reduced oxygen concentration. The net CO_2 selectivity becomes zero when the CO_2 feed flow rate is 40 cc/min or greater. This, again, is because the rate of destruction of CO_2 is greater than the rate of creation at this partial pressure of CO_2. These results suggest that CO_2, like CO, does not enhance liquid production. Of great interest, however, is the fact that CO_2 is evidently converted to CO, without the loss of liquids production except under oxygen limited conditions. The decrease in methane conversion observed in these experiments is also relatively small. Thus, the presence of CO_2 does not materially interfere with methane conversion or oxygenated production and is to some extent converted to a more useful product. Due to recent enhanced analysis capabilities it has been shown that hydrogen is being produced in significant amounts.

Table 3.3: CO_2 Experimental results (3:1 $CH_4:O_2$, 8.5 kV, 100 Hz, 200 cc/min flow rate)

CO_2 Flow Rate (cc/min)	Mole % CH_4 Conv.	Mole % CO_2 Conv.	Mole % O_2 Conv.	% CO Select.	% CO_2 Select.	% Methan -ol Select.	% Methyl- formate Select.	%. Formic Acid Select.	% Formal- dehyde Select.	Org. Liq. Sum	% Ethane Select.
0	20	-	67	15	12	15	10	16	12	53	4
10	15	-	53	23	14	14	9	10	12	45	5
20	22	-	70	21	2	19	18	8	7	52	3
40	26	4	77	29	0.0	12	21	21	13	67	3
60	22	3	71	42	0.0	11	8	7	8	34	4

The third set of experiments examined addition of both CO and CO_2 to the methane and oxygen feed stream. These results can be seen in Table 3.4. The total flow rate, frequency, and voltage are the same as the previous experiments. When both CO and CO_2 flow rates are both set at 17 cc/min, net CO_2 selectivity is 15% while net CO selectivity is 7%. This suggests the rate for CO conversion to CO_2 is greater than the rate of CO_2 conversion to CO at these partial pressures and one minute residence time. The second experiment reduces the CO flow rate to 10 cc/min while keeping the CO_2 flow rate at 17 cc/min. This causes both selectivities to be around 15%. This is due to the fact that with more CO_2 in the feed stream more CO is produced, as was also seen in the CO_2 experiments, and the rates are in balance.

Table 3.4: CO₂/CO Experimental results (8.5 kV, 100 Hz, Experiment 1: CH₄=125 cc/min, O₂=41 cc/min, CO₂=17 cc/min, CO=17 cc/min, Experiment 2: CH₄=130 cc/min, O₂=49 cc/min, CO₂=17 cc/min, CO=10 cc/min)

Exper.	Mole % CH_4 Conv	Mole % O_2 Conv.	% CO Select.	% CO_2 Select.	% Ethane Select.	% Methanol Select.	% Methyl-formate Select.	%. Formic Acid Select.	% Formal-dehyde Select.	Org. Liq. Sum
1	20	79	7	15	5	17	12	15	12	56
2	19	77	15	15	5	20	13	18	14	65

The last set of experiments shown in Table 3.5, are with a pure CH_4 feed or gas mixtures of 150 cc/min of methane with 50 cc/min of helium, or CO_2, or CO, or 40 cc/min of CO and CO_2. The first three experiments in Table 3.5 give ethane selectivities which range from 37% to 57%. Little or no liquid products or solid accumulation in the reactor was observed. The rest of the products are assumed to be C_3+ compounds, but analysis of these was not available. When methane is the only feed gas, ethane selectivity is 49%. It is interesting to note that the mixture of CH_4 and CO_2 produced a total selectivity for liquid products of less than 5%. When methane is fed with CO, less than 2% of the total selectivity is for liquids. This again indicates that the contribution from CO or CO_2 to liquid products formation is negligible. The selectivity for ethane is 82% when methane and CO are fed. This suggests, as is shown in the CO experiments, that CO in the feed stream appears to promote methane coupling. It seems to be a better promoter than CO_2 since with CO_2 an ethane selectivity of only 37% is obtained. Note in all these cases, the absence of oxygen dramatically reduces the conversion of methane. The successful activation of methane to cause its conversion significantly depends upon active species generated by O_2 which are not formed from CO or CO_2.

Table 3.5: No O_2 Experimental Results

CH_4 Flow Rate (cc/min)	He, CO_2, and/or CO Flow Rate (cc/min)	Mole % CH_4 Conv	Mole % CO Conv.	Mole % CO_2 Conv	% CO Select.	% CO_2 Select.	% Ethane Select.
200	0	3	0	0	0	0	49
150	50 He	4	0	0	0	0	57
150	50 CO_2	3	0	1	45	0	37
150	50 CO	3	0	0	0	1	82
150	40 CO 40 CO_2	7	2	3	0	0	48

Pathways that could be occurring in the homogeneous partial oxidation of methane have been studied.[9,10] A study involving O_2 and O_3 in the feed with CH_4 show that at 401 °C no methanol could be detected with just O_2 and CH_4 but methanol was detected when O_3 was present at the same temperature. The authors suggested that O_3 decomposed to O_2 and O and the O atom could abstract hydrogen from methane to form CH_3 and OH. Once the methyl radical is generated a series of reactions can occur which ultimately leads to the products.[9] At ambient temperature, Mallinson found no reaction between Methane and O_3/O_2 mixtures.[7] Also, the possible reaction of activation of CO_2 via dissociation:

$$CO_2 + e^- \rightarrow CO + O + e^-$$
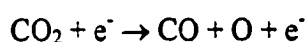
or by electron attachment:

$$CO_2 + e^- \rightarrow CO + O^-$$
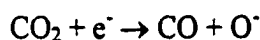
do not appear to generate the required energetic species for significant methane activation.

3.4 Conclusions

Methane and oxygen mixtures may be converted to a significant extent to liquid products: methanol, formaldehyde, formic acid, and methyl formate in a low-temperature, atmospheric pressure, plasma environment. CO, CO_2, H_2, and ethane are also products. Ethane becomes the primary product in an oxygen limited environment. High conversions of methane to significant liquid oxygenates require O_2 to be present. It is believed that the oxygen species generated in the plasma field

somehow activates the methane in such a manner that allows for these higher conversions. At this point the pathways appear to generate CO from stepwise oxidation from methane which is then oxidized to CO_2 via the water gas shift reaction. Recent hydrogen detection enhancements to the gas chromatograph have shown that hydrogen is being produced when methane is combined with oxygen which, therefore, allows the water gas shift reaction to take place. A pseudo-equilibrium is established which can be driven towards the shift or towards the reverse shift depending on the composition. Reduction of CO to more useful products does not occur to a significant degree under the present conditions, although CO_2 hydrogenation is known to be possible[11]. The presence of CO_2 inhibits further production of CO_2 from over oxidation and contributes to "recycling" of carbon.

Literature Cited

(1) Fox III, Joseph M., CATAL. REV.-SCI. ENG. 1993, 35(2), 169-212

(2) Liu, C. A., A. Marafee, B. Hill, G. Xu, R. G. Mallinson and L. L. Lobban, Ind. Eng. Chem. Research,1996, 35, 3295

(3) Bhatnagar, Rajat, Mallinson, Richard G.; "Methane and Alkane Conversion Chemistry," Plenum Press, 1995, 249

(4) Marafee, A. C. Liu, G. Xu, R. G. Mallinson and L.L. Lobban, Ind. Eng. Chem. Research, 1997, 36, 632 (1997).

(5) Liu, C.A., A. Marafee, B. Hill, R.G. Mallinson and L.L. Lobban; "Methane Conversion to Higher Hydrocarbons over Charged Metal Oxide Catalysts," in press Applied Catalysis, A., July 1997.

(6) Chang, J.S.; Lawless, P.A.; Yamamoto, IEEE Transactions on Plasma Science, Vol. 19, NO. 6, 1991

(7) Mallinson, R.B. unpublished results, 1987

(8) Caldwell, T, Larkin, D.W., Lobban, L.L, Mallinson, R.G.; "Geometric Effects on Methane Conversion and Product Selectivity in a Planar Silent Electric Discharge Reactor," publication in progress

(9) Gesser, H.D. Hunter, N.R. and Das, P.A.; "The Ozone Sensitized Oxidation Conversion of Methane to Methanol and Ethane to Ethanol," Catal. Lett., 1992, Vol. 16, 217-221

(10) Rotzoll, G.; " Mass Spectrometric Investigation and Computer Modeling of the CH_4-O_2-O_3 Reaction from 480 to 830 K," J. Phys. Chem., 90, 677, 1986

(11) Eliason, B., Kogelschatz, U, Xue, B., Zhou, L.M.; "Application of Dielectric-Barrier Discharges To The Decomposition And Utilisation of Greenhouse Gases," 13[th]International Synposium on Plasma Chemistry (ISPC-13), Beijing, Aug, 1997

CHAPTER FOUR: Carbon Pathways, CO₂ Utilization, and *In Situ* Product Removal in Low Temperature Plasma Methane Conversion to Methanol

Abstract

This study examines a non-equilibrium "cold" plasma reaction system for the partial oxidation of methane as well as the water-gas shift reaction and CO_2 reforming of methane. Annular and planar plasma reactors are used. Both systems have a glass dielectric interposed between two metal electrodes. The electrodes are supplied with kV ac power with frequencies ranging from 50 Hz to 100 Hz. The results show that lowering the reaction temperature from 75 °C to 28 °C in the partial oxidation experiments increases overall organic oxygenate liquid selectivities from 24% to 52%. The lower temperatures reduce these products' vapor pressures to their equilibrium partial pressures allowing condensation within the reactor. Experiments involving CO and H_2O, and CO_2 and H_2 confirm that the water-gas shift reaction pathway occurs along with the partial oxidation of methane. Results of carbon dioxide reforming of methane indicates that the CO_2:CH_4 ratio strongly affects the results. The ethane and hydrogen selectivity decrease when the CO_2:CH_4 ratio is reduced from 1:2 to 1:1. This decrease in partial pressure of methane decreases direct coupling to ethane. Increasing the partial pressure of CO_2 from a 1:2 to 1:1 CO_2:CH_4 ratio causes increased CO_2 conversion to CO. The selectivity for methanol under reforming conditions is less than 1 %. A further increase in the CO_2:CH_4 ratio from a 1:1 to 2:1 causes an increase in ethane and hydrogen selectivity indicating that an

oxidative coupling pathway may play a role under these conditions. Finally, the results show that the presence of helium enhances methane conversion and alters the reaction selectivities despite lowering methane partial pressures. This potentially is due to the fact that increasing the partial pressure of helium within the system increases the system's average electron energy.[1] Thus, the number of electrons capable of initiating reactions increases.

4.1 Introduction

Presently, natural gas is being used as a combustion fuel in industrialized areas that are close to large natural gas reserves. Steam reforming and further conversion to methanol is a major process that utilizes natural gas for its chemical value. This commercial technology is a complex multi-step process which is energy intensive.

There is also a considerable amount of natural gas in "remote" areas around the world. Many of these natural gas reserves cannot be utilized presently due to high transportation costs. This problem could be potentially reduced if those resources could be converted into organic liquids, such as methanol, that did not need refrigeration or compression for transport.[2] However, multi-step processes such as steam reforming and then synthesis are too expensive to implement for remote locations or for fuel value, rather than chemical value. Thus, a one-step partial

oxidation process which substantially reduces the processing cost could allow effective utilization of these gas reserves.

This study uses a silent electric discharge reactor to generate a nonequilibrium plasma which causes the direct partial oxidation of methane to organic liquid oxygenates (e.q. methanol). The reactor operates at near ambient temperatures and atmospheric pressure. Planar and annular geometries with about the same volume and gap distance are used in this study. A comparison of their performance is made when processing identical 3:1 CH_4:O_2 feeds with the same 1 minute residence time.

The effect of reactor wall temperature is investigated in this study to determine if lowering the reactor temperature increases liquid organic oxygenate production while decreasing CO_x production in the partial oxidation of methane. Lowering the reaction temperature lowers the vapor pressures of the "liquid" oxygenate products and, thus, causes more of these desirable products to be condensed *in-situ*. This decreases their chances of being over- oxidized since they are no longer in the gas phase reaction zone.

In partial oxidation experiments, shown in previous work, the rate of destruction of CO_2 was found to be greater than the rate of creation of CO_2 when the CO_2 partial pressure was significant.[3] This paper studies the role of the water-gas

shift reaction (and its reverse) in CO_2 production and destruction in the partial oxidation system.

Also in this study, the utilization of carbon dioxide in carbon dioxide reforming of methane is examined. The use of CO_2 for reforming may reduce net CO_2 production when synthesis gas (or hydrogen) is produced. Additionally, since CO_2 is present in many natural gas resources, its ability to be tolerated and even enhance partial oxidation is of interest.

4.2 Experimental Section

The overall experimental setup is shown in Figure 2.1. The experimental procedure and design for the partial oxidation experiments are discussed in section 2.1. The gap through which the gas flows in the annular silent electric discharge reactor (Figure 2.2) is a 0.27 cm wide annular space. The active reaction area is 920 cm^2 and the effective annular volume of the reactor is 225 milliliters.

In addition, a planar plasma reactor is also utilized in the partial oxidation of methane (reactor geometry experiments) and in the CO_2 methane reforming experiments. Two flat aluminum plates are used as the electrodes for this reactor. A glass dielectric and a teflon spacer, which creates the volume for the gas flow, are located between the top and bottom aluminum plates. The electrode without the glass dielectric has a water jacket on its exterior side. In the partial oxidation experiments,

the gas gap and reactor volume are .25 cm and 200 cm^3, respectively. These dimensions are very similar to the annular reactor system; however, this design allows for variation of reactor geometry. The reactor volume in the CO_2 reforming experiments is 216 cm^3. For the partial oxidation experiments, the system used in the collection and analysis of the products is the same as that used in the annular reactor. However, the gases in the CO_2 reforming of methane experiments are analyzed by a Perkin-Elmer "Autosystem" Gas Chromatography apparatus which has both TCD and FID detectors. Haysep DB and T columns are used to separate the methane, CO_2, CO, acetylene, ethylene, ethane, hydrogen, and methanol.

In the first series of experiments, the annular reactor performance is compared with the planar reactor system. For these experiments, the residence time is one minute and the $CH_4:O_2$ ratio is kept constant at 3:1. The difference in power used by the two reactors for these experiments is 15 %.

Experiments to examine the effect of in-situ product condensation on product selectivities used the annular reactor. Methane and oxygen are fed to the reactor at a ratio of 3:1 with a total flow rate of 200 cc/min. This gives a residence time of 1 minute. The frequency and voltage are set at 100 Hz and 7.6 kV, respectively. The experimental variable for the four experiments conducted is the water jacket temperature.

In the next series of experiments the reverse water-gas shift reaction is studied by feeding hydrogen and carbon dioxide to the annular reactor. The $H_2:CO_2$ ratios used are 3:1, 4:1, 5:1, and 6:1. For all four experiments the residence time is 2 minutes. The frequency and voltage are 87 Hz and 5.9 kV, respectively. The water temperature in the water jacket is maintained at 15 degrees C.

The water-gas shift reaction is studied by feeding CO and H_2O to the annular reactor. Carbon monoxide is bubbled through a flask of water at 57.8 degrees C. This provides an inlet mole fraction of water of 0.18 based upon saturation calculations. The water in the water jacket for this experiment is set at 80 degrees C. Thus, water fed to the reactor should be retained in the vapor phase. The residence time is 2 minutes. The frequency and voltage are 90 Hz and 7 kV, respectively.

In the first series of methane reforming experiments, the $CO_2:CH_4$ ratio is varied from pure methane, 1:2, 1:1, and 2:1. For each $CH_4:CO_2$ ratio, the experiment is repeated at voltages of 5.5 kV, 6.6 kV, and 7.7 kV. For all of these experiments, the space time is 4 minutes and 80% of the feed is helium.

In the next series of experiments the helium concentration is varied with the balance of the feed gas being CH_4 and CO_2 at a 1:1 ratio. For a given helium concentration the experiment is conducted with four minute and six minute space times. For each space time the voltage is also varied from 5.5 kV to 7.7 kV.

4.3 Results and Discussion

The results of the partial oxidation experiments in the annular and planar reactors are shown in Tables 4.1 and 4.2. The plasma reactors operate at the same 1 min. residence time and within 15 % of the power of one another. The annular reactor has a gap thickness of .27 cm while the planar reactor's gap thicknesses is .25 cm. Comparing the two systems, it can be seen that the methane and oxygen conversions are within 4% and 10% of one another, respectively. The only significant difference comes in formaldehyde selectivity in which the planar system has a much lower selectivity for it. Thus, the different reactor geometries produce generally similar results.

The results obtained for partial oxidation and water-gas shift(and its reverse)experiments, presented in Tables 4.3-4.6, are carried out in the annular reactor. Tables 4.3-4.4 show the partial oxidation results when the reactor wall temperature is varied. The results show that changes in water jacket temperature from 6 to 75 degrees C, results in only small changes in methane conversion, while oxygen conversion increased significantly from 67% to 88%. The ethane selectivity remains relatively constant with increasing temperature but the CO and CO_2

Table 4.1: 3:1 CH$_4$:O$_2$, 1 min. residence time(Reactor type: p= planar, a = annular)

Geo-metry & gap d. (cm)	Mole % CH$_4$ Conv.	Mole % O$_2$ Conv	% Ethane Select.	% CO Select	% CO$_2$ Select	% Me Select.	% MF Select.	% FA Select.	% F Select.	% Et Select.	Org. Liquid Sum
.27 (a)	24	74	4	14	13	17	5	16	13	1	52
.25 (p)	25	82	5	18	15	23	8	22	2	0	55

Note: Me=Methanol, MF = Methyl Formate, FA = Formic Acid, F = Formaldehyde, Et =Ethanol

Table 4.2: 3:1 CH$_4$:O$_2$, 1 min. residence time(Reactor type: p = planar, a = annular)

Geometry & Gap dis.(cm)	Power (Watts)	% CH$_4$ Conv.	Reacted CH$_4$ (moles/min)	Freq. (Hz)	Volt. (kV)	eV/(molecule of conv. CH$_4$)
.27 (a)	118	24	.0015	100	7.6	49
.25 (p)	100	25	.0015	100	5.0	41

Table 4.3: Annular Reactor, 3:1 $CH_4:O_2$, 7.6 kV, 100 hz, 200 cc/min flow rate

H_2O Temp. °C	Mole % CH_4 Conv.	Mole % O_2 Conv	% E Select.	% CO Select	% CO_2 Select	% Me Select.	% MF Select.	% FA Select.	% F Select.	% Et Select.	%Org. Liquid Sum	%Gas Phase Sum
6	23	67	3	11	10	11	3	15	15	1	45	24
28	24	74	4	14	13	17	5	16	13	1	52	31
54	24	81	4	25	22	9	5	12	7	1	34	51
75	25	88	3	36	26	9	4	7	4	0	24	65

Note: E=Ethane, Me=Methanol, MF = Methyl Formate, FA = Formic Acid, F = Formaldehyde, Et =Ethanol

Table 4.4: Annular Reactor, 3:1 $CH_4:O_2$, 7.6 kV, 100 Hz, 200 cc/min

H_2O Temp.(° C)	Power(Watts)	Mole % CH_4 Conv.	eV/(molecule of conv. CH_4)
6	112	23	48
28	118	24	49
54	119	24	49
75	135	25	53

Table 4.5: Annular Reactor, H_2:CO_2, 5.9 kV, 87 Hz, total flow rate =106 cc/min, H_2O jacket temp. =15°C

H_2:CO_2 Ratio	% CO_2 Conv.	% H_2 Conv.	% CO Select.	Power (Watts)	eV/(molecule of conv. CO_2)
3:1	10	3.9	117	96	570
4:1	11	3.5	104	100	614
5:1	13	3.3	94	102	640
6:1	13	2.6	101	103	788

Table 4.6: Annular Reactor CO:H_2O, 7.0 kV, 90 Hz, total flow rate =106 cc/min, H_2O jacket temp. =80°C

% CO Conv.	% CO_2 Select.	% H_2O Conv.	Power (watts)	eV/(molecule of conv. CO)
3.5	58	11	38	154

selectivities both increase. The "liquid" selectivities, except for methyl formate and ethanol, which shows little change, generally decrease with increasing temperature. Thus, as can be seen in the last two columns of Table 4.3, the overall trend for increasing water jacket temperature is that the sum of the "liquid" selectivities decreases while the sum of the "gas" selectivities increase. The increased selectivities for CO_x at higher temperatures due to "over" oxidation of the "liquid" products is consistent with higher oxygen conversion with little change in methane conversion. Because the reactor operates at such low temperatures, as the methane conversion increases as the gases pass along the length of the reactor, the partial pressures of the products increase. The partial pressures of the heavier "liquid" components reach their vapor pressures at sufficiently low temperatures that condensation on the cooled wall occurs. Thus, under ideal conditions, the low temperatures achievable in these reactors result in low partial pressures of these products in the gas phase, thus minimizing their availability to be further oxidized to "gas" products, CO_x.

Table 4.4 shows that the power and eV per molecule of converted CH_4 for these experiments increase 17% and 9.4%, respectively, as the temperature increases from 6 to 75 degrees C. The change in eV per molecule is primarily the result of the significant change in the power used. Thus at the lower temperatures, not only are more liquid products being recovered, but energy efficiency is higher.

The results of the water-gas shift reaction experiments are shown in Table 5. The only two products observed in any of the four experiments are CO and water. As shown in the table, increasing partial pressure of hydrogen results in decreased hydrogen conversion while CO_2 conversion increases. An increase in partial pressure of hydrogen also results in an increase in the eV/molecule of converted CO_2. Table 4.6 shows the results of having CO and H_2O as the feed gas where the products are hydrogen and CO_2, as expected. The $H_2:CO_2$ ratio of the products is 1:2 which suggests that half of the O atoms combining with CO to form CO_2 came from CO. These results demonstrate that the water-gas shift reaction pathway occurs in these systems. These results also indicate that when CO and CO_2 are present in methane partial oxidation, a balance between CO and H_2 production is established. Thus, CO_2 production can be minimized or eliminated, as shown in previous work[5], while producing a synthesis gas that could be used for methanol production.

The results for the first series of CO_2 reforming experiments (conducted by M. Leethochawalit and S. Chavadej from the Petroleum and Petrochemical College, Chulalongkorn University), as outlined in the experimental section, can be seen in Tables 4.7-4.9. As may be seen in all three tables, an increase in voltage increases the conversion. These results also generally indicate that as the $CO_2:CH_4$ ratio increases, the methane conversion becomes greater as can be seen most clearly in Table 4.9 at 7.7 kV. In previous work[7] with the annular

85

Table 4.7: CO_2:CH_4 experiments(5.5 kV, 80 % helium concentration, space time = 4 min.)

CO_2:CH_4 Ratio	% CH_4 Conv.	% CO_2 Conv.	% Ethane Select.	% CO Select.	% Hydrogen Select.
1:2	22	16	65	34	9
1:1	16	9	23	76	2
2:1	28	13	65	34	14

Table 4.8: CO_2:CH_4 experiments(6.6 kV, 80 % helium concentration, space time = 4 min.)

CO_2:CH_4	% CH_4 Conv.	% CO_2 Conv.	% Ethane Select.	% CO Select.	% Hydrogen Select.
1:2	25	16	67	32	10
1:1	24	14	13	87	1
2:1	34	15	34	66	16

Table 4.9: CO_2:CH_4 experiments(7.7 kV, 80 % helium concentration, space time = 4 min.)

CO_2:CH_4	% CH_4 Conv.	% CO_2 Conv.	% Ethane Select.	% CO Select.	% Hydrogen Select.
0:1	15	-------	99	-------	4
1:2	29	21	65	34	12
1:1	30	18	17	82	7
2:1	40	18	31	68	20

reactor, the methane conversion in pure methane was about 3 %. For the same residence time, frequency, and voltage with a 3:1 methane to oxygen feed, the methane conversion was 14 %. The methane conversion in the 2:1 CO_2:CH_4 (at 7.7 kV) is intermediate to these other two cases. The lower conversions in the experiments with CO_2 compared to the experiments with molecular oxygen present suggest that an active oxygen species, which CO_2 is not capable of producing in the same quantity, if at all, helps initiate the conversion of methane. One simple explanation for this result is that the energies required to dissociate oxygen due to an inelastic collision with an electron are 6.0 and 8.4 eV, while the dissociation energies of carbon dioxide due to an inelastic electron collision with an electron are 6.9 and 11.4 eV.[4] Therefore, a more energetic process may be required to "abstract" an oxygen atom from CO_2 than from O_2, though there is no evidence offered in this study of the important active species in these different systems.

The highest fractional conversion of CO_2 occurs at a 1:2 CO_2:CH_4 ratio. The fractional conversion for the 1:1 and 2:1 ratios of CO_2:CH_4 is lower than 1:2, but fairly similar with each other at the same voltage. Once again, for all the experiments, an increase in voltage increases CO_2 conversion for a given feed ratio.

The selectivity for ethane is also shown in Tables 4.7-4.9. In these experiments at least 98% of the C_2 products formed is ethane. The highest selectivity for ethane occurred with pure methane as the feed where the only initially observable

88

products are C_2 species and H_2. With a CO_2:CH_4 ratio of 1:1, ethane selectivity is lower, presumably due to the lower partial pressure of CH_4, and a decreased rate of direct methane coupling is observed. At the higher CO_2 ratio of 2:1 CO_2:CH_4, ethane selectivity is higher than for the 1:1 experiments. This is consistent at all the voltages and space times. These results suggest that while direct methane coupling is a major pathway in ethane formation, an oxidative pathway may play a role at higher CO_2 partial pressures.

The hydrogen selectivity in these experiments appears to be related to ethane production because hydrogen is produced in the methane coupling reaction.

Carbon monoxide is the other major carbon product in these experiments. Until experiments with isotopically labeled CO_2 are conducted, it cannot be established how much of the CO comes from methane under these conditions. In partial oxidation experiments when neither CO or CO_2 is present in the feed, CO is clearly produced from methane.

The effect of adding helium to a 1:1 CO_2:CH_4 ratio feed stream was studied in a series of experiments conducted at 5.5, 6.6, and 7.7 kV with 4 minute and 6 minute space times. Table 4.10 shows the results for 5.5 kV and a 4 minute space time. All the experiments show the same trends, though some trends are not as uniform as those in Table 4.10. In these experiments, as the helium partial pressure is increased,

the methane conversion increases despite lower partial pressures of the reactant gases. When the helium partial pressure is increased, ethane selectivity decreases, while the carbon monoxide selectivity increases. These experiments suggest that helium may be affecting the electrical properties of the system rather than acting solely as a diluent. Due to the high excitation levels of helium, the effective free mean path of an electron increases within the reaction zone.[1] This results in an increase in the average electron energy. Therefore, the number of electrons capable of initiating reactions within the system increases and, hence, might be affecting product selectivities as well as methane and carbon dioxide conversions. In addition, the decrease in ethane selectivity with higher methane conversion may be due simply to the dilution of the second order coupling reaction.

Table 4.10: Effect of helium concentration on methane conversion($CO_2:CH_4$ ratio 1:1, 5.5 kV, 4 min. space time)

Helium Conc.	% CH_4 Conv.	% CO_2 Conv.	% Ethane Select.	% CO Select.	% Hydrogen Select.
20 %	<1		89	0	0
50 %	6		69	30	2
80 %	16	9	23	76	2

4.4 Conclusions

The results of this study show that product selectivities are strongly influenced by *in-situ* product condensation in partial oxidation of methane in a silent electric discharge reactor when reactor wall temperature is varied. At 28 ° C, 52 percent of the reacted carbon is recovered as these liquid organic oxygenates. At 75 ° C only 24 percent of the reacted carbon is recovered as "liquid" organic products. When the temperature of the system is lowered sufficiently the vapor pressures of the liquid organic oxygenates are reduced and condensation can occur, thus limiting the partial pressures of these desirable products in the gas phase. This results in reduced oxidation of these products to CO_x.

Experiments with hydrogen and carbon dioxide and with carbon monoxide and water suggest that the water-gas shift reaction pathway takes place in these systems. These results explain previous observations[5], where CO_2 inhibition and increased CO production were observed with higher CO_2 partial pressures, by demonstrating that the reverse water-gas shift reaction occurs.

Carbon dioxide reforming of methane in these systems also occurs along with methane coupling. The production of CO from methane under these conditions has not been established, and methane partial oxidation from CO_2 is very limited. Finally, helium increases the average electron energy within the system,[1] which potentially

92

enhances methane conversion and affects product selectivities. The exact role of helium in these reaction systems needs to be studied further.

Acknowledgment

4.5 Literature Cited

(1) Tas, Marnix A., thesis, "Plasma-Induced Catalysis: A Feasibility Study and Fundamentals," Eindhoven University of Technolgy, 1995

(2) Crabtree, Robert H. Aspects of Methane Chemistry. Chem. Rev. 1995, 95, 987-1007

(3) Larkin, D.W.; Caldwell, T.A., Lobban L.L.; Mallinson, R.G. Energy and Fuels Vol 12. n. 4 pp. 740-744

(4) Eliasson, B., Egli, W., Kogelschatz, U.; "Modeling of Dielectric Barrier Discharge Chemistry," Pure & Appl. Chem., Vol. 66, No. 6, 1994, 1275-1286

CHAPTER FIVE: Production of Organic Oxygenates in the Partial Oxidation

of Methane in a Silent Electric Discharge Reactor

Abstract

This study on the partial oxidation of methane in a silent electric discharge uses an annular reactor consisting of two metal electrodes separated by a gas gap and a glass dielectric covering the outer surface of the inner electrode. The reactor operates at 7000 volts and 26 to 178 W of AC power. The frequency ranges from 100 to 200 Hz. The organic liquid oxygenates formed from the partial oxidation of methane are principally methanol, formaldehyde, methyl formate, and formic acid. This study showed that when the oxygen partial pressure became limited in the reaction zone, the energy efficiency of the system significantly decreased. It was also shown that with a recycle, as opposed to without, the selectivity for organic liquids was enhanced by 12% while the CO_x selectivity decreased by 19% because the recycle had a short per pass residence time with removal of organic liquid oxygenate products via a condenser. Finally, experimentally simulating reactors in series with intermediate oxygen additions obtained an overall methane conversion of 59% with 35% yield in organic liquid oxygenates.

5.1 Introduction

Currently, research using non-equilibrium plasmas is being done to convert methane into useful products such as higher hydrocarbons, synthesis gas, and organic oxygenate liquid products. [1-7] This study, which is a continuation of Bhatnagar et al. work [3,4], uses a silent dielectric barrier discharge (DBD) reactor, which creates a non-equilibrium plasma to cause the direct partial oxidation of methane. The reactor typically operated at atmospheric pressure with an operating temperature of either 28 or 75 °C. The reactor geometry is annular with a fixed gap distance.

The ability to efficiently convert a significant amount of the natural gas to useful products at a remote site is important in order for a process to have commercial potential. Thus, this study examines the effect methane and oxygen conversion has on the energy efficiency for the system.

In previous work, it was demonstrated that the water-gas shift and reverse water-gas shift reactions were taking place when CO or CO_2 was added to a methane-oxygen feed. [5,6] This work studies the influence hydrogen has on CO and CO_2 selectivities via these pathways.

Earlier work also has shown that decreasing the reactor temperature increased the organic oxygenate selectivity due to *in-situ* removal of these products from the reaction zone via condensation. [6] The current work studies how the organic oxygenate

selectivity is affected when a recycle stream is added. The recycle stream in this study has a high recycle ratio and low residence time per pass in which the organic oxygenates are condensed out in a low temperature liquid trap. In addition, evidence of a direct oxidative route from methane to CO_x is explored.

This study also investigates methane-oxygen-nitrogen systems to determine the effect of nitrogen on energy efficiency and product selectivity. If methanol could be produced from a methane-air feed, or with oxygen enriched air, the cost for oxygen could be reduced or eliminated.

Finally, some types of natural gas have significant amounts of ethane within them. When ethane and oxygen are present in a DBD reactor, ethanol is one of the products formed. Currently, ethanol is looked upon as a potential future fuel source. Commercially, it is produced by acid-catalyzed hydration of ethylene or fermentation.[8] This study investigates the effect of ethane composition on energy efficiency and product selectivity.

5.2 Experimental Section

The experimental design and procedures are discussed in section 2.1. The overall experimental setup is shown in Figure 2.1. For this work, the partial oxidation of methane occurs in an annular DBD reactor (shown in Figure 2.2). The gap in the

DBD reactor the gas flows through is 1.9 mm. The active reaction area is 728 cm^2 and the effective annular volume of the reactor is 141 cm^3.

The power factor for each experiment in this work is one. This is obtained by setting the frequency to the value that produces this power factor. The power input for these experiments is 118 W, except when power is the experimental variable. This power input value of 118 W was chosen in order for a significant amount of methane and/or ethane to be converted in all the experiments that did not have power as the experimental variable. The water jacket temperature for all but one of the experimental series is 28 °C. This temperature enables *in situ* removal of organic oxygenates to occur within the reaction zone of single pass systems. The experimental series that does not have a water jacket temperature of 28 °C is the hydrogen experimental series, in which the temperature is 75 °C. This higher setting is used in order to allow water that is formed in the reaction zone to remain in the gas phase and, hence, be a potential reactant in the water-gas shift reaction.

In order to demonstrate that the experiments in this work can be acceptably reproduced, Table 5.1 compares two methane-oxygen experiments at identical

Table 5.1: Experimental Reproducibility

CH$_4$:O$_2$ feed ratio = 2:1, Power = 118 W, Freq.= 174 Hz, Residence Time = 20 seconds, Water Temp. in Water Jacket = 28 °C													
Experiment #	Moles of CH$_4$ conv. (moles/min)	eV/molecule of CH$_4$ conv.	H$_2$ sel.	Mole % CH$_4$ conv.	Mole % O$_2$ conv.	% C Selectivity (mole Basis)							
						CO$_2$	CO	Ethane	M	MF	FA	F	Sum
1	.0014	51	11	12	26	13	19	2	16	9	17	12	88
2	.0014	53	12	12	27	14	20	2	14	8	16	14	88
M = Methanol, MF = Methyl Formate, FA = Formic Acid, F = Formaldehyde, Sum = Sum of Carbon Selectivity													

conditions. The material balances (reactive molar carbon basis) for all the non-ethane experiments are fairly close to closing. However, since most of them account for 83% to 96% of the carbon reacted, the possibility of undetected gas phase products does exist. This is because no significant solid residue has been found within the reactor after an experiment has been completed.

In the methane-ethane-oxygen and ethane-oxygen systems, the Varian 3300 GC detects significant identified organic liquid products due to ethane chemistry. Thus, their carbon material balances are not as close to closing as the rest of the experiments done in this work.

5.3 Results and Discussion

5.3.1 Energy Efficiency Experiments

The first two series of experiments examine the effect of feed flow rate and power input on energy efficiency (eV per molecule of methane converted) for a methane-oxygen system. For all of these experiments, the $CH_4:O_2$ feed ratio is 2:1, the water temperature in the water jacket is 28 °C, the frequency is set at 174 Hz, and the system pressure is 1 atm. In the first series of experiments, the power is constant at 118 watts and the feed flow rate is varied from 40 cc/min to 430 cc/min. In the second series of experiments, the feed flow rate is constant at 70 cc/min while the power is varied from 26 watts to 178 watts.

The results of the energy efficiency experiments are shown in Figure 5.1. As the methane conversion increased, the eV per molecule of methane converted increased. The oxygen conversion, like the methane conversion, also increased and, therefore, the partial pressure of oxygen down the length of the reactor decreased. Figure 5.1 shows that methane conversions of 44% or greater had corresponding oxygen conversions of 100%. At these higher methane conversions, methanol production is completely shut off in the latter stages of the reactor and methane coupling forming ethane is the predominant reaction occurring. Our previous work has shown that when going from a pure methane feed to a 3:1 methane-oxygen feed, in which both experiments are done at 16 kV and 200 Hz with a 1 minute residence time, the methane conversion rate (*MCR*), as defined below, increased by a factor of 3.[5]

MCR = *CH₄ molar flowrate entering reactor* – *CH₄ molar flowrate exiting reactor*

This indicates active species generated by O_2 significantly enhance the methane reaction rate, resulting in an increase in the methane conversion rate. In addition, Bhatnagar showed that increasing the partial pressure of oxygen in a methane-oxygen

Figure 5.1: % CH$_4$ & O$_2$ Conversion vs. Energy Efficiency
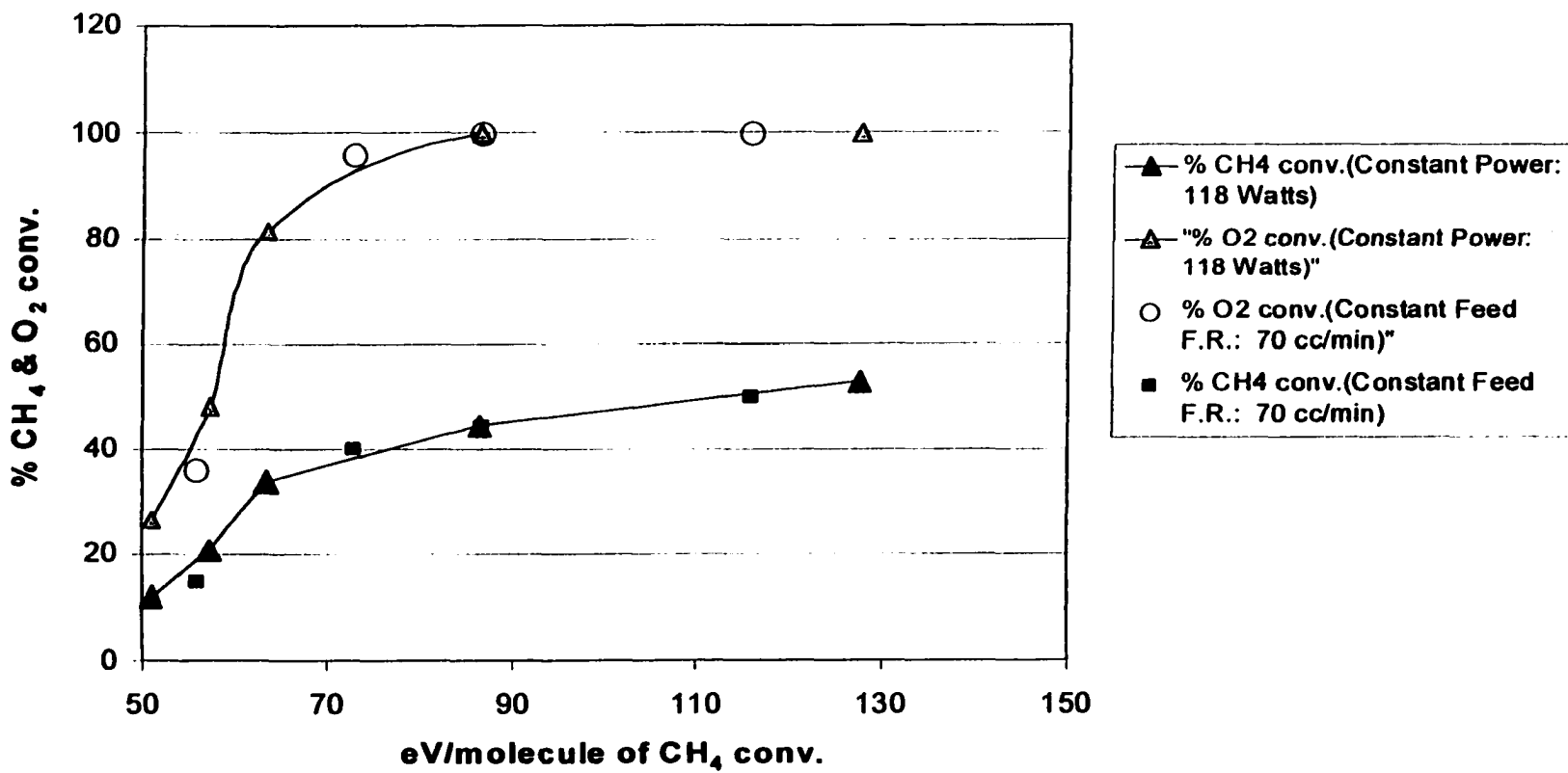
feed for a silent DBD reactor, while keeping the residence time and voltage input constant, also resulted in an increase in the methane conversion rate.[3,4] This means the methane reaction rate increased. Thus, lower partial pressures of oxygen in the reaction zone, due to increases in oxygen conversion, lead to decreases in energy efficiency for methane conversion, as shown in Figure 5.1.

Figure 5.1 also shows that varying the power while holding the flow rate constant or vice versa produces the same energy efficiency. Thus, when holding the feed composition, gap distance, and system pressure constant, the partial pressure of oxygen is the key variable affecting the energy efficiency of the system.

Eliasson and Kogelshatz's group, in contrast, has shown that better energy efficiency at higher conversions is obtained by higher power inputs at constant flow rates, as opposed to lower flow rates at constant power inputs.[1] These results, however, were obtained at a significantly higher power input range, 100 to 800 W, which may suggest that, at some point, power input per surface area may significantly affect energy efficiency.

Finally, the active oxygen species responsible for the increased energy efficiency for methane conversion could be atomic oxygen, since it has been shown that a significant amount of the energy input into a DBD *ozone* reactor is directed

toward the oxygen dissociation reaction, shown below:[9]

$$O_2 \rightarrow O + O$$
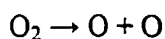
The atomic oxygen could then activate methane and form CO_x or organic oxygenate liquids.

5.3.2 Hydrogen Experiments

Previous work[6, 7] has shown that the water-gas shift reaction and reverse water-gas shift reaction, shown below, are taking place in the partial oxidation of methane in a silent electric discharge reactor:

$$CO + H_2O \rightarrow CO_2 + H_2$$

$$CO_2 + H_2 \rightarrow CO + H_2O$$
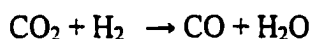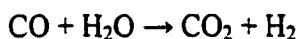
This series of experiments examines the role these reactions play when methane, oxygen, and hydrogen are fed to the silent electric discharge reactor. The power and frequency in these experiments are set at 118 watts and 174 Hz , respectively. The methane:oxygen feed ratio is kept constant at 2:1 and the total feed flow rate is 125 cc/min. The temperature in the water jacket is 75 °C and the system pressure is 1 atm. The hydrogen mole percent in the feed is varied from 0 to 40 percent.

Table 5.2 shows the results of increasing the partial pressure of hydrogen in a methane-oxygen-hydrogen feed stream in which the methane-oxygen ratio is 2:1.

104

The results show that, when going from 0 to 40 mole percent H_2 in the feed stream, the selectivity of CO remained relatively constant, while the selectivity of CO_2 increased from 38 % to 47%. In both experiments in which hydrogen was in the feed, the net rate of hydrogen creation was less than the net rate of hydrogen destruction. This suggests that hydrogen primarily reacts with oxygen and forms water and the water-gas shift reaction is secondary. Since hydrogen is a reactant it cannot be looked upon as a diluent. A possible reason why the CO selectivity does not significantly change is that less O_2 in the feed may favor partial oxidation of the organic oxygenates to CO instead of complete over-oxidation to CO_2. Thus, CO destruction from the water-gas shift reaction is approximately balanced by CO production from the partial oxidation of organic oxygenates, as shown below:

$$CO + H_2O \rightarrow CO_2 + H_2$$

Organic Oxygenates $\rightarrow$ CO + non-carbon species
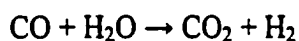
The eV per molecule of methane converted increased 44% when going from no hydrogen in the feed to 40 mole percent hydrogen in the feed. This happens for two reasons. As the hydrogen partial pressure is increased in the feed, the oxygen partial

Table 5.2: Hydrogen Experimental Results

Power = 118 W, Freq.= 174 Hz, Residence Time = 1.1 min., Water Temp. in Water Jacket = 75 °C															
Feed Mole Fraction			Moles of CH_4 conv.	eV/molecule of CH_4	$H_{2(product)}/H_{2(Feed)}$	Mole %	Mole %	% C Selectivity (mole Basis)							
CH_4	O_2	H_2	(moles/min)	conv.		CH_4 conv.	O_2 conv.	CO_2	CO	Ethane	M	MF	FA	F	Sum
0.67	0.33	0.00	0.0008	88		29	81	38	42	2	9	2	0	0	93
0.53	0.27	0.20	0.0007	111	0.98	28	91	43	41	2	9	1	0	0	96
0.40	0.20	0.40	0.0005	156	0.87	27	100	47	40	3	6	0	0	0	96
M = Methanol, MF = Methyl Formate, FA = Formic Acid, F = Formaldehyde, Sum = Sum of Carbon Selectivity															

pressure is decreased, which means the average partial pressure of oxygen down the length of the reactor is lower and the resulting lower methane activation rate lowers the energy efficiency for methane conversion. Secondly, as the partial pressure of hydrogen is increased in the reaction zone, the probability of oxygen reacting with hydrogen, as opposed to methane, increased. Increasing the partial pressure of hydrogen to 40 mole percent also reduced the production of organic oxygenates, shown by the 70% decrease in the organic oxygenate products that were produced. Finally, the increase in hydrogen in the feed caused only a slight decrease in the fractional methane conversion, but due to the decreased partial pressure of methane, the methane reaction rate decreased.

5.3.3 "Staged" Reactors in Series Experiments

The next type of experiment is referred to as a "staged" experiment. The purpose is to emulate reactors in series with oxygen addition to each reactor to bring the methane-oxygen ratio back to a set value so that an oxygen depleted condition does not occur. This is accomplished by doing single reactor experiments in which the feed is adjusted to reflect the composition of the effluent of a reactor that would precede it, with liquid products removed and oxygen added to achieve the desired methane-oxygen ratio. Note that because carbon oxides and hydrogen are produced, they remain in the feed to the next "downstream" reactor. The composition of the feed to a "downstream" reactor experiment, thus, consists of methane, oxygen, carbon monoxide, carbon dioxide, and hydrogen. The very small amount of ethane produced

under these conditions is neglected. The first experiment, which represents the first reactor in series, has a $CH_4:O_2$ feed ratio of 2:1 and a feed flow rate of 225 cc/min. Experimentally emulating the second reactor in series is done by making the feed stream of the second experiment the same as the gas product stream of the first experiment and adding oxygen to it so that the $CH_4:O_2$ ratio is 2:1. The third experiment represents the final reactor in the series. The feed stream of the third experiment is adjusted to the composition of the gas product stream of the second experiment, and oxygen is added to the feed in order for the $CH_4:O_2$ ratio to be 2:1. In all of these experiments, the frequency and power are kept constant at 174 Hz and 118 watts, respectively.

Tables 5.3 and 5.4 show the conditions and results of the "staged"-reactors-in-series experiments. The results show that when going from stage one to stage three, the individual methane conversion for a given stage went from 21% to 30%, making the overall methane conversion 59%. The *molar rate* of methane conversion, however, decreased 19%. That indicates that the increase in overall methane conversion does not compensate for the decrease in methane throughput (partial pressure) in stages two and three. Thus, the energy efficiency decreased 19% when going from stage one to three.

Table 5.3: "Staged" Reactors in Series Experimental Results

Stage	Feed mole fraction					Residence time (sec)	CH$_4$:O$_2$	eV per molecule of CH$_4$ conv.	Moles of CH$_4$ conv. (moles/min)	Mole % CH$_4$ conv.	Mole % O$_2$ conv.	H$_2$/CO	H2/CO$_2$	H$_2$ Sel.
	CH$_4$	O$_2$	H$_2$	CO$_2$	CO									
1	0.67	0.33	0.00	0.00	0.00	38	2:1	57	0.0013	21	48	1.3	1.5	12
2	0.60	0.30	0.04	0.03	0.03	49	2:1	60	0.0012	26	61	2.0	1.1	9
3	0.53	0.27	0.08	0.06	0.05	52	2:1	70	0.0010	30	75	1.3	0.6	7

Power = 118 W, Freq.= 174 Hz, Water Temp. in Water Jacket = 28 °C

Table 5.4: "Staged" Reactors in Series Experimental Results

St	Feed mole fraction					% C Selectivity (mole Basis)							
	CH$_4$	O$_2$	H$_2$	CO$_2$	CO	CO$_2$	CO	E	M	MF	FA	F	S
1	0.67	0.33	0.00	0.00	0.00	16	18	2	17	9	25	15	102
2	0.60	0.30	0.04	0.03	0.03	18	10	2	14	8	21	17	90
3	0.53	0.27	0.08	0.06	0.05	22	10	3	10	11	14	13	83

Power = 118 W, Freq.= 174 Hz, Water Temp. in Water Jacket = 28 °C.

St = Stage, E = Ethane, M = Methanol, MF = Methyl Formate, FA = Formic Acid, F = Formaldehyde, S = Sum of Carbon Selectivity

This decrease in energy efficiency occurs for two reasons. The first reason is that methane is being converted to other carbon products when in the reaction zone of a given stage and, therefore, the methane throughput for the next stage is smaller. This means the oxygen feed partial pressure is less than if it were fresh feed, meaning less active oxygen species being generated to enhance the methane reaction rate.

The second reason for decreased energy efficiency is that as the partial pressure of carbon monoxide, carbon dioxide, and hydrogen build up from one stage to the next, the probability of oxygen reacting with methane decreases. However, since carbon monoxide, carbon dioxide, and hydrogen can react with other gas species in the reaction zone, they cannot be looked upon only as diluents. The results also show that the oxygen conversion increased 36% because the residence time increased 27% from stage one to stage three as the flow rate decreased. Thus, oxygen has more time to be converted when going from one stage to the next. Furthermore, the results showed that the CO selectivity decreased by 44% while the CO_2 selectivity increased 27% when going from stage one to stage three. The 44% drop in CO selectivity is a result of the CO formed in previous stages being over-oxidized to CO_2. Finally, there was a 30% decrease in the molar rate of organic oxygenate species production from stage one to three because there was less oxygen and methane in stage three available to form organic oxygenate species. However, the overall organic oxygenate yield of this system was 35%. This is significant because, although there has been much research done in the area of methane conversion, the

yields to organic liquid products, like methanol, have not been that high in one-step processes.[10-12]

5.3.4 Recycle Experiments

The next experiments examine the changes that occur in the partial oxidation of methane when recycle operation at a high recycle ratio is used with a short per-pass residence time. The first experiment of this series has a $CH_4:O_2$ feed ratio of 2.5:1 and a feed flow rate of 40 cc/min *to the system*. The power and frequency are set at 118 watts and 174 Hz, respectively. The system pressure is 1 atm and the water temperature in the water jacket is 28 °C. This experiment has no recycle stream. The second experiment is identical to the first, except a pump is placed downstream of the liquid traps. The liquid traps, that condense the organic oxygenates, are directly downstream of the reactor outlet. The pump recycles 3590 cc/min of gas product stream. This recycle stream then combines with the 40 cc/min 2.5:1 $CH_4:O_2$ system feed stream, and the combined stream is then fed to the reactor. These conditions give a "per pass" residence time of 2.3 seconds. A gas stream purge, located after the traps, flows to the Carle GC for analysis.

Table 5.5 compares the partial oxidation of methane occurring in the silent electric discharge reactor both with and without recycle. The methane conversion showed little change when comparing the recycle with the non-recycle experiment,

111

Table 5.5: Recycle Experimental Results

Power = 118 W, Freq. = 174 Hz, Water Temp. in Water Jacket = 28 °C, $CH_4:O_2$ Flow Rate Input Ratio = 2.5:1																			
Recycle Ratio	Moles of CH_4 Conv. (moles/min)	eV per m. of CH_4 conv.	Mole % CH_4 conv.	Mole % CH_4 conv. per pass	Mole % O_2 conv.	H_2/CO	$H2/CO_2$	H_2 Sel.	% C Selectivity (mole Basis)										
									CO_2	CO	E	Pr	n-B	M	MF	FA	F	El	Sum
0	.0005	138	46	46	100	2.9	4.4	28	13	19	13	3	1	6	8	19	11	1	94
160	.0006	129	49	.6	100	2.9	2.2	16	15	11	4	0	0	17	5	12	10	7	81
E = Ethane, Pr = Propane, n-B = n-Butane, M = Methanol, MF = Methyl Formate, FA = Formic Acid, F = Formaldehyde, El = Ethanol, Sum = Sum of Carbon Selectivity																			

despite better gas mixing in the recycle experiment. In both experiments the oxygen conversion was 100 %, but the non-recycle experiment was 69% higher in ethane selectivity when compared to the recycle experiment. In addition, the non-recycle experiment had a 4% overall selectivity for propane and n-butane, while the recycle experiment showed no selectivity toward these compounds. The reason for these differences is that the high recycle ratio in the recycle experiment causes the gases within the reactor to be well mixed and, therefore, increases the probability of ethane reacting with oxygen and forming ethanol. This can be seen in the ethanol selectivity: 1% in the non-recycle experiment compared to 7% in the recycle experiment. In the non-recycle experiment, however, the gases within the reactor are near plug flow conditions. Thus, as the ethane partial pressure increased to a significant amount, the oxygen partial pressure was already extremely limited or zero. This meant ethane reacted with ethane and methane molecules to form n-butane and propane, respectively. This chain building behavior has been studied by Caldwell et al.[7] Finally, the sum of organic oxygenate products was 12% higher, while the CO_x selectivity was 19% lower in the recycle experiment. Since, the methane conversion per pass in the recycle experiment was only 0.6%, due to very low residence times per pass, the low partial pressures of the organic oxygenate species did not permit these products to be condensed in the reactor at 28 °C, but they were able to condense in the liquid trap at −55 °C. Thus, using a recycle at high recycle ratios with a low temperature liquid trap minimizes the organic oxygenates' chances of becoming over-oxidized, and, therefore, increases their yield while decreasing CO_x production.

Finally, even at the high recycle ratio, the CO_x selectivity was still 26%. This, therefore, suggests there is a parallel direct oxidative pathway between CH_4 and CO_x.

5.3.5 Nitrogen Experiments

The next series of experiments examines the effect of nitrogen on the partial oxidation of methane in the DBD reactor. In all of these experiments, the total feed flow rate is 430 cc/min to give a residence time of 20 seconds and the $CH_4:O_2$ feed ratio is kept constant at 2:1. The power and frequency are set at 118 watts and 174 Hz, respectively. The water temperature in the water jacket is 28 ^{o}C and the system pressure is 1 atm. The mole percent of nitrogen in the feed is varied from 0 to 40 percent.

Tables 5.6 and 5.7 show the results of the methane-oxygen-nitrogen experiments. The results show that as the $N_2:O_2$ ratio went from 0:1 to 2:1, the rate of methane converted went from .0014 moles/min to .0011 moles/min, which in turn caused the energy efficiency to decrease 23%. This occurred because N_2 was acting as a diluent since it was virtually non-reactive in the reaction zone. The CO and CO_2 selectivities increased 27% and 28%, respectively when going from a $N_2:O_2$ ratio of 0:1 to 2:1, although the organic oxygenate liquid sum does not decrease, as would be expected with over-oxidation of these products.

Table 5.6: Nitrogen Experimental Results

Power = 118 Watts, Freq. = 174 Hz, Water Temp. in Water Jacket = 28 °C, Residence Time = 20 sec.								
Feed Mole Fraction		N_2: O_2	Moles of CH_4 conv. (moles/min)	eV per m. of CH_4 conv.	Mol % CH_4 conv.	Mol% O_2 conv.	H_2/CO	H2/CO2
Mole% CH_4+O_2 (CH_4:O_2 = 2:1)	Mole % N_2							
100	0	0	0.0014	51	12	26	1.1	1.6
90	10	0.3	0.0014	52	13	29	1.2	1.5
80	20	0.8	0.0012	63	12	24	1.1	1.5
70	30	1.3	0.0010	70	13	33	1.0	1.5
60	40	2	0.0011	66	16	39	1.1	1.5

Table 5.7: Nitrogen Experimental Results

Power = 118 Watts, Freq. = 174 Hz, Water Temp. in Water Jacket = 28 °C, Residence Time = 20 sec.										
Feed Mole Fraction		% C Selectivity (mole Basis)								
Mole% CH_4+O_2 (CH_4:O_2 = 2:1)	Mole% N_2	CO_2	CO	E	M	MF	FA	F	Org. liq. Sum	Sum
100	0	13	19	2	16	9	17	12	54	88
90	10	16	20	2	11	17	14	9	51	89
80	20	17	23	2	14	19	19	12	64	106
70	30	18	27	2	11	12	19	11	53	100
60	40	18	26	2	10	12	20	9	51	97
E = Ethane, M = Methanol, MF = Methyl Formate, FA = Formic Acid, F = Formaldehyde, Sum = Sum of Carbon Selectivity										

5.3.6 Methane-Ethane-Oxygen Experiments

The final series of experiments examines methane-ethane-oxygen systems. In all but one of the experiments, the hydrocarbon to oxygen feed ratio is 2:1. The one exception is the experiment that has only ethane and a $C_2H_6 : O_2$ feed ratio of 1.8:1. All of the experiments have a total feed flow rate of 430 cc/min. The power and frequency are kept at 118 watts and 174 Hz, respectively. The water temperature in the water jacket in all the experiments is 28 °C. In these experiments, the $CH_4:C_2H_6$ feed ratio is varied from 14.6:1 to 1:1. Three other experiments consist of a methane-oxygen experiment with a $CH_4:O_2$ feed ratio of 2:1, an ethane-oxygen experiment with a $C_2H_6:O_2$ feed ratio of 2:1, and an ethane-oxygen experiment with a $C_2H_6:O_2$ feed ratio of 1.8:1.

Table 5.8 shows the methane-ethane-oxygen experimental results. The results show, compared to the 2:1 $CH_4:O_2$ feed, that the energy efficiency increased 49% for 2:1 $C_2H_6:O_2$ feed. While their conversions are the same, for every mole of ethane reacting, 2 moles of carbon are converted, while for each mole of methane reacting, only one mole of carbon is converted. This result shows that even though the bond energy in a carbon-carbon bond in ethane is 16% less than the carbon-hydrogen bond in methane, the ethane conversion is not enhanced compared to the methane conversion. The energy efficiency for the ethane-oxygen system was further

Table 5.8: Methane-Ethane-Oxygen Experimental Results

Power = 118 W, Freq. = 174 Hz, Residence Time = 20 sec., Water Temp. in Water Jacket = 28 °C																
Feed Mole Fraction			Moles of C conv. (moles/min)	eV per atom of C conv.	Mole % CH_3CH_3 conv.	Mole % CH_4 conv.	Mole % O_2 conv.	% C Selectivity (mole Basis)								
CH_4	E	O_2						CO_2	CO	E	M	MF	FA	F	El	Sum*
.67	0.00	.33	.0014	51	0	12	26	13	19	2	16	9	17	12	0	88
.64	.04	.31	.0018	41	36	11	30	13	14		13	5	14	12	3	74
.47	.20	.33	.0026	28	25	10	31	10	9		8	3	9	10	6	55
.33	.33	.33	.0025	29	19	6	30	9	9		8	3	11	11	10	61
0.00	.67	.33	.0028	26	12	0	26	8	8		5	2	7	8	13	51
0.00	.64	.36	.0032	23	14	0	27	8	6		5	1	8	8	13	49

E = Ethane, M = Methanol, MF = Methyl Formate, FA = Formic Acid, F = Formaldehyde, El = Ethanol, Sum* = Sum of Carbon Selectivity (Acetaldehyde, ethyl formate, and acetic acid have been detected but not quantified. They account for 33% of the total TCD GC area count of the organic oxygenate products for the 2:1 ethane-oxygen system.)

increased by 12% by lowering the 2:1 $C_2H_6:O_2$ ratio to 1.8:1. This is also due to the enhancement of the reaction rate by oxygen.

The liquid selectivities of quantified organic oxygenate liquid compounds decreased when going from a 2:1 $CH_4:O_2$ feed to a 2:1 $C_2H_6:O_2$ feed. The exception to this trend was ethanol's selectivity, which increased and can account for 9% to 13% of the ethane reacted. Three identified (acetaldehyde, ethyl formate, and acetic acid) but not quantified organic oxygenate liquid products also substantially increased in selectivity when ethane partial pressure increased in the feed. This was determined by the fact that their integrated *areas* on the Varian GC analysis increased with increasing partial pressure of ethane. The sum of these three products' *areas* accounted for 33% of the total organic liquid *area* in the 2:1 ethane-oxygen experiment. Evidently, ethane is reacting with oxygen and forming C_2 and C_2+ (ethyl formate) organic oxygenate species.

The CO_x selectivity decreased 50% when going from a 2:1 $CH_4:O_2$ feed stream to a 2:1 $C_2H_6:O_2$ feed stream. The reason for this decrease in CO_x is uncertain. Potentially, this is because of the fact that the additional organic oxygenates that formed due to ethane chemistry (ethanol, acetaldehyde, ethyl formate, and acetic acid) have higher dew points than their corresponding organic oxygenate counterparts that are traditionally formed due to methane chemistry (methanol, formaldehyde, methyl formate, and formic acid). Thus, the fraction of organic

118

oxygenates in the liquid phase might be higher which decreases the chances of over-oxidation. Ethane-oxygen experiments at a high recycle ratio might also give further insight into whether there is a direct oxidative pathway from ethane to CO_x, and how significant it is. At this point with the present experiments it is difficult to determine what relationship exists between methane and ethane in the methane-ethane-oxygen experiments since the observed methane-ethane conversions might not accurately represent the actual conversions because of interconversion between the two.[7]

5.4 Conclusions

Previous work has shown that decreasing the oxygen partial pressure in a methane-oxygen feed for a silent electric discharge reactor decreased the methane conversion rate.[3] With this in mind, the "energy efficiency" experimental results of this work showed that when the gap distance, methane-oxygen feed ratio, and system pressure were fixed in the partial oxidation of methane in a silent electric discharge reactor, the energy efficiency of the system was determined by the partial pressure of oxygen within the reactor.

The "hydrogen" experimental results showed that increasing the partial pressure of hydrogen in a methane-oxygen-hydrogen experiment increased the CO_2 selectivity with little change in the CO selectivity. In addition, the net rate of hydrogen destruction was greater than the net rate of hydrogen creation. This

indicates that hydrogen was reacting with oxygen to form water and the water-gas shift reaction was a secondary reaction.

The energy efficiency of methane-oxygen-hydrogen systems as well as methane-oxygen-nitrogen systems were affected by both the partial pressure of hydrogen (or nitrogen) and the partial pressure of oxygen when the methane oxygen feed ratio was fixed. Increasing the hydrogen (or nitrogen) partial pressure in the feed decreased the probability of methane colliding with and then reacting with an active oxygen species. In the case of hydrogen, the probability was even further decreased because hydrogen was evidently reacting with oxygen and forming water. The "staged-reactors-in-series" experimental results showed that decreasing the partial pressures of oxygen and methane and increasing the partial pressures of CO, CO_2, and H_2 in the feed decreases the energy efficiency and organic oxygenate production.

The "recycle" experimental results showed that organic oxygenate liquid production can be enhanced while minimizing CO_x production through use of high recycle ratios. In addition, CO and CO_2 were still present in the high recycle ratio experiment, suggesting a direct oxidation pathway from CH_4 to CO and CO_2.

Replacing methane with ethane in an oxygen-rich feed stream did not show an increase in conversion in ethane, but the eV per atom of carbon converted is about halved.

The current large-scale industrial process for methanol production, steam reforming of methane to synthesis gas and then methanol synthesis, requires about 11 eV per molecule of methanol produced.[13] However, at a remote natural gas site the efficiency of this process would probably be lower because the plant size would have to be scaled down due to the limited gas reserves. The best result obtained in this work is 51 eV per molecule of methane converted with a 13% selectivity of CO_2. Thus, the system consumes 59 eV per molecule of usable carbon products, which is less efficient than the industrial methanol synthesis process. However, this might not represent the true difference between the two processes because they are scaled to different sizes (Large industrial scale vs bench scale). Both processes would have to be of similar scale in order to make a fair comparison.

High methane conversion can be obtained in the silent electric discharge reactor, but at the expense of energy efficiency. This problem can be lessened by having "staged" reactors in series with intermediate oxygen addition, which allowed high methane conversions with better energy efficiency. In fact, the "staged" experiments also produced a 35% liquid oxygenate *yield*, the best results to date.

5.5 Literature Cited

(1)   Zhou, L.M., Xue, B., Kogelschatz; U., Eliasson, B.; "Partial Oxidation of Methane to Methanol with Oxygen or Air in a Nonequilibrium Discharge Plasma," Plasma Chemistry and Plasma Processing, Vol. 18, No. 3 , 1998, 375-393

(2) Yao, S., Takemoto, T., Ouyang, F., Nakayama, A., Suzuki, E.; "Selective Oxidation of Methane Using a Non-Thermal Pulsed Plasma," Energy & Fuels, Vol. 14, No.2, 2000, 459-463

(3)   Bhatnagar, Rajat, Mallinson, R.G.; "Methane Conversion in AC Electric Discharges at Ambient Conditions," Methane and Alkane Conversion Chemistry, Plenium Press 1995, 249-264

(4)   Bhatnagar, Rajat, M.S. thesis, "A Study of the Partial Oxidation of Methane Under the Influence of an AC Electric Discharge," University of Oklahoma, 1993

(5) Larkin, D.W., Caldwell, T.A., Lobban, L.L., Mallinson, R.G.; "Oxygen Pathways and Carbon Dioxide Utilization in Methane Partial Oxidation in Ambient Temperature Electric Discharges," Energy & Fuels, Vol. 12, No. 4, 1998, 740-744

(6) Larkin, D.W., Leethochawalit, S., Caldwell, T.A., Lobban, L.L., Mallinson, R.G.; "Carbon Pathways, CO_2 Utilizaton, and *In Situ* Product Removal in Low Temperature Plasma Methane Conversion to Methanol," Greenhouse Gas Control Technologies, Elsevier Science Ltd., 1999, 397-402

(7) Caldwell, T.A., Poonphatanaricha, P., Chavadej, S., Mallinson, R.G., Lobban, L.L., Third-Body Enhanced Methane Conversion In a Dielectric-Barrier Discharge Reactor," *ACS National Meeting*, August, 1998, Boston, MA

(8) McMurry, John Organic Chemistry 2nd Edition. Brooks/Cole Publishing Company, 1988

(9) Eliasson, B., Egli, W., Kogelschatz, U.; "Modeling of Dielectric Barrier Discharge Chemistry," Pure & Appl. Chem., Vol. 66, No. 6, 1994, 1275-1286

(10) Hunter, N.R., Gesser, H.D., Morton, L.A., Yarlagadda, P.S.; "Methanol Formation at High Pressure," Appl. Catal., Vol. 57, 1990, 45-54

(11) Rytz, D.W. and Baiker, A.; "Partial Oxidation of Methane to Methanol in a Flow Reactor at Elevated Pressure," Ind. Eng. Chem. Res., Vol. 30, 1991, 2287-2292

(12) Foulds, G.A., Gray, B.F.; "Homogeneous Gas-Phase Partial Oxidation of Methane to Methanol and Formaldehyde," Fuel Processing Technology, Vol 42, 1995, 129-150

(13) Rostrup-Nielson, Jens R. Catalysis and Large-Scale Conversion of Natural Gas. Catalysis Today, Vol. 21, 1994, 257-267

CHAPTER SIX: Organic Oxygenate Pathways from Partial Oxidation of

Methane in a Silent Electric Discharge Reactor

6.1 Abstract

This study of methane conversion involves the use of a glass dielectric interposed between metal electrodes, and applies kilovolt AC voltage and 118 watts power with frequencies in the range of 173 to 264 hertz. The geometry of the system is cylindrical, with gas flowing axially in the annulus between two electrodes. The partial oxidation reactions in this configuration produce methanol, formaldehyde, formic acid, methyl formate, ethane, hydrogen, water, carbon monoxide, and carbon dioxide. The outer electrode is maintained at a low temperature (12 °C or 15 °C), allowing the organic oxygenates to condense on the plate itself inside the reactor. The results show, through residence time experiments, that methane and oxygen react to form methanol, which further reacts to form formaldehyde, methyl formate, and formic acid. Increasing the gas gap from 4.0 mm to 12.0 mm decreases the reduced electric field from 30 volts/cm/torr to18 volts/cm/torr which results in a shift in the product distribution from organic oxygenate products to ethane, ethylene, and acetylene. This is because the energy deposition directed toward oxygen dissociation decreases and the energy deposition directed toward methane and oxygen excitations increases. Finally, this work shows that increasing the pressure from one to two atmospheres with a 1.9 mm gas gap decreases the energy consumption per methane converted of the system by 35% because the feed concentration doubles, while

maintaining 46% selectivity in organic oxygenate products because the reduced electric field strength has a significant fraction of the energy directed toward oxygen dissociation under these conditions.

6.2 Introduction

The electron energy distribution in a DBD reactor can be altered by changing various system parameters (e.g., gas gap and system pressure). This in turn affects the energy deposition directed toward the various electron-gas specie collision processes. Hence, the chemistry occurring within the reaction zone can be influenced by changing the electrical properties of a gas phase system within the DBD reactor.

These electrical properties can be characterized through Bolsig, an electron Boltzmann equation by Kinema Software and CPAT.[2] This electron boltzmann solver is designed for systems that have steady-state, uniform electric fields (E) with weakly ionized gases, which is the case for a DBD system.[4] This program numerically solves for the Boltzmann Equation, shown below, which describes the electron energy distribution function (f) in terms of space (x), velocity (v), and time (t).[2,4,5]

$$\frac{\partial}{\partial t}f(x,v,t)+a\nabla_v f(x,v,t)+v\bullet\nabla_x f(x,v,t)=J[f(x,v,t)] \quad \text{(eq. 1)}$$

126

According to the presentation of Baldur Eliasson et al.[2] regarding the Boltzmann equation, the a is the acceleration term, a = (c·E)/m (c= electron charge, m = mass of electron), which is proportional to the force from the electric field (E) acting upon the electron. The term on the right hand side of the equation, $J[f(x,v,t)]$, is the collision term. It accounts for the electron energy distribution change due to collisions between electrons and gas species present in the reaction zone.[2] Therefore, this program can determine the energy deposition directed toward the various collision processes: elastic, inelastic, ionization, and attachment. Since the DBD system has a steady state, uniform electric field at high pressure (1 atm or greater), the electron energy distribution becomes simply a function of velocity. Once $f(v)$ is known, the average electron energy (e_{avg}) can be found for a given reduced electric field, as shown in the following equation:[6]

$$e_{avg} = \int_0^\infty e(v)f(v)dv \,(\text{eq. 2})$$

where $e(v) = \frac{1}{2}mv^2$

In addition, since the electron energies within the system are affected by the electric field strength and interactions with gas species present, the average electron energy can be described as a function of the reduced electric field (E/P), which is the electric field divided by the system pressure (P), at the condition of breakdown. Changes that increase the reduced electric field results in an increase in the average electron energy. The reduced electric field is also related to the breakdown strength and is a

function of breakdown voltage (V), gas gap distance (D), and system pressure($E = V/D$ and therefore $E/P = V/(D \cdot P)$). Increasing the system pressure or gas gap distance will result in a decrease in the reduced electric field and, hence, the average electron energy within the system.[2]

This work, which is a continuation of previous efforts[7-10], uses a DBD reactor to directly partially oxidize methane to organic oxygenates, such as methanol. In order to determine the effects the reduced electric field and, therefore, the average electron energy has on product selectivities, methane and oxygen conversion, and the energy consumption within the system, the gas gap distance was varied. In addition, the effects of changing the system pressure from one to two atmospheres is studied in order to determine the similarities with the results of the gap distance experiments at similar reduced electric field strengths. Further, the effect pressure has at different gap distances in regards to organic oxygenate production is also investigated.

Previous results have shown that a 3:1 methane-oxygen feed has a greater methane conversion rate than a pure methane feed (all other experimental parameters are held constant).[8] In addition, organic oxygenate products were formed only when oxygen was present in the feed. This work examines the effect that partial pressure of oxygen has on methane reaction rate, energy efficiency, and product selectivity for methane-oxygen systems at one and two atmospheres. This is done at both of these system pressures by decreasing the methane-oxygen ratio from 5:1 to 2:1.

Finally, this study conducts residence time experiments in a DBD reactor. These experiments are conducted in order to better understand the sequential and parallel product formation pathways that are occurring within the methane-oxygen system.

6.3 Experimental Section

The breakdown voltage for the annular reactor is measured using a Tektronix P6015A high voltage probe in conjunction with a Tektronix TDS 754C digital oscilloscope. The power is measured with a Microvip 1.2 Energy Analyzer on the primary side. This allows the system's energy consumption on a per molecule of methane converted basis to be determined (The energy consumption as used in this work is eV per molecule of methane converted and 1 eV/molecule of CH_4 converted = 96.4 kJ/mol = 1.67 * 10^{-3} kWh/g). As a result of measuring the power on the primary side, the energy losses from the DBD reactor, high voltage wires, and transformer are all included in the measured value. Additionally, the components (DBD reactor, high voltage wires, and transformer) have not been optimized to minimize these energy losses and, therefore, this work underestimates how energy efficient this process may be.

In order to demonstrate that the experiments performed in this work can be acceptably reproduced, Table 6.1 compares two 5:1 methane-oxygen experiments at identical conditions. The material balances (carbon molar basis) for all the experiments done in this work are close to closing (80 to 100%). Potentially, the unaccounted carbon comes from undetected products in the gas phase since no solid residue has been found within the reactor after experiments.

Table 6.1: Experimental Reproducibility

Experiment #	Moles of CH$_4$ conv. (moles/min)	eV/molecule of CH$_4$ conv.	H$_2$ sel.	Mole % CH$_4$ conv.	Mole % O$_2$ conv.	% C Selectivity (mole Basis)							
						CO$_2$	CO	Ethane	M	MF	FA	F	Sum
1	.0009	79	18	10	61	13	16	5	19	5	17	10	85
2	.0010	76	16	10	56	13	16	5	18	6	16	13	87

CH$_4$:O$_2$ feed ratio = 5:1, Gap Distance = 1.9 mm, Power = 118 W, Pressure = 1 atm, Residence Time = 29 seconds, Water Temp. in Water Jacket = 15 °C

M = Methanol, MF = Methyl Formate, FA = Formic Acid, F = Formaldehyde, Sum = Sum of Carbon Product Selectivity (mole basis)

In all the experiments, the power input was 118 watts which was sufficient to convert a significant amount of the methane. The frequency in each experiment was set such that the power factor on the low voltage side of the transformer was one. The water temperature within the water jacket for this work was set at 12 °C or 15 °C (Only the residence time experimental series had a 12 °C water temperature). Both these temperatures allowed *in situ* removal of organic oxygenates from the reaction zone, as seen in previous work[9], for experiments with residence times of 5 seconds or greater.

The first series of experiments varied the gas gap distance from 1.9 mm to 12.0 mm in order to determine how changes in the reduced electric field strength affected the results of a 2:1 methane-oxygen system. The residence time for these experiments was 1 minute and the reaction area was 688 cm^2. When changing from a gap distance of 1.9 mm to 12.0 mm, the frequency was increased from 174 Hz to 216 Hz in order to maintain the power factor at a value of 1, due to the fact that the capacitance of the system changes when the gas gap is altered.

The second series of experiments varied the system pressure from one to two atmospheres for a 2:1 methane-oxygen system with a residence time of 29 seconds in order to have methane and oxygen conversions similar to those of the gap distance experiments. This provides a comparison of product selectivities between the pressure and gap distance experimental series at similar reduced electric fields. The

pressure experimental series had a gap distance of 4.0 mm and a reaction electrode area was 688 cm^2. At one atmosphere the frequency was set at 173 Hz and at two atmospheres it was 241 Hz.

For the third series of experiments the methane-oxygen feed ratio was varied from 5:1 to 2:1 at one and two atmospheres with a gap distance of 4.0 mm, an electrode reaction area of 688 cm^2, and a residence time of 29 seconds. The frequency was 173 Hz at one atmosphere and 241 Hz at two atmospheres.

The fourth series of experiments varied system pressure from one to three atmospheres, while maintaining the gap distance at 1.9 mm and a 5:1 methane-oxygen feed ratio. This was done in order to determine the effects pressure had on a system in which a significant amount of the energy input into the system was directed toward oxygen dissociation at all system pressures as a result of the smaller gap distance (1.9 mm as opposed to 4.0 mm). The electrode reaction area for these experiments was 688 cm^2 and the residence time was 29 seconds. The frequency was adjusted to maintain the power factor at one and at one atmosphere this was 167 Hz, at two atmosphere it was 217 Hz, and at three atmospheres it was 264 Hz.

The last series of experiments varied the residence time from 2.5 to 40 seconds in order to better determine the carbon pathways occurring within the system. The reaction area for these experiments was 430 cm^2 and the frequency was 198 Hz.

Finally, Bolsig, the numerical electron boltzmann solver by Kinema Software and CPAT, was used to plot all the energy deposition graphs (energy deposition directed toward a given collision process as a function of reduced electric field strength). In addition, it was used to determine the average electron energy within methane-oxygen systems for given reduced electric field strengths.[4, 12]

6.4 Results and Discussion

As previously mentioned, altering the gas gap affects the reduced electric field of a DBD system. Table 6.2 shows how the electrical and discharge properties change when the gas gap is varied from 1.9 mm to 12.0 mm. Increasing the gas gap distance decreases the reduced electric field strength (E/P), and this results in a decrease in the average electron energy of the plasma. Decreasing the reaction zone's average electron energy in turn affects the energy deposition directed toward the various types of collision processes. Figure 6.1 shows the energy deposition for the significant collision processes as a function of reduced electric field strength (E/P) in a barrier discharge reactor for a 2:1 methane-oxygen system. The experimental operating region for this study lies within the gray region seen in this figure. Within this operating region at least 97% of the energy being input into the reaction zone is directed toward inelastic methane and oxygen collision processes. Processes such as attachment ($e + A_2 \rightarrow A_2^-$), ionization ($e + A_2 \rightarrow A_2^+ + 2e$), and elastic ($e + A_2 \rightarrow e + A_2$) collision processes are not significant in this range.

Table 6.2: Electrical Parameters

2:1 CH_4:O_2 System at 1 atmosphere				
Gap Distance (mm)	1.9	4.0	6.7	12.0
E/P (volts/cm/torr)	49.0	30.0	24.0	18.0
Average Electron Energy (eV)	5.0	4.2	4.0	3.6

Figure 6.1: Energy Deposition (Group Processes) vs. E/P (2:1 CH_4:O_2 System)
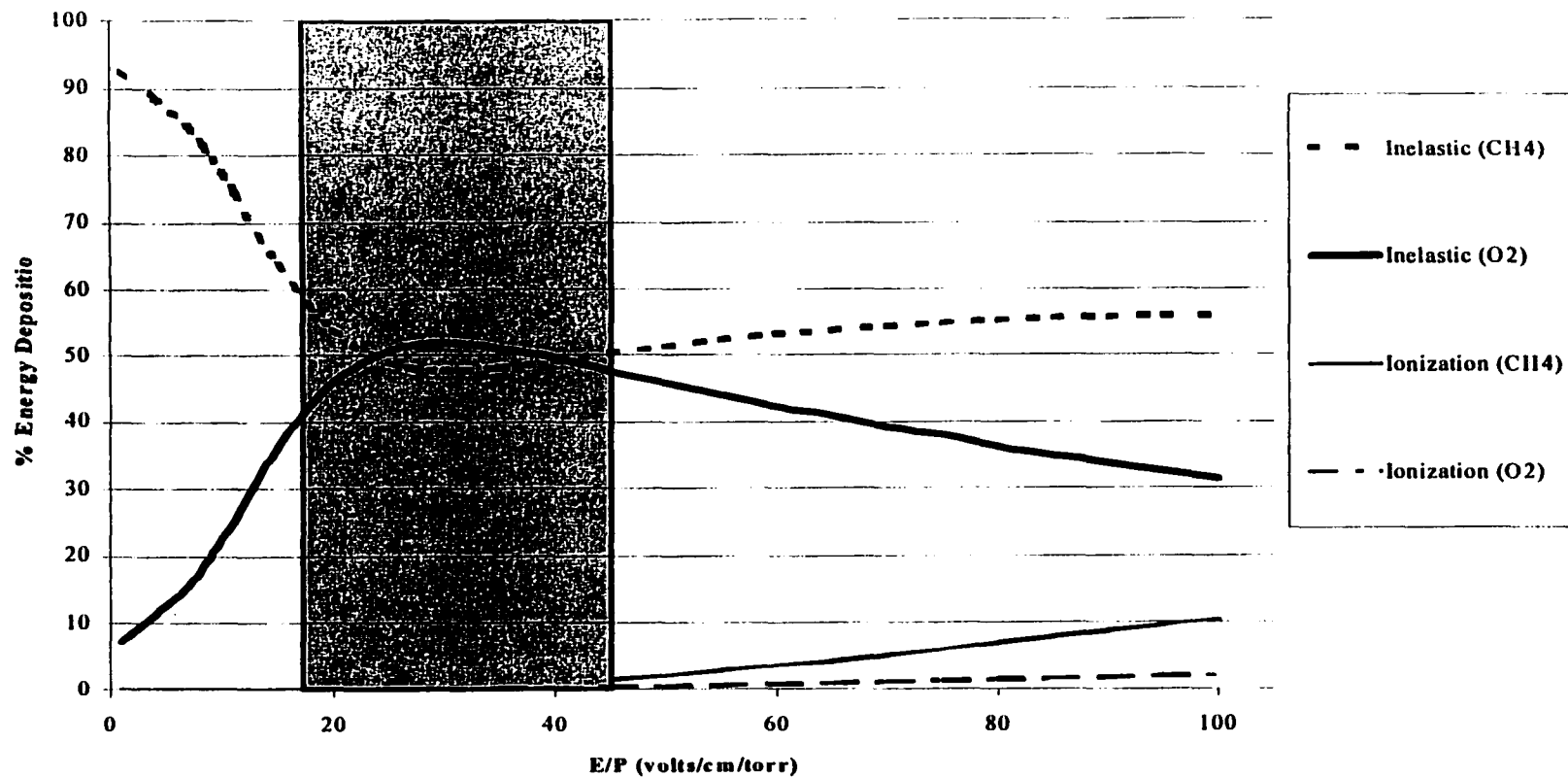
Figure 6.2 separates the energy deposition for the inelastic methane collision processes into its two primary components: methane excitation and methane dissociation. The two components have electron impact formation energy ranges of .2 to .4 eV and from 9.0 to 12.0 eV, respectively. The figure shows that, within the experimental operating region, when the reduced electric field is decreased, the energy deposition directed toward methane excitation increases while that towards methane dissociation decreases. When the reduced electric field is decreased, the average electron energies decrease and the fraction of electrons capable of dissociating methane is reduced. This also means the fraction of electrons capable of exciting, but not dissociating, methane molecules increases and the energy fraction deposited into the excitation process increases.

Figure 6.2: Energy Deposition vs. E/P (2:1 CH_4:O_2 System)
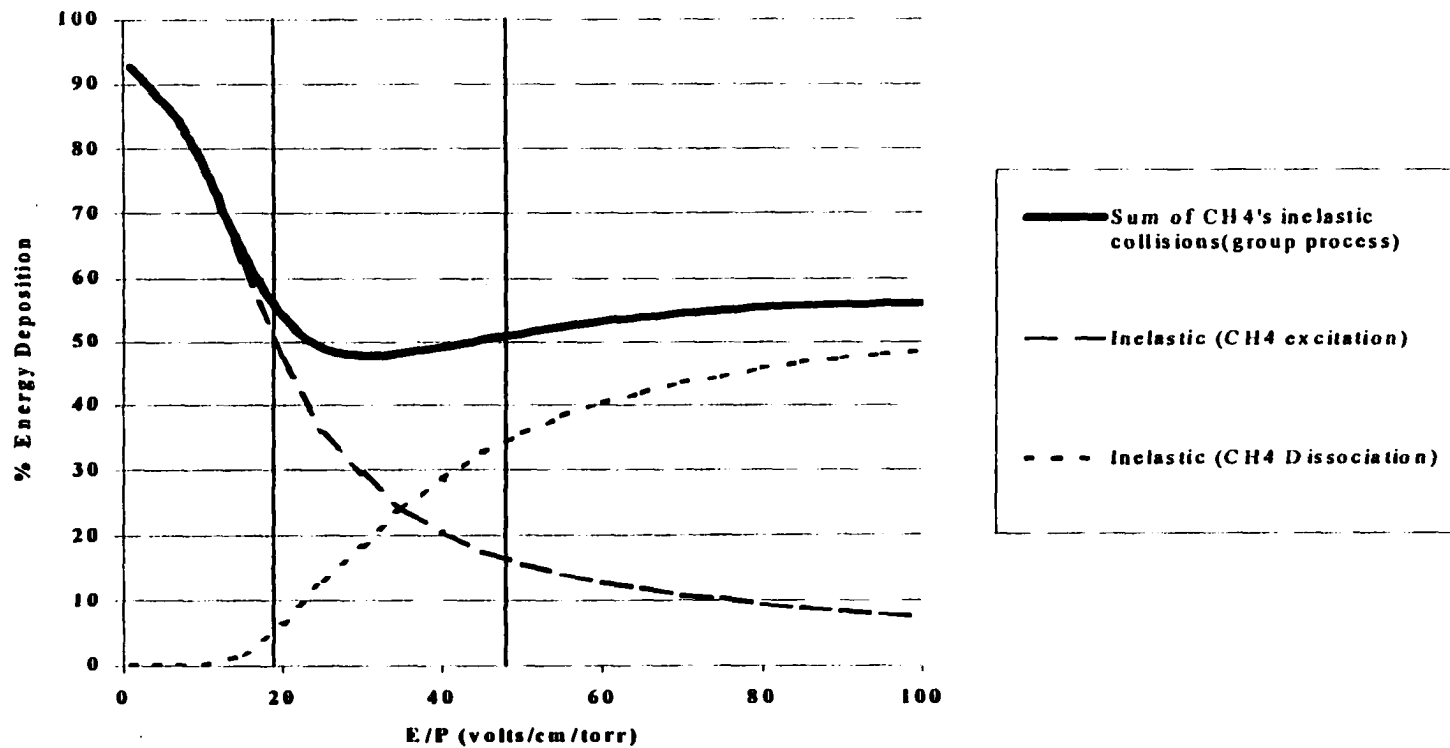
Figure 6.3 separates the energy deposition for the inelastic oxygen collision processes into its two components: oxygen excitation and oxygen dissociation. The two components have electron impact formation energy ranges of .2 to 4.0 eV and from 6.0 to 8.4 eV, respectively. Within the experimental operating region seen in this figure, a decrease in the reduced electric field strength results in an increase in the energy deposition directed toward the excitation of the oxygen molecules without dissociation. In this same range, the energy deposition directed toward oxygen dissociation remains around 40% for reduced electric field values above 30 volts/cm/torr and drops off significantly below this value. This drop-off occurs because the average electron energy decreases to the point that there is a significant reduction in the fraction of electrons having enough energy to dissociate oxygen molecules and an increasing portion of the electrons will only have enough energy to excite oxygen (and methane) molecules.

In addition to the inelastic oxygen collision processes, Figure 6.3 also shows the organic oxygenate product selectivity (organic oxygenate product selectivity = sum of organic oxygenate selectivities) as a function of reduced electric field. The results show that when going from 48 volts/cm/torr to 30 volts/cm/torr, the organic oxygenate selectivity and the energy deposition going into oxygen dissociation stay relatively constant. However, from 30 volts/cm/torr to 18 volts/cm/torr, the organic oxygenate product selectivity and the energy deposition going into oxygen dissociation both sharply decrease. Finally, the energy deposition going into oxygen

139

excitation without dissociation does not follow the organic oxygenate product selectivity trend since it increases over the entire operating range, 48 volts/cm/torr to 18 volts/cm/torr. These results suggest that an atomic oxygen species generated from oxygen dissociation is responsible for the direct partial oxidation of methane to organic oxygenate species.

Figure 6.3: Energy Deposition & Organic Oxygenate Product Selectivity vs E/P (2:1 CH_4:O_2 System, 118 Watts Power Input, 15 °C Water Jacket Temp)
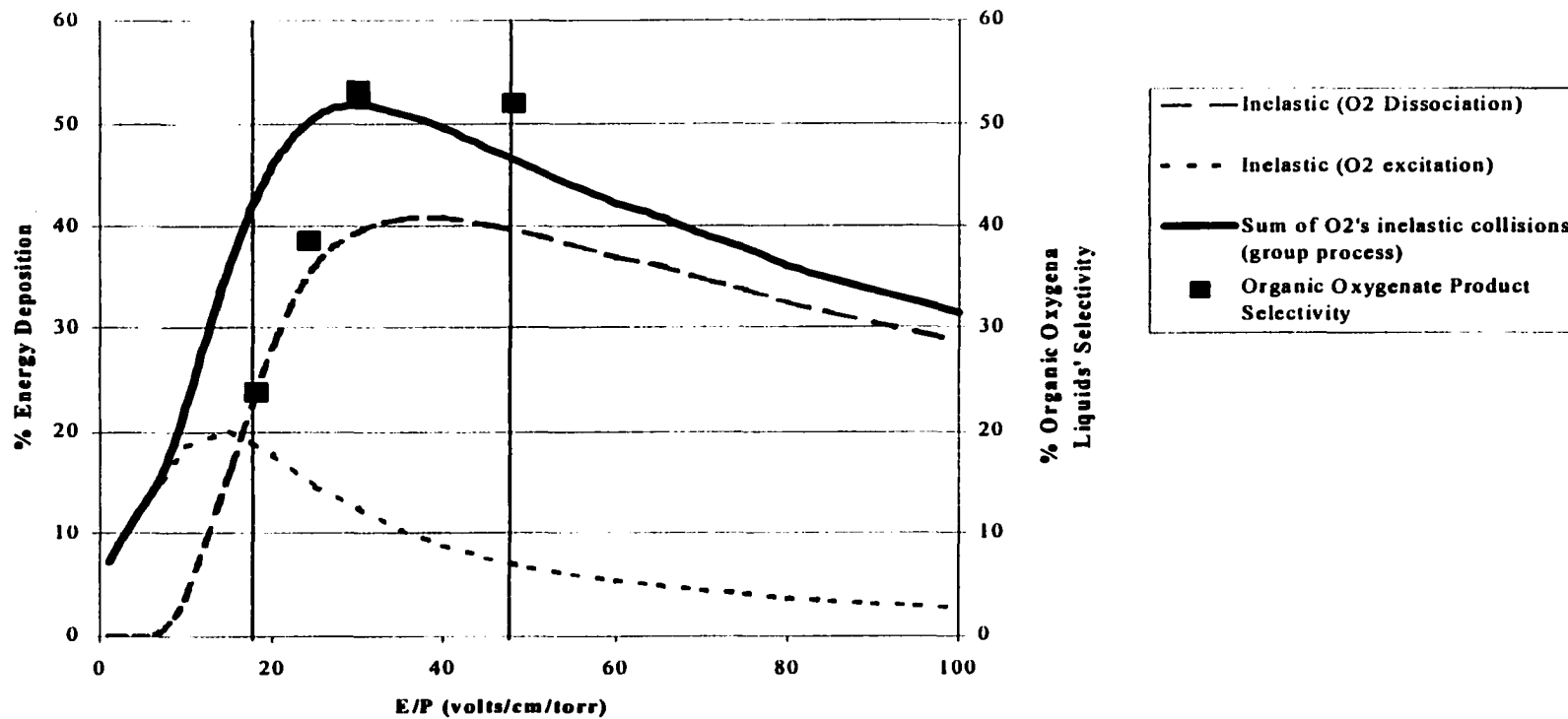
Figure 6.4 shows the CO and CO_2 selectivities for the gap distance experiments as a function of reduced electric field. In addition, the H_2 selectivity and energy deposition directed toward the two inelastic oxygen processes are included in this figure. As can be seen in the figure, the CO and CO_2 selectivities and energy deposition directed toward oxygen dissociation remain relatively constant in the range from 48 volts/cm/torr to 30 volts/cm/torr, but from 30 volts/cm/torr to 18 volts/cm/torr, the CO selectivity increases while the CO_2 selectivity decreases. Since the energy deposition directed toward oxygen dissociation decreases over this same reduced electric field range, atomic oxygen species are evidently involved in oxidation of CO to CO_2. However, as will be seen in the discussion of the pressure experiments, a high CO/CO_2 ratio can be obtained under conditions where significant O_2 dissociation does occur and this appears to be inconsistent with the above explanation. This will be discussed further in that section.

Figure 6.4: Energy Deposition, CO_x Selectivity, H_2 Selectivity vs E/P (2:1 CH_4:O_2 System, 118 Watts Power Input, 15 °C Water Jacket Temp)
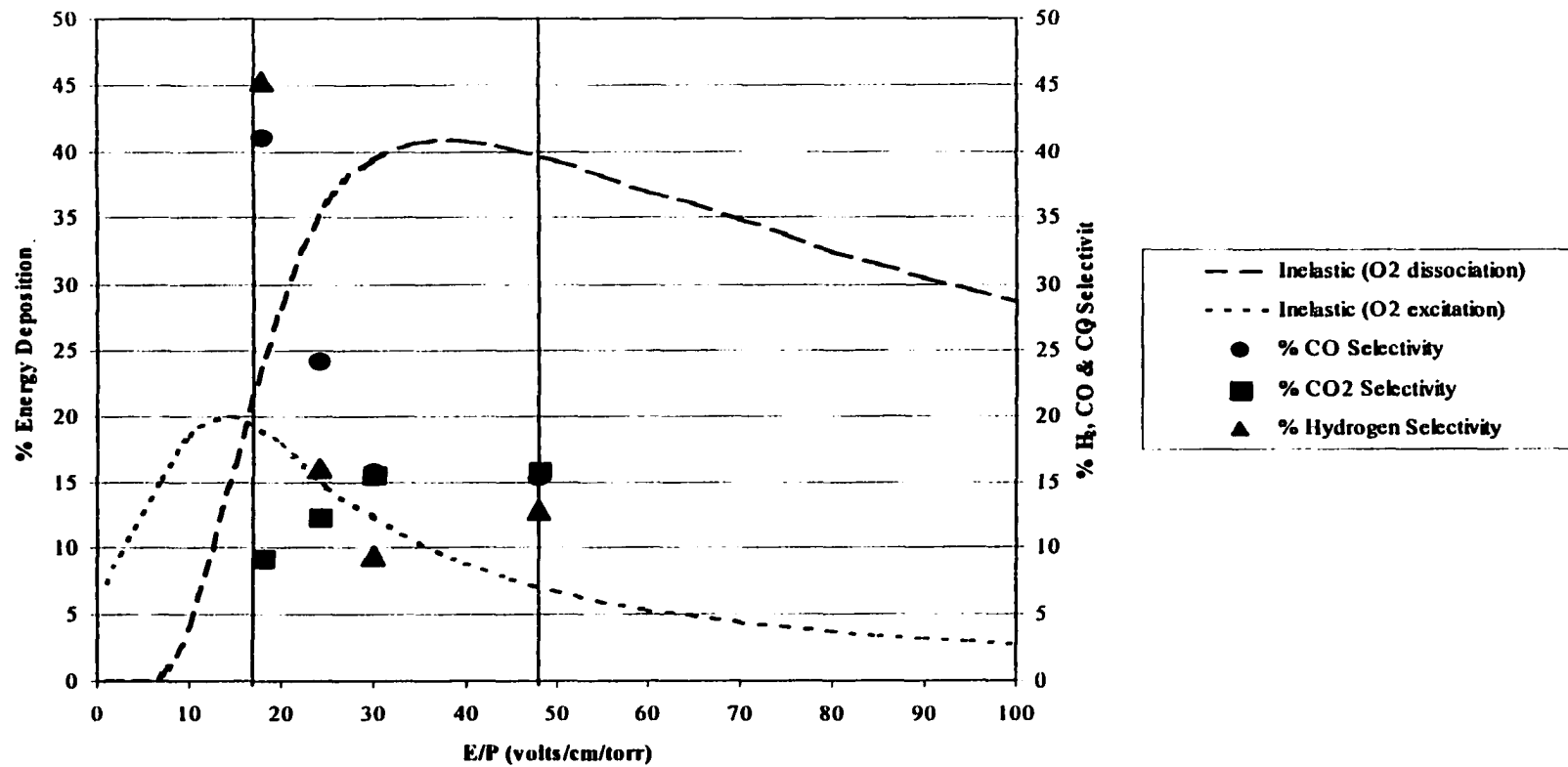
Another factor affecting the CO and CO_2 selectivities, shown in previous work, is that increasing the partial pressure of CO in a methane-carbon monoxide-oxygen system shifts the selectivity between CO and CO_2 via the water-gas shift pathway.[8] In the range where the CO selectivity is higher, the hydrogen selectivity (and partial pressure) is also increasing, also shown in Figure 6.4. In addition, significant *in situ* removal of water from the reaction zone via condensation occurs at these conditions over the entire range of reduced electric field. This is shown by the fact that 72% of the water exiting the 12 mm gap reactor was collected in the liquid phase. Both these factors inhibit the water-gas shift reaction and CO_2 formation from this pathway.

Finally, Figure 6.4 shows that the energy deposition directed toward the excitation of the oxygen molecules without dissociation increases over the entire operating range, and this also suggests that excited oxygen molecules are not nearly as effective at oxidizing CO to CO_2 and are not significantly involved in direct oxidation of other species to CO_2.

Figure 6.5 shows the gap distance experiments for C_2 hydrocarbon selectivity (sum of acetylene, ethylene, and ethane), the energy deposition directed toward the inelastic methane collision processes and its two components, and the two components for the inelastic oxygen collision processes, as functions of reduced electric field. Table 6.3 shows the acetylene-ethylene-ethane ratio at a given reduced

144

electric field for these experiments. The results show that when the energy deposition directed toward oxygen dissociation drops off and the energy deposition directed toward the inelastic methane collision process increases (the latter due to the increase in the energy deposition directed toward methane excitation), the C_2 hydrocarbon selectivity increases. The increased C_2 hydrocarbon selectivity is due to increases in ethane and acetylene production. Caldwell has shown in a pure methane system that, when varying the gas gap and, therefore, the reduced electric field over the same range, the product distribution is composed of ethane and hydrogen with some higher alkanes, but no ethylene of acetylene and is relatively constant.[14] Those pure methane results suggest that ethane formation in the 2:1 methane-oxygen system at the lower reduced electric field strengths (where oxygen dissociation is not significant) comes from methane coupling from direct methane activation, as diagrammed in Figure 6.6. In this range of reduced electric field, oxygen dissociation and its consumption of activated methane is not significant. Also in this same range, with oxygen, increased oxygen excitation occurs ($O_2^\bullet$) with significant acetylene selectivity. This suggests $O_2^\bullet$ involvement in the production of acetylene, as shown in Figure 6.6. Additional evidence that active molecular oxygen species are involved in C_2 hydrocarbon formation comes from the fact that methane conversion rates for the pure methane results[14] are less than the methane conversion rates in this study. Further, the $CO:CO_2$ ratio is increasing over this same reduced electric field range, which suggests that CO formation is favored over CO_2 formation, as already discussed.

At high reduced electric field strengths (E/P $\geq$ 30 volts/cm/torr) the energy deposition directed toward molecular oxygen excitation is small and, therefore, the O_2^* hydrocarbon pathway shown in Figure 6.6 is a minor one with little acetylene formation. The dissociated O^* species lead to organic oxygenate formation in part by reacting with activated methane thus reducing ethane selectivity from the ethane production pathway shown in both figures 6.6 and 6.7. In addition, previous work, as well as residence time experiments discussed later in this study, provide evidence that a direct oxidative pathway to CO and/or CO_2 exists.[10] Hence, the overall carbon pathway for the 2:1 methane-oxygen system at high reduced electric field strengths includes direct and indirect pathways for CO_x formation as well as the pathway for organic oxygenate formation , as shown in Figure 6.7.

For all reduced electric field strengths, little to no ethylene is observed and this may suggest that acetylene may be formed, as diagramed in Figure 6.6, from the coupling of two CH group species as opposed to ethane reacting sequentially to form ethylene and then acetylene since the reactions' thermodynamics suggests that this is unlikely to preferentially *not* favor ethylene. Evidence for the presence of CH groups in low temperature plasmas has been shown by M. Okumoto et al.[13], in which CH groups were detected spectroscopically in a methane-oxygen system using a pulsed DBD reactor. In addition, Caldwell [14] has shown in a DBD reactor that increasing the partial pressure of hydrogen in an ethane-hydrogen system inhibits the production of ethylene and acetylene. In contrast, these results show that acetylene selectivity

increases when hydrogen selectivity increases, and this also suggests a different pathway other than sequential dehydrogenation.

Figure 6.5: Energy Deposition & C_2 Selectivity vs. E/P (2:1 CH_4:O_2 System, 118 Watts Power Input, 15 °C Water Jacket Temp)
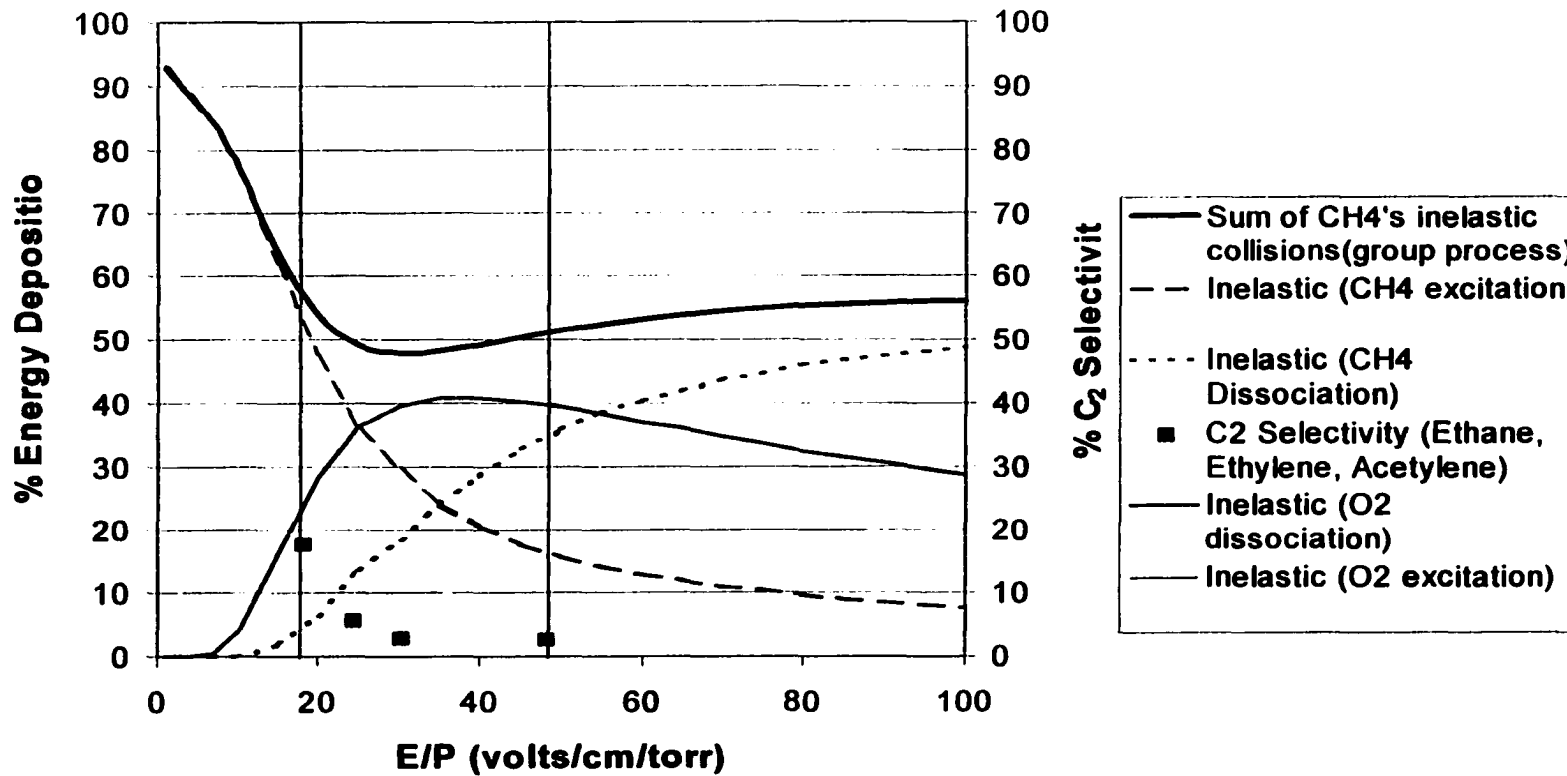
Table 6.3: Acetylene:Ethylene:Ethane Ratio for Gap Distance Experiments

2:1 CH_4:O_2 System at 1 atmosphere				
Gap Distance (mm)	1.9	4.0	6.7	12.0
E/P (volts/cm/torr)	49.0	30.0	24.0	18.0
Acetylene:Ethylene:Ethane	0:0:1	1:0:2	1:0:2	10:1:7
C_2 hydrocarbon sum	3	3	6	18

Figure 6.6: Hydrocarbon Formation Pathways for C_2 Hydrocarbons at Low Reduced Electric Fields (E/P less than 30 volts/cm/torr)

$$CH_4 + electron \longrightarrow \longrightarrow \longrightarrow C_2H_6 + H_2$$

$$CH_4 + O_2^\bullet \longrightarrow \longrightarrow \longrightarrow C_2H_2 + 3H_2$$

Figure 6.7: Hydrocarbon Formation Pathways at High Reduced Electric Fields (E/P greater than 30 volts/cm/torr)
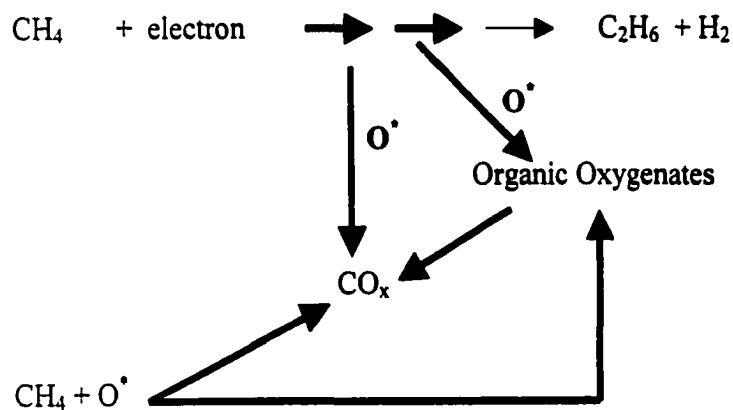
Note: This figure includes CH_4 activation that occurs in Figure 7a

149

Figure 6.8 plots the methane conversion, oxygen conversion, and energy consumption as functions of reduced electric field for the gap distance experiments. The figure shows that when going from 48 volts/cm/torr to 18 volts/cm/torr, the methane and oxygen conversions decrease 61% and 71%, respectively. The system's energy consumption per molecule of methane converted, however, decreases over the same change in the reduced electric field because the methane throughput increased by 82%. The decrease in energy consumption per molecule of methane converted seen when going from 30 volts/cm/torr to 18 volts/cm/torr is largely because of the shift in the energy deposition from oxygen dissociation to methane excitation. In other words, energy is shifting from collision processes that form atomic oxygen, which can react with methane and also carbon monoxide, organic oxygenate products, and hydrogen, to a collision process that forms excited methane, which when it reacts with other species always consumes methane thereby increasing the methane reaction rate and, hence, decreases the energy consumption per methane converted. In addition, excited oxygen molecules may have a higher probability of *reacting* with methane than other species at the lower reduced electric fields (e.g., CO does not seem to become over oxidized to CO_2 when the energy deposition directed toward oxygen excitation increases).

Figure 6.8: CH₄ Conversion, O₂ Conversion, & Energy Consumption (2:1 CH₄:O₂ System, 118 Watts Power Input, 15 °C Water Jacket Temp)
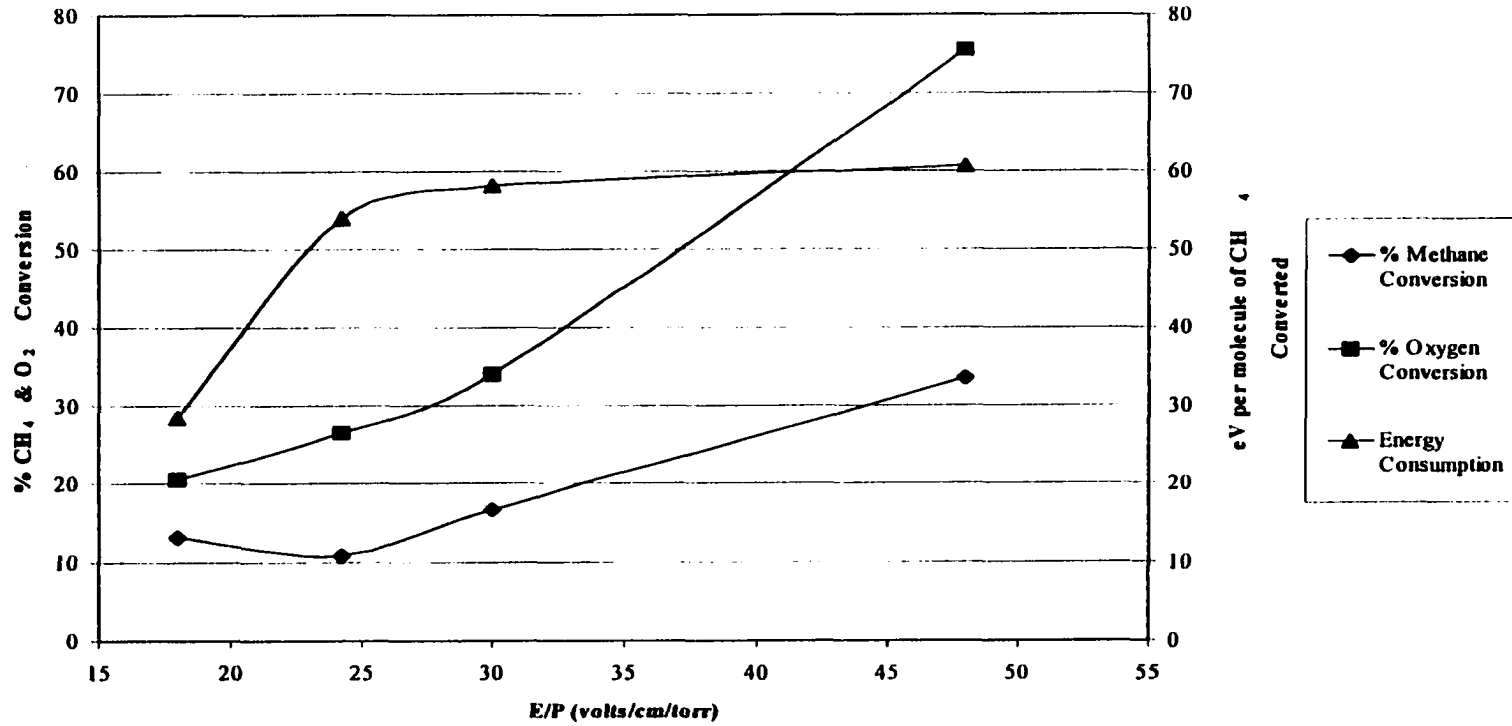
The system's energy consumption can also be affected by the reaction volume to electrode surface area ratio. Previous work has shown that the ratio of reactor wall quenching to gas phase quenching for atomic oxygen is around one when the atomic oxygen is within 1 mm of the cylindrical reactor wall (p = 1 bar, bulk gas = helium, reactor temperature = 500 °C). However, when atomic oxygen is within 6 mm of the wall, the reactor wall quenching to gas phase quenching ratio for atomic oxygen significantly decreases.[15] Other research has given evidence that significant oxygen recombination can take place in a DBD reactor with a 1 mm gas gap.[16] Hence, electrode surfaces can quench radical species thereby wasting the energy consumed in forming these species since they are no longer able to initiate or propagate reactions. Therefore, increasing the reaction volume to electrode surface area ratio decreases the overall effect radical quenching on the electrode surface has on the overall chemical processes. Figure 6.9 plots the system's energy consumption as a function of reaction volume to electrode surface area ratio and shows that the energy consumption does decrease when increasing the ratio from .2 to 1.2.

Figure 6.9: Energy Consumption vs. Reaction Volume to Electrode Surface Area Ratio (2:1 $CH_4:O_2$ System, 118 Watts Power, 15 ^oC Water Jacket Temp)
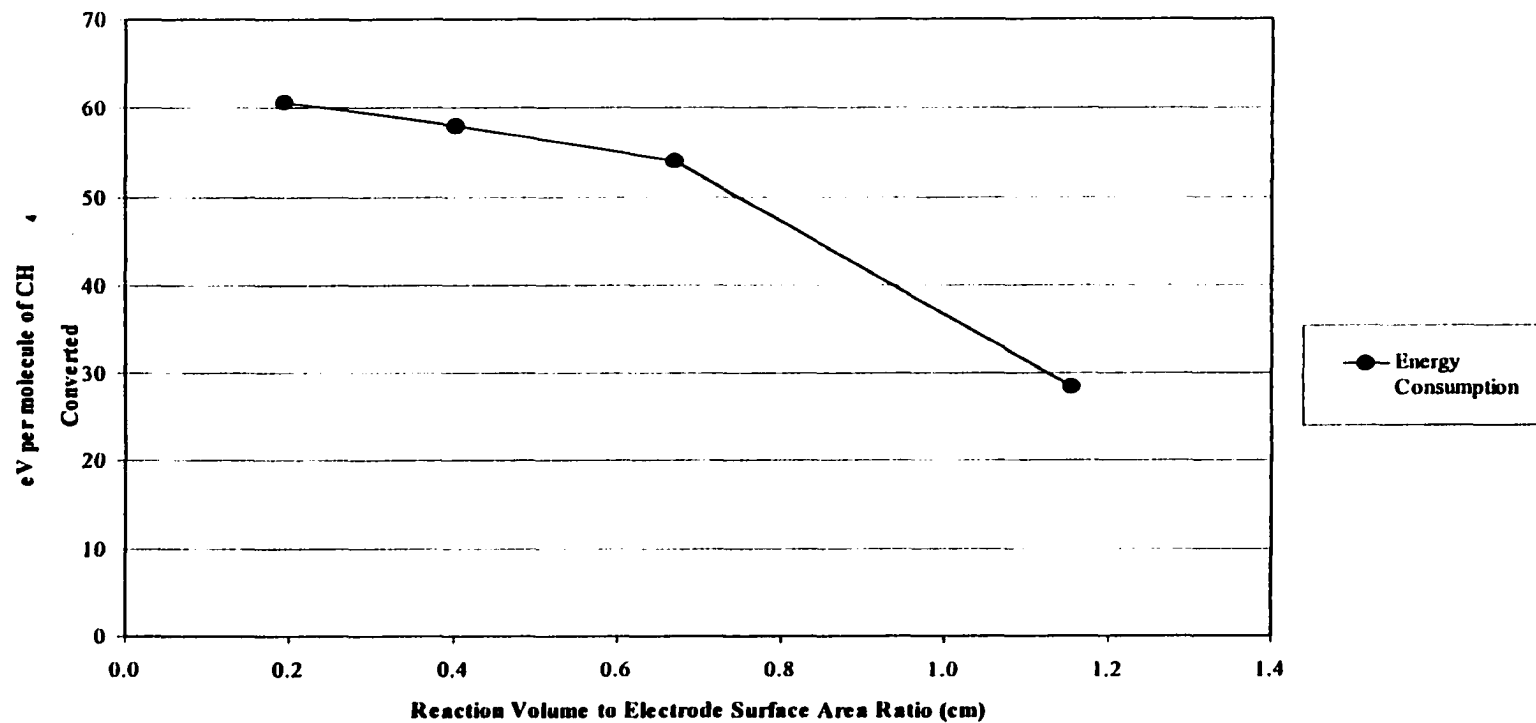
Another way of decreasing the reduced electric field strength is by increasing the pressure within the system. In this series of experiments, the system pressure was increased from one to two atmospheres in a 2:1 methane-oxygen system with a 4 mm gap distance. This was done in order to support the conclusion that changes to the reduced electric field and the resultant change in electron energy is a key variable that controls selectivity between organic oxygenates and C_2s and between CO and CO_2. The results of the 4 mm gap 2:1 methane-oxygen experiments, presented in Table 6.4, show that, when going from one to two atmospheres, the organic oxygenate sum decreases from 59% to 37% and C_2 selectivity increases from 1% to 17%. The change in the reduced electric field from 30 volts/cm/torr to 23 volts/cm/torr is in the region where the energy deposition directed toward oxygen dissociation decreases and that of methane and oxygen excitations increases, as was shown in Figures 6.2 and 6.3. This is consistent with the behavior in the gap-distance experiments. In addition, doubling the system pressure causes the methane feed concentration to double, which also promotes methane coupling reactions. As for CO and CO_2, when going from one to two atmospheres, the $CO:CO_2$ ratio increases from 1.2:1 to 4.1:1. This is also consistent with the observations from the gap-distance results. At two atmospheres, 81% of the water exiting the reactor was in the liquid phase. Thus, water in the gas phase, which can participate in the water-gas shift reaction, does not appear to participate in a major reaction pathway. Finally, increasing the system pressure from one to two atmospheres decreases the energy consumption per methane converted by 46%. Assuming positive order kinetics, the methane reaction rate may

be expected to increase due to the doubling of the feed partial pressure. In addition, the energy consumption per molecule of methane converted also decreases because some of the energy input into the system is shifted from processes that don't directly consume methane to processes that do. Further, the energy consumption decreases because the energy deposition directed toward oxygen excitation increases as already explained in the gap distance results.

Table 6.4: Pressure Experimental Results (4.0 mm Gap Distance, E/P = 30 volt/cm/torr at 1 atmosphere, E/P = 23 volts/cm/torr at 2 atmosphere)

Reactor Pressure (atm)	eV per molecule of CH4 Conv.	Moles of CH₄ conv. (moles/min)	% CH4 Conv.	% O2 Conv.	% H₂ Select.	% CO Select.	% CO2 Select.	% C₂ Select. (Ethane, Ethylene, & Acetylene)	% Org. Oxy. Liquids' Select.	Sum
1	48	.0015	8	22	8	16	13	1	59	89
2	26	.0028	9	17	39	33	8	17	37	95

Previous work has shown that when going from a pure methane feed to a 3:1 methane-oxygen feed, the methane reaction rate is enhanced due to active oxygen species. In addition, organic oxygenate products are formed only when oxygen is present.[8] This work varies the methane-oxygen feed ratio from 5:1 to 2:1 at one and two atmospheres. This is done in order to determine the effect of the partial pressure of oxygen on the methane reaction rate, the system's energy consumption per methane converted, and product selectivities. Table 6.5 shows that, at both one and two atmospheres, increasing the oxygen partial pressure decreases the systems' energy consumption per methane converted when going from a 5:1 to 2:1 methane-oxygen system. This is because the methane conversion increased enough to more than compensate for the 20% decrease in methane partial pressure and throughput in both cases. The methane reaction rate, therefore, increased with increasing partial pressure of *oxygen* in the feed, which caused the decrease in energy consumption per methane converted.

Table 6.5: $CH_4:O_2$ Ratio Experimental Results

4 mm Gas Gap, 118 Watt Power Input, Water Jacket Temp. = 15 °C						
$CH_4:O_2$	Pressure (atm)	E/P (volt/cm/torr)	% CH_4 conv.	% O_2 conv.	eV per molecule of CH_4 conv.	Moles of CH_4 conv. (moles/min)
5:1	1	30	6	31	61	.0012
4:1	1	30	6	27	60	.0012
3:1	1	30	7	23	58	.0013
2:1	1	30	9	22	48	.0015
5:1	2	23	5	21	39	.0019
4:1	2	23	6	19	32	.0023
3:1	2	23	7	19	27	.0027
2:1	2	23	8	17	26	.0028

Figure 6.10 shows the energy deposition directed toward methane and oxygen inelastic collision processes as a function of reduced electric field for the 5:1 to 2:1 experiments. The figure shows that, as the methane-oxygen ratio decreases, the energy deposition directed toward inelastic methane collision processes decreases and the energy deposition directed toward inelastic oxygen collision processes increases. This is because the probability of methane colliding with an electron decreases and that of oxygen increases, when the methane-oxygen ratio decreases. However, the trends seen in each inelastic methane and oxygen collision process curve are similar to the trends seen in all the other inelastic collision process curves for the same group. Figures 6.11, 6.12, and 6.13 show the 5:1 to 2:1 methane-oxygen systems' energy deposition directed toward methane excitation, oxygen excitation, and oxygen dissociation, respectively. Here again, as the methane-oxygen ratio decreases, the energy deposition directed toward methane excitation decreases while energy directed toward oxygen excitation and dissociation increases due to the decreased probability of electrons impacting methane molecules rather than oxygen molecules. However, the trend in each curve within a group (methane excitation group, oxygen excitation group, and oxygen dissociation group) is similar to the trend of all the other curves within that group. Hence, regardless of the methane-oxygen ratio, the trends of the changes in the energy deposition directed toward these collision processes due to changes of the reduced electric field are the same.

Figure 6.10: Energy Deposition (Group Process) vs. E/P
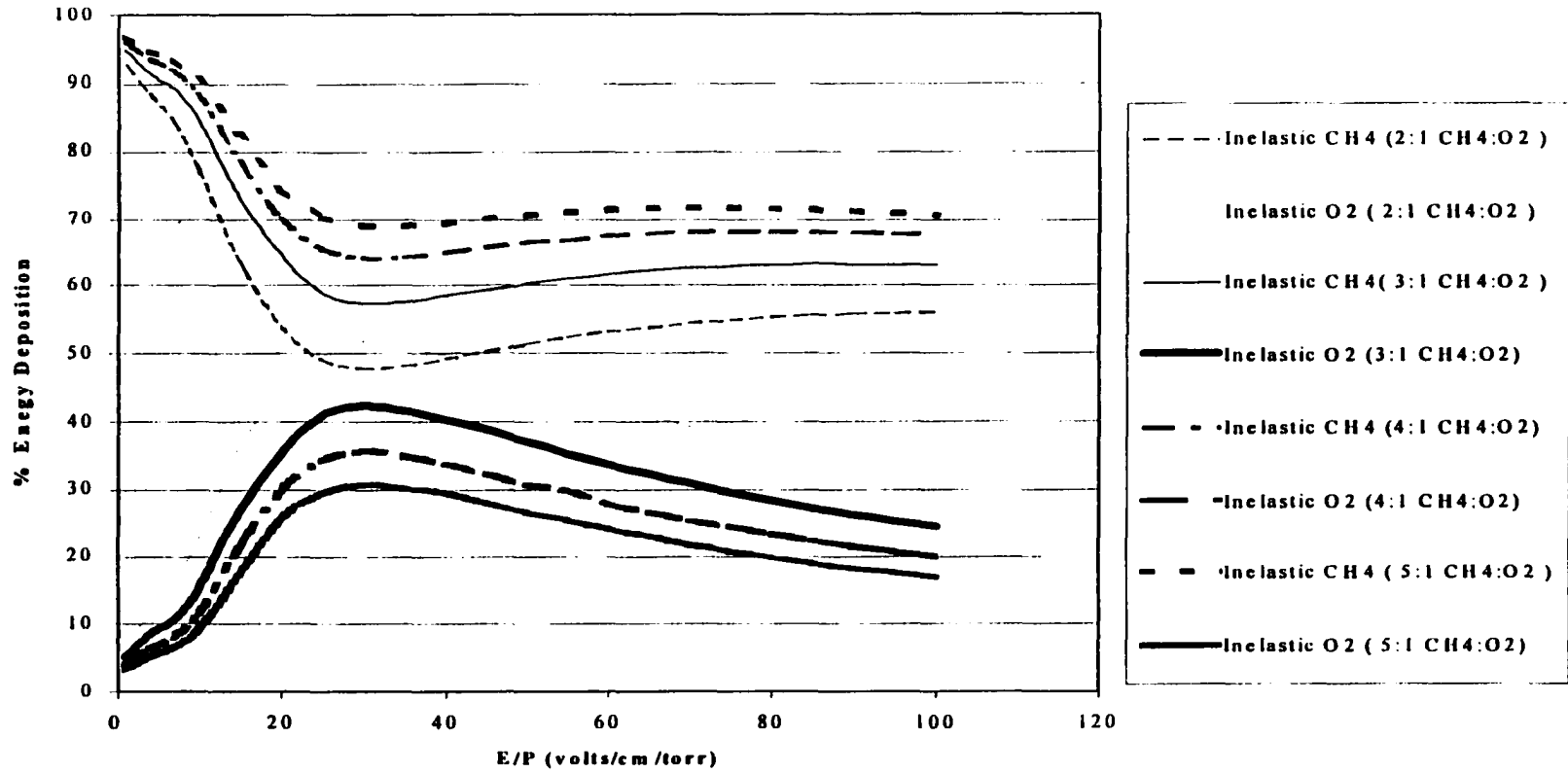
Figure 6.11: CH_4 Excitation Energy Deposition vs. E/P

191
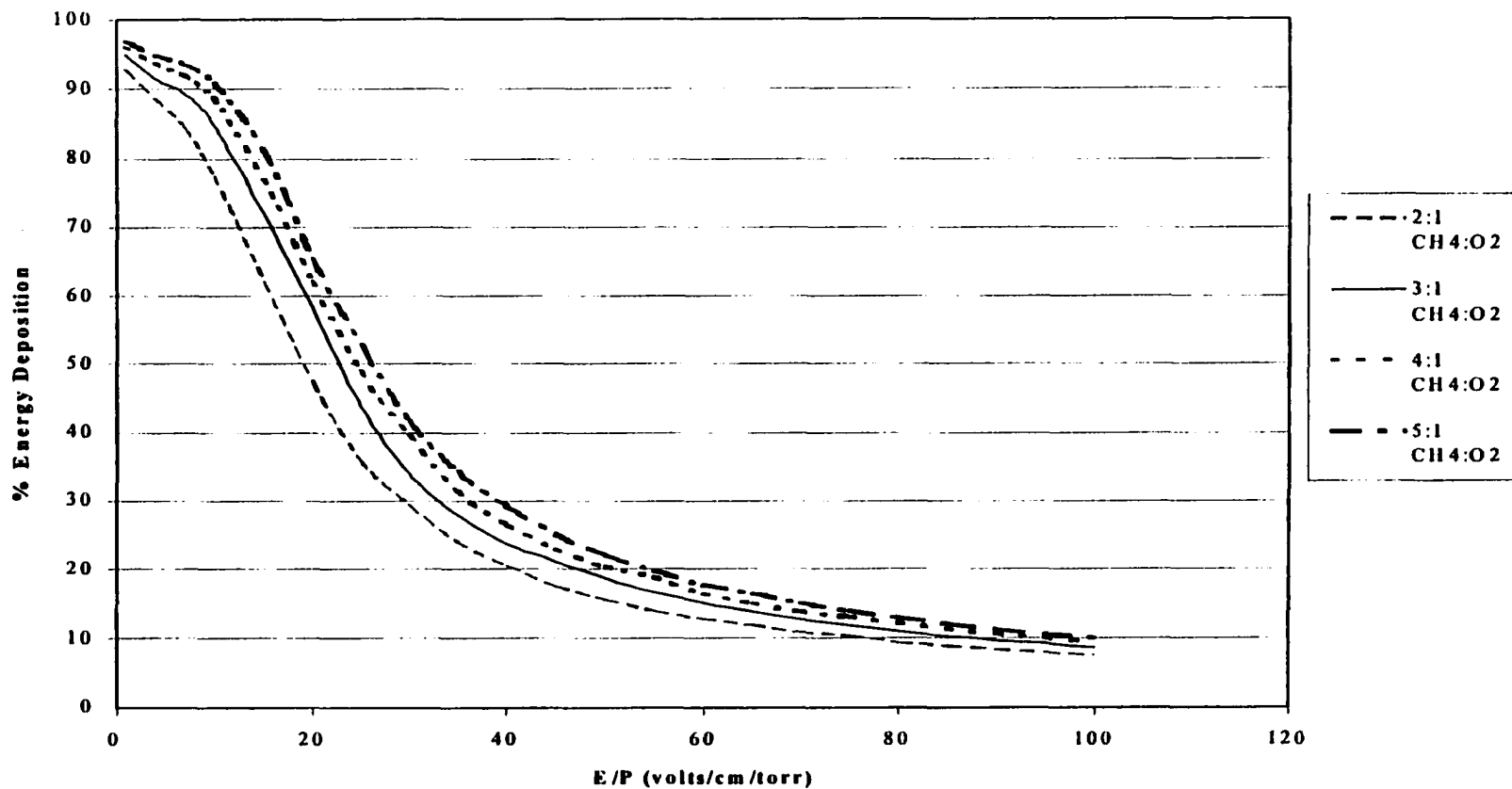
Figure 6.12: O_2 Excitation Energy Deposition vs. E/P
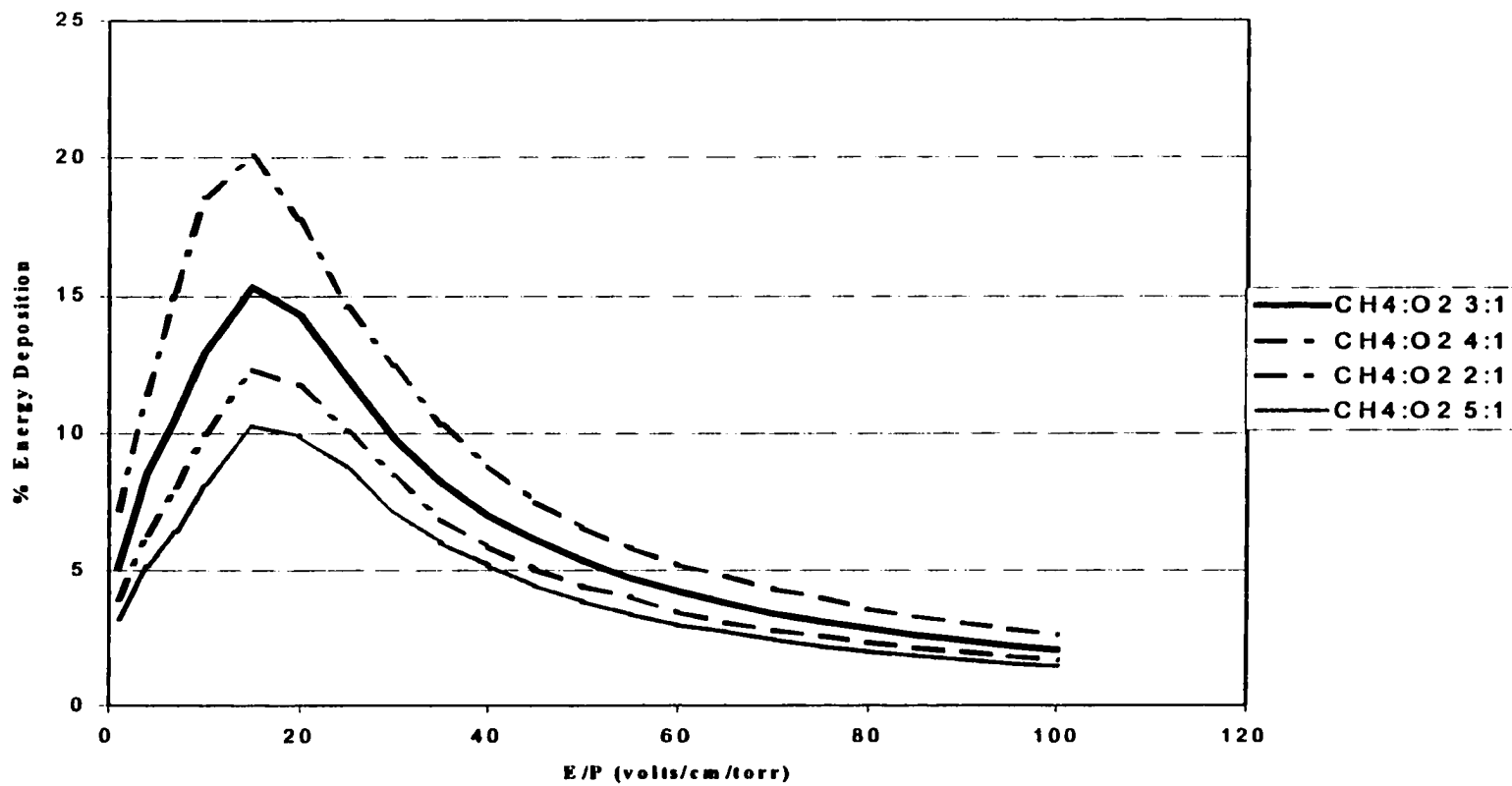
Figure 6.13: O_2 Dissociation Energy Deposition vs. E/P
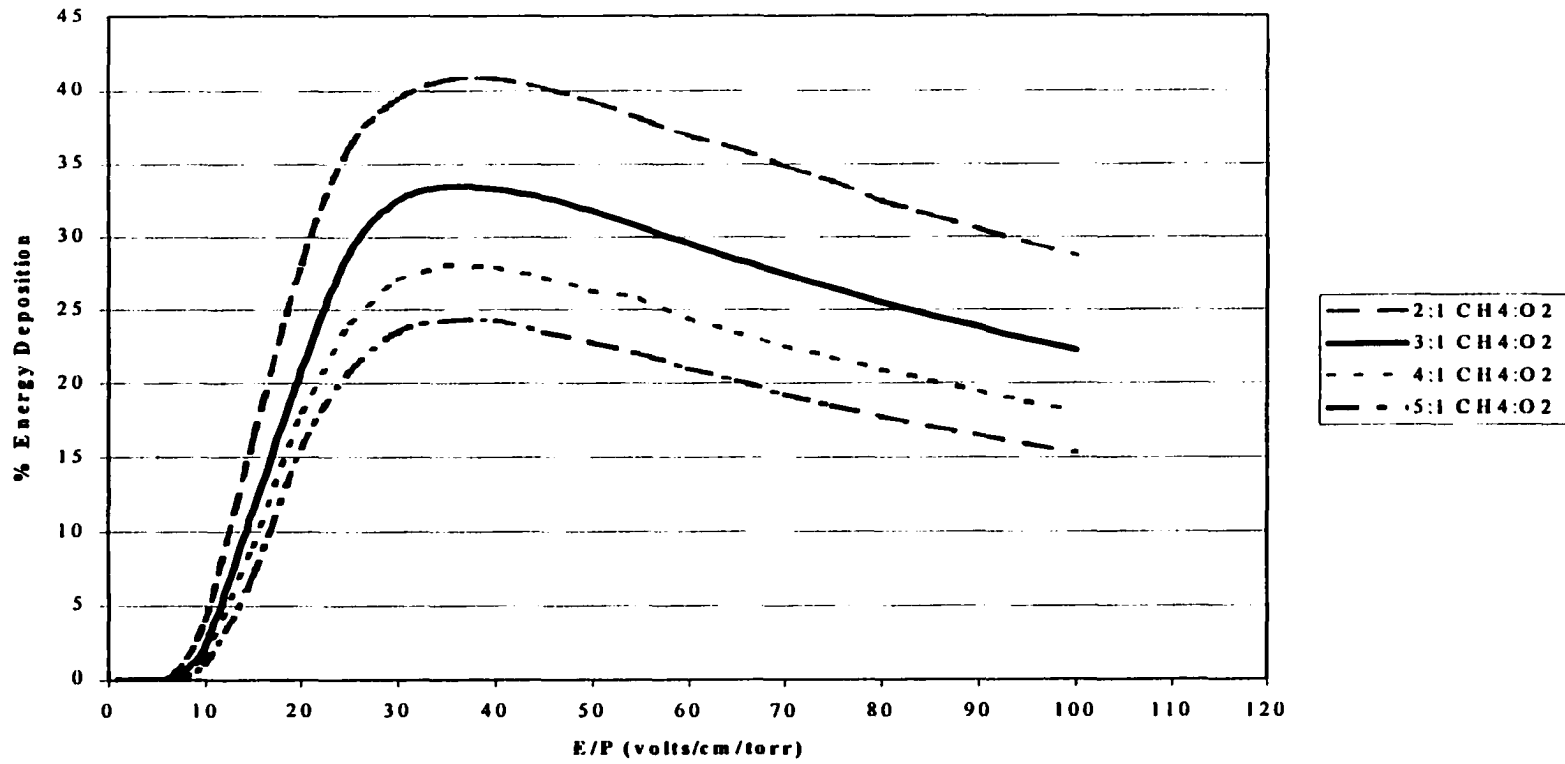
Table 6.6 shows the product selectivity results for the methane-oxygen feed ratio experiments at one and two atmospheres. At a system pressure of one atmosphere, the results show that when going from a 5:1 to 2:1 methane-oxygen feed ratio, the CO_x, C_2, and organic oxygenate selectivities remain relatively constant. Previous work as well as the residence time experiments discussed later in this work provide evidence that there is a pathway for partial oxidation of methane directly to CO and CO_2 in the dielectric barrier discharge methane-oxygen system.[10] With this is mind, the CO_x and organic oxygenate selectivities remain relatively constant when the partial pressure of oxygen is increased in the feed because both pathways are enhanced. The net effect is that changes in the rates of these two oxidative pathways balance one another out. In addition, the ethane selectivity always remains low because enough atomic oxygen is present at this reduced electric field strength to consume activated methane which limits methane coupling.

Table 6.6: $CH_4:O_2$ Ratio Experimental Results

4 mm Gas Gap, 118 Watt Power Input, Water Jacket Temp. = 15 degrees C, E/P = 30 volt/cm/torr at 1 atmosphere, E/P = 23 volts/cm/torr at 2 atmosphere														
$CH_4:O_2$	Pressure (atm)	% H_2 Select.	% CO Select.	% CO_2 Select.	% Ethane Select.	% Ethylene Select.	% Acetylene Select.	% M Select.	% F Select.	% MF Select.	% FA Select.	C_2 sum	Org. Oxy. Liquid sum	S
5:1	1	12	16	10	4	0	0	19	12	8	13	4	51	81
4:1	1	11	16	10	4	0	0	19	15	10	15	4	59	89
3:1	1	9	15	10	2	0	0	16	15	7	16	2	53	80
2:1	1	8	16	13	1	0	0	15	14	10	20	1	59	89
5:1	2	48	26	8	14	5	14	5	7	2	11	33	24	91
4:1	2	42	25	7	11	3	11	5	8	2	12	25	27	84
3:1	2	39	27	7	9	2	10	5	8	2	13	21	29	84
2:1	2	39	33	8	7	1	9	7	10	3	17	17	37	95
M = Methanol, F = Formaldehyde, MF = Methyl Formate, FA = Formic Acid, Selectivity for Carbon Compounds is on a Carbon Mole Basis, S = Sum of carbon selectivity (mole basis)														

At a system pressure of two atmospheres, Table 6.6 shows that, when going from a 5:1 to a 2:1 methane-oxygen system, the C_2 selectivity decreases and the organic oxygenate selectivity increases. At this reduced electric field the energy deposition directed toward oxygen dissociation becomes sufficiently limited that increasing the partial pressure of oxygen in the feed increases the energy deposition directed to oxygen dissociation enough to result in shifting the selectivity from C_2s to organic oxygenate products. Finally, the CO_x selectivity in this range remains relatively constant because both the direct and indirect methane oxidation routes to CO_x as well as the methane oxidation routes to organic oxygenates are being enhanced.

Increasing the system's pressure increases the feed concentration and, therefore, contributes (assuming positive order kinetics) to the enhancement of the methane reaction rate, resulting in a decrease in the energy consumption per methane converted, as was shown in Table 6.5. However, as shown in Table 6.6, the increase in pressure also results in a decrease in the organic oxygenate selectivities because energy deposition directed toward oxygen dissociation significantly drops off.

The next series of experiments increased the system pressure from one to two atmospheres in a 5:1 methane-system with a 1.9 mm gas gap, to compare the other results to those of the 4 mm gas gap. In addition, a 3 atm experiment with a 1.9 mm gas gap (5:1 methane-oxygen system) was also done. Table 6.7 shows that when

166

going from one to two atmospheres, the 1.9 mm and 4.0 mm gap distance systems show 25% and 22% decreases in methane conversion, respectively. The energy consumption per molecule converted decreases 35% for the 1.9 mm gap distance experiment and 36% for the 4.0 mm gap distance system because the methane throughput doubled for both systems. This means the methane reaction rate increased for both gap distances. Assuming positive order kinetics, this increase could be expected since the feed concentration was doubled in both cases. In addition, for the 4.0 mm gap distance experiment, the energy consumption per methane converted also decreased which is attributable to an increase in the energy deposition directed toward methane and oxygen excitations and a decrease in the energy deposition directed toward oxygen dissociation. The 4 mm gap system's energy consumption per methane converted was 22% less at one atmosphere and 23% less at two atmospheres, than the 1.9 mm gap system's energy consumption per methane converted. The difference seen in energy consumption per converted methane at one atmosphere is due to the fact that the reaction volume to electrode surface area ratio decreases (increases radical quenching) when going from the 4.0 mm to the 1.9 mm gap distance.

Table 6.7: Pressure Experimental Results (1.9 mm and 4.0 mm Gap Distance)

5:1 CH_4:O_2 Ratio, 118 Watt Power Input, 15 °C Water Jacket Temp.												
Reactor Pressure (atm)	Gap Distance (mm)	E/P (volts/cm/torr)	eV per molecule of CH4 Conv.	Moles of CH_4 conv. (moles/min)	% CH4 Conv.	% O2 Conv.	% H_2 Select.	% CO Select.	% CO_2 Select.	C_2 Sum	Organic Oxy. Liq. Sum	S
1	1.9	49	79	.0009	10	61	18	16	13	5	51	85
2	1.9	37	51	.0014	8	37	32	19	7	29	46	101
3	1.9	32	43	.0017	6	24	40	22	6	30	42	100
1	4.0	30	61	.0012	6	31	12	16	10	4	51	81
2	4.0	23	39	.0019	5	21	48	26	8	33	24	91
Selectivity for Carbon Compounds is on a Carbon Mole Basis, S = Sum of carbon selectivity (mole basis)												

At two atmospheres pressure, the increase in energy consumption per methane converted when going from the 4.0 mm to the 1.9 mm gap distance is because of radical quenching (the reaction volume to electrode surface area ratio is decreasing). Once again, the energy consumption per methane converted also increases when decreasing the gap distance because of the shift in the energy deposition from excitations of methane and oxygen to oxygen dissociation. Finally, going from two to three atmospheres in the 1.9 mm gas gap resulted in a 20% decrease in the methane conversion. However, the energy consumption per methane converted decreased 17% because the methane throughput increased 33%. More specifically, the energy consumption per methane converted decreased due to an increase in the methane reaction rate because of the increase in the feed concentration.

Table 6.7 shows that going from one to two atmospheres in the 1.9 mm gas gap system shifts the selectivity from organic oxygenate products to C_2s. Again, the increase in pressure promotes methane coupling. In this same range, however, the CO selectivity increases and the CO_2 selectivity decreases, despite the fact that the energy deposition directed toward oxygen dissociation remains significant. This suggests that oxidation of C_2s to CO is favored over complete over-oxidation to CO_2. In addition, shifts in selectivity from CO to CO_2 via the water-gas shift reaction are not seen because the selectivity to hydrogen is high and, therefore, the reverse water-gas shift reaction prevents an overall shift back to CO_2, as previously explained.

Table 6.7 also shows that the product selectivities at one atmosphere for the 1.9 mm and 4 mm gap distance systems are similar. This is because the energy depositions into inelastic methane and oxygen collisions processes are similar. However, when going from one to two atmospheres, there is a greater shift in selectivity from organic oxygenate products to C_2s in the 4 mm gas gap system because of both the increase in pressure and the change in energy deposition. Thus, under all of the system variables tested, higher energy deposition directed toward oxygen dissociation enhances the organic oxygenate production.

The last experimental series studied the organic oxygenate pathways that occur once atomic oxygen initiates the process. This was done by varying the residence time for a 3:1 methane-oxygen system at one atmosphere. In addition, the effects of residence time on CO_x and ethane selectivity as well as methane and oxygen conversion were examined. Figure 6.14 shows the results of the latter. As the residence time is increased from 2.5 seconds to 40 seconds, both the methane and oxygen conversions increase 89%. The increase for both methane and oxygen conversion was linear over this range, but previous work has shown that at greater methane and oxygen conversions the methane and oxygen conversions become nonlinear, and therefore, methane and oxygen concentrations do affect the methane reaction rate.[10]

Figure 6.14: CH_4 & O_2 Conversion vs. Residence Time
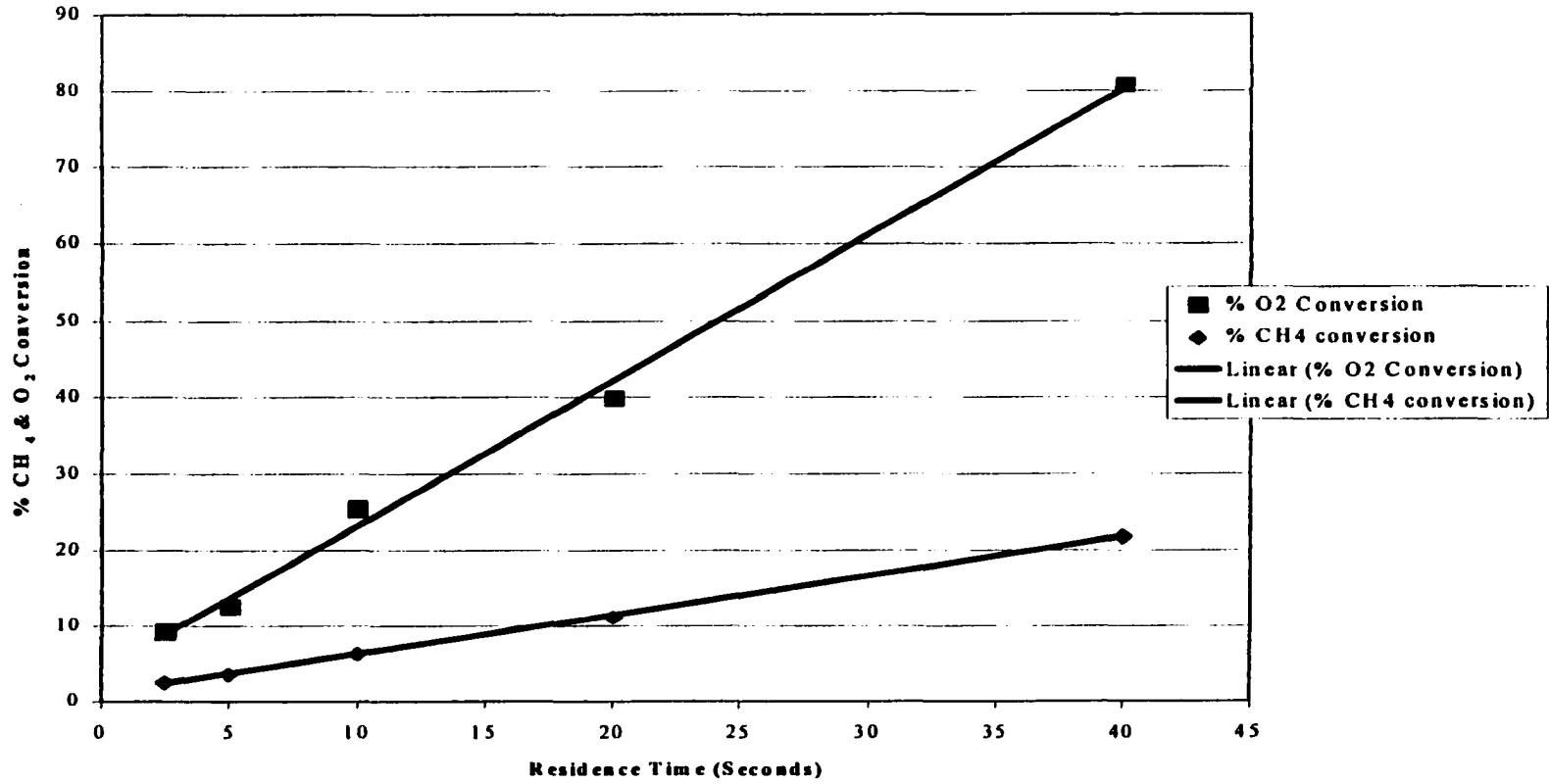
Figure 6.15 shows the effects of residence time on CO, CO_2, and ethane selectivity. As can be seen in the figure, the CO and CO_2 selectivities were always high. This suggests a direct oxidative pathway from methane to CO and/or CO_2. In addition, the CO_2 selectivity remains constant throughout the entire residence time range, but the CO selectivity decreases initially and then levels off at about 20 seconds residence time where it then remains constant at longer residence times. The initial decrease in the CO selectivity is due to the water-gas shift reaction and the fact that *in situ* organic oxygenate product removal is starting to occur as these partial pressures increase above their vapor pressures with longer residence times resulting in condensation within the reaction zone.[9] *In situ* product removal also causes a decrease in the CO_2 production since less over oxidation results. The water-gas shift reaction, which increases CO_2 production, balances this out and, as shown in earlier work[9], the CO_2 selectivity remains relatively constant.

Figure 6.15: CO, CO_2, & C_2H_6 Selectivity vs. Residence Time
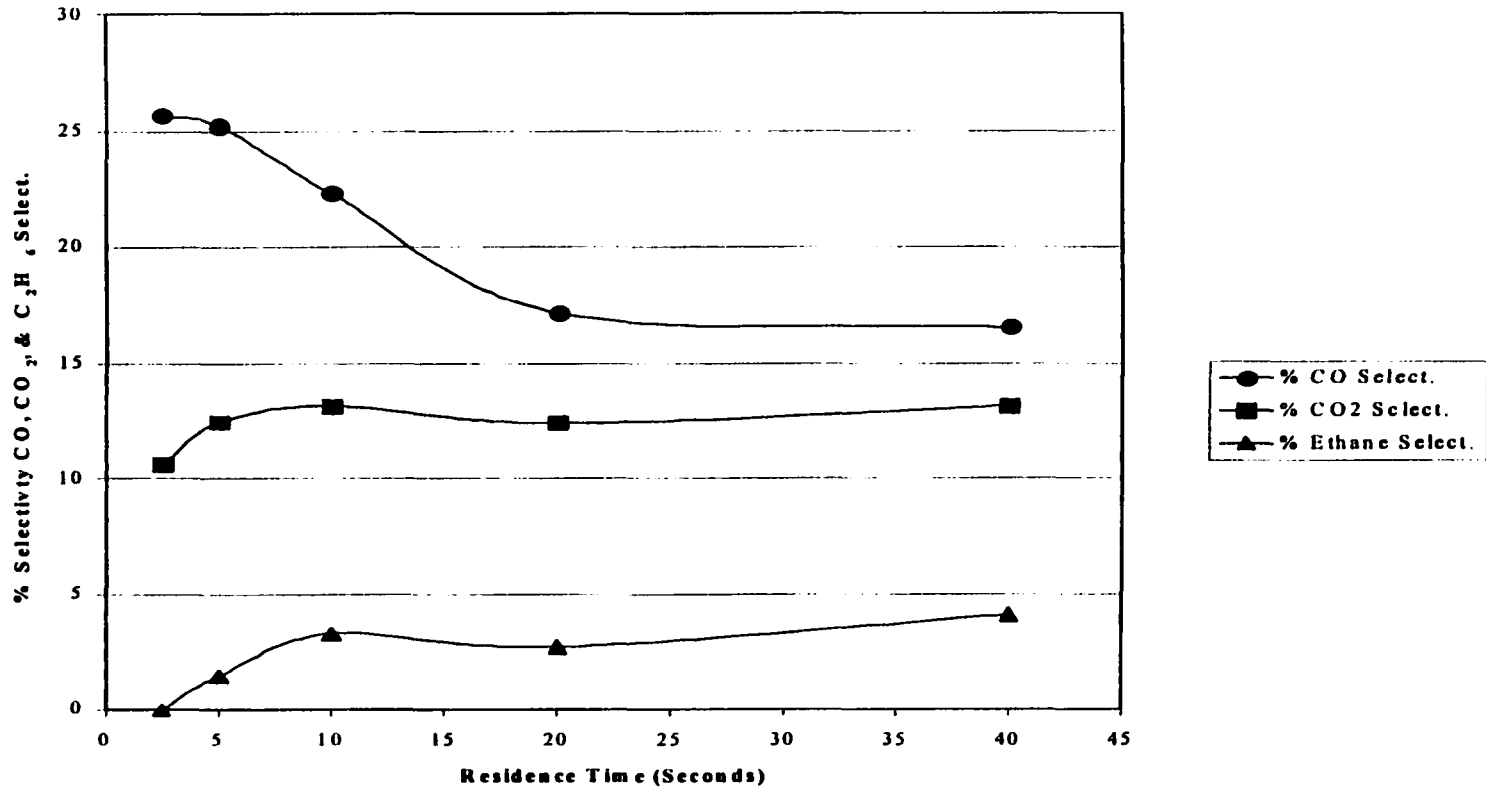
Figure 6.16 shows the residence time experiment results for the organic oxygenate selectivities. The figure shows that when the residence time increases from 2.5 seconds to 40 seconds, the methanol selectivity initially decreases rapidly and then decreases more gradually over time. The formic acid selectivity initially increases rapidly, then at a lower rate. Formaldehyde and methyl formate selectivities increase at a uniform rate. These results indicate that methane and oxygen react to form methanol as an initial product, which further reacts to form formic acid and formaldehyde. Significant amounts of formic acid are evidently formed from methanol at relatively short residence times and can then react with methanol to form methyl formate. Finally, the organic oxygenate selectivities at 40 seconds residence time represent the typical selectivities seen with longer residence time experiments (residence time $\geq$ 40 seconds).

Figure 6.16: Organic Oxygenate Select. vs. Residence Time
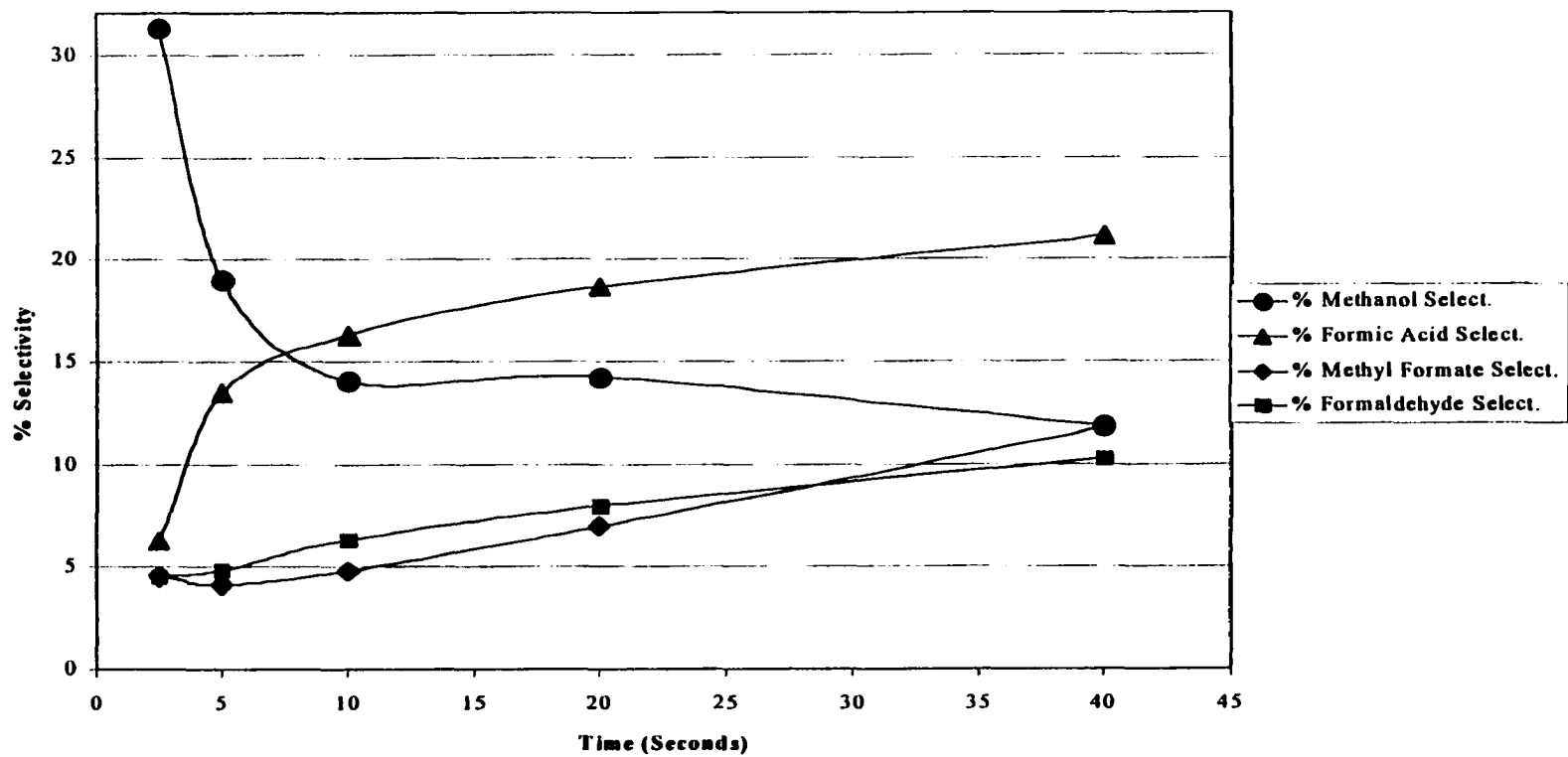
6.5 Conclusions

The product selectivities in a methane-oxygen system within a DBD system can be affected by altering the reduced electric field strength by changing the geometry or operating conditions. These changes affect the average electron energy within the system and can shift the energy deposition among the various collision processes. This was shown in a 2:1 methane-oxygen system through the shift in product selectivities from organic oxygenate products to C_2s when the reduced electric field strength is changed from 30 volts/cm/torr to 18 volts/cm/torr by increasing the gap distance from 4.0 mm to 12.0 mm.

The results for a 2:1 methane-oxygen system with a 4 mm gap distance at elevated pressure verified that the shift in product selectivities from organic oxygenates to C_2s could be attributed to the decrease in the reduced electric field. The effect of pressure on the results showed a similar shift in product selectivities when the reduced electric field was changed over the same range as in the gap distance experiments. However, it was found that increasing the system pressure also promotes methane coupling.

Energy consumption per methane converted was affected by the methane-oxygen feed ratio, the system pressure, the reduced electric field strength, and the reaction volume to electrode surface area ratio. Higher partial pressures of oxygen in the feed were found to decrease the energy consumption per methane converted and is consistent with prior work.[7] Increasing the pressure also reduces the system's energy consumption per molecule of methane converted due to increases in the feed concentration. However, significant reductions in the organic oxygenate selectivity

occur if the reduced electric field strength is too low. Large decreases in the system's energy consumption per methane converted (as high as 55%) which are solely due to decreases in the reduced electric field strength (at constant feed concentration) come with significant losses (as high as 65%) in the organic oxygenate product selectivity.

The increase in the $CO:CO_2$ ratio when the pressure is increased from one to two atmospheres, or the gap distance is increased from 4.0 mm to 12.0 mm, may be a result of partial oxidation of C_2s to CO being favored over complete over-oxidation to CO_2. In addition, if the reduced electric field is low enough that a drop-off in energy deposition directed toward atomic oxygen occurs, the $CO:CO_2$ ratio may be expected to increase.

Residence time studies showed that methane partially oxidizes to form methanol, which further reacts to form formic acid, formaldehyde, and methyl formate. This experimental series supports the conclusion that there is a direct oxidative route from methane to CO and/or CO_2 since there is a significant amount of both of them present at even low residence times, and this is consistent with previous work.[10] All of the results are consistent with the changes of the populations of active species with changes in energy deposition due to changes in the reduced electric field. In the range studied, a lower reduced electric field reduces oxygen dissociation and increases methane and oxygen excitations. Lower oxygen dissociation reduces organic oxygenates, but higher methane and oxygen excitations decrease energy consumption per molecule of methane converted.

Finally, in regards to energy usage, the best results in this study are 26 eV per molecule of methane converted. Since all products except for CO_2 might be considered useful, the system requires 28 eV per molecule of useable carbon produced. A large-scale commercial methanol synthesis process consumes 11 eV per molecule of methanol produced.[17] However, at a remote site the one-step partial oxidation of methane to organic oxygenates using a DBD reactor may be feasible despite higher energy consumptions due to increase simplicity and lower capital costs than conventional processes. Therefore, further reductions in power consumption remain desirable, but the exact level that is required will depend on the specifics of a given gas conversion project.

6.6 Literature Cited

(1) Chang, J.S., Lawless, P.A., Yamamoto, IEEE Transactions on Plasma Science, Vol. 19, NO. 6, 1991

(2) Eliasson, Baldur, Kogelschatz, Ulrich ; "Nonequilibrium Volume Plasma Chemical Processing," IEEE Transactions On Plasma Science, Vol. 19, No 6, December 1991

(3) Bruno, Giovanni, Capezzuto, Pio, Cicala, Grazia Chemistry of Amorphous Silicon Deposition Processes: Fundamentals and Controversial Aspects. Academic Press, Boston, 1995

(4) "Bolsig, CPAT and Kinema Software, http://www.csn.net/siglo/bolsig.htm (1998)"

(5) Pitchford, L.C., Oneil, S.V., Rumble, J.R.; "Extended Boltzmann Analysis of Electron Swarm Parameters," Physical Review A, Vol. 23, No 1, 1980

(6) Dr Li-Ming Zhou; "Non-Thermal Plasma Features in Dielectric Barrier Discharges" Written report to Institute for Gas Utiliaztion Technologies at the University of Oklahoma, November of 1998

(7)   Bhatnagar, Rajat, Mallinson, R.G.; "Methane Conversion in AC Electric Discharges at Ambient Conditions," Methane and Alkane Conversion Chemistry, Plenium Press 1995, 249-264

(8) Larkin, D.W., Caldwell, T.A., Lobban, L.L., Mallinson, R.G.; "Oxygen Pathways and Carbon Dioxide Utilization in Methane Partial Oxidation in Ambient Temperature Electric Discharges," Energy & Fuels, Vol. 12, No. 4, 1998, 740-744

(9) Larkin, D.W., Leethochawalit, S., Caldwell, T.A., Lobban, L.L., Mallinson, R.G.; "Carbon Pathways, CO_2 Utilizaton, and *In Situ* Product Removal in Low Temperature Plasma Methane Conversion to Methanol," Greenhouse Gas Control Technologies, Elsevier Science Ltd., 1999, 397-402

(10)   Larkin, D.W., Lobban, L.L., Mallinson, R.G.; "Production of Organic Oxygenates in the Partial Oxidation of Methane in a Silent Electric Discharge Reactor" publication pending

(11) Eliasson, B, Elgi, W., Kogelschatz, U.; "Modeling of Dielectric Barrier Discharge Chemistry," Pure & Appl. Chem., Vol. 66, No 6, 1994, 1275-1286

(12)   "The Siglo Data Base, CPAT and Kinema Software, http:// www.csn.net/siglo (1998)"

(13) Mizuno, A., Katsura, S., Okumoto, M.; "Direct Synthesis of Methanol using Non-Thermal Plasma," Reports of Project Research (No. 256) Ministry of Education of Japan, 1998, 21-27

(14) T.A. Caldwell, Personal Communication

(15) Tas, Marnix A., thesis, "Plasma-Induced Catalysis: A Feasibility Study and Fundamentals," Eindhoven University of Technolgy, 1995

(16) Khan, A.A.; "Studies on the Inhomogeneous Nature of the Silent Discharge Reactor: Part 1. Experimental Investigations," The Canadian Journal of Chemical Engineering, Vol. 67, 1989, 102-106

(17) Rostrup-Nielson, Jens R. Catalysis and Large-Scale Conversion of Natural Gas. Catalysis Today, Vol. 21, 1994, 257-267

CHAPTER SEVEN: CONCLUSIONS AND FUTURE WORK

7.1 General Conclusions

The direct partial oxidation of methane to organic oxygenates requires oxygen activation. Oxygen cannot be replaced with carbon dioxide or carbon monoxide and still produce significant amounts of organic oxygenates. However, the presence of carbon dioxide in a methane-oxygen-carbon dioxide feed results in inhibition of production of carbon dioxide via the reverse water-gas shift reaction.

Lowering the reactor wall temperature from 75 °C to 28 °C enhances the organic oxygenate selectivity. This is due to *in situ* removal of organic oxygenates in the reaction zone via condensation By lowering the reactor wall temperature to the point where the organic oxygenates' partial pressures are above their equilibrium partial pressures, condensation is allowed to occur.

In carbon dioxide reforming of methane, the partial pressure of carbon dioxide in the feed affects product selectivities (carbon monoxide and ethane) and methane and carbon dioxide conversions. Increasing the partial pressure of helium in a methane-carbon dioxide-helium feed (1:1 methane-carbon dioxide ratio) shifts the product selectivity from ethane to carbon monoxide. Potentially, this is due to the fact that increasing the partial pressure of helium in the feed both causes an increase in the average electron energies within the system and dilutes the methane in the feed.

For a DBD reactor with a methane-oxygen feed, an increase in energy consumption results in an increase in methane conversion within the system. This occurs because of lower partial pressures of oxygen in the reaction zone. However, a methane-oxygen feed with intermediate oxygen addition, as opposed to without such addition, can decrease the energy consumption required for high methane conversion as well as increase the organic oxygenate yield.

A methane-oxygen system within a DBD reactor can also have its product selectivities altered by changing the reduced electric field strengths because the change affects the energy deposition directed toward the various collision processes that provide activation and reaction. In addition, it appears that atomic oxygen species play an important role in organic oxygenate formation. This is due to the fact that a significant decrease in the energy deposition directed toward oxygen dissociation results in a decrease in organic oxygenate selectivity.

In regards to carbon pathways present in the direct partial oxidation of methane in a DBD system, methane and oxygen react to form methanol. Methanol further reacts to form formaldehyde, methyl formate, and formic acid. In addition, the fact that significant selectivities toward CO_x still exist at low residence times suggests a direct partial oxidation route from methane to carbon monoxide and/or carbon dioxide.

The industrial methanol synthesis process requires 11 eV per molecule of methanol produced. This works best result is 28 eV per molecule of useable carbon produced. However, at a remote site the direct partial oxidation of methane to organic oxygenates might be feasible because of increased simplicity and lower capital costs than conventional processes.

7.2 Recommendations for Further Work

The current work uses glass as the dielectric. However, a study varying the type of dielectric used in this system should be done in order to determine if changing the dielectric affects the methane and oxygen conversions, product selectivities, and energy consumption of the system. Studies of other systems have shown that the type of dielectric material used does affect the experimental results.[2,3] For example, a study of nitric oxide destruction within a DBD reactor has shown that when changing from a glass dielectric to a Teflon PFA (perflouroalkoxy) dielectric, it resulted in a 23% decrease in the eV per molecule of NO oxidized. Due to the facts that the power levels used for both dielectric systems (glass and Teflon PFA) were the same and no differences in the discharge characteristics were observed, the authors concluded that the decrease in energy consumption was due to a chemical effect.[2] In addition, Khan has seen increased ozone conversion efficiency when using a P.T.F.E (polytetrafluoroethylene) coated glass dielectric and has attributed the increase in

efficiency to the fact that a P.T.F.E. surface exhibits lower recombination rates of atomic oxygen than does a silica surface.[3]

Another area that should be studied is the use of a pulsed DBD reactor. In a DBD system, an extremely fast rising voltages (comparable to the duration of a microdischarge) causes a large number of discharges to start simultaneously.[4] This might increase the number gas molecules exposed to the discharge and, therefore, potentially enhance the direct partial oxidation of methane to organic oxygenates.

Currently, the energy consumption of the system is determined on the primary side of the transformer. Obtaining the power usage within the reaction zone, however, would indicate the energy consumption the system used to enable chemical reactions to take place. Assuming the power consumed in the reaction zone is significantly less than the system's overall power consumption, studying how system components (e.g. transformer) can be altered in order to decrease energy losses from them should be done.

Studies have shown the potential importance of OH groups in the partial oxidation of methane in a DBD reactor.[5,6] Hence, methane-oxygen-water systems in a DBD reactor should be investigated in order to determine the effects water has on the system. For example, it could be useful to examine whether water enhances the organic oxygenate liquid selectivities.

Finally, an economic analysis of the direct partial oxidation of methane to organic oxygenates in a DBD reactor should be conducted. In addition, an economic analysis of the current commercial methanol process should also be completed for comparison purposes. However, the scale of both systems when implementing the economic analyses should be similar in order to make an accurate comparison.

7.3 Literature Cited

(1) Rostrup-Nielson, Jens R. Catalysis and Large-Scale Conversion of Natural Gas. Catalysis Today, Vol. 21, 1994, 257-267

(2) Rogers, John W., Nejezchleb, Allen J., Rolader, Glenn E., Federle, Steven P., Littrel, Donald M., Neely, William C., Newhouse, E. Irene; "Barrier Discharge Optimization for Nitric Oxide Destruction," This paper has been accepted for publication in a special non-thermal discharge issue of the Journal of Advanced Oxidation Technologies

(3) Khan, A.A.; "Studies on the Inhomogeneous Nature of the Silent Discharge Reactor: Part 1. Experimental Investigations," The Canadian Journal of Chemical Engineering, Vol. 67, 1989, 102-106

(4) Kogelschatz, Ulrich; Eliasson, Baldur; Egli, Walter Dielectric-Barrier Discharges Principle and Applications. J. PHYS IV France 7 , Colloque C4, 1997, 47-64

(5) Okumoto, M., Takshima, K., Katsura, S., Mizuno, A.; "Direct Synthesis of Methanol from Methane using Non-thermal Plasma," The Asia-Pacific Workshop on Water and Air Treatment by Advanced Oxidation Treatments, 1998

(5)   Zhou, L.M., Xue, B., Kogelschatz; U., Eliasson, B.; "Partial Oxidation of Methane to Methanol with Oxygen or Air in a Nonequilibrium Discharge Plasma," Plasma Chemistry and Plasma Processing, Vol. 18, No. 3 , 1998, 375-393

APPENDIX A. Sample Set of Mass Flow Controller and GC Calibrations

A.1 Sample Set of Mass Flow Controller Calibrations

GAS	Controller Full Scale (SCCM), Serial # (S/N)	Mass Flow Controller Calibration Equations (F.R. = Flow Rate in cc/min, S = set point)
CH_4	He (1000), S/N 9201904	F.R. = 5.99*S - .18
CH_4	CH_4 (1000), S/N 9201909	F.R. = 11.70*S + 13.59
CH_4	CH_4 (200), S/N 9100015	F.R. = 2.28*S - 5.02
CH_4	C_2H_6 (20), S/N 9100014	F.R. = .33*S - .18
O_2	He (1000), S/N 88CO327	F.R. = 7.11*S + 10.25
O_2	C_2H_6 (20), S/N 9100014	F.R. = .44*S - .35
O_2	O_2 (250), S/N 9201910	F.R. = 2.63*S - 1.63
CO	C_2H_6 (20), S/N 9100014	F.R. = .45*S - .25
CO	CH_4 (300), S/N 90CO251	F.R. = 4.54*S +3.17
CO_2	C_2H_6 (20), S/N 9100014	F.R. = .34*S - .33
CO_2	CH_4 (200), S/N 9100015	F.R. = 2.21*S + 5.22
C_2H_6	C_2H_6 (20), S/N 9100014	F.R. = .23*S - .47
C_2H_6	He (1000), S/N 88CO327	F.R. = 3.47*S + 8.27
C_2H_6	CH_4 (100), S/N 9702202	F.R = .74*S + .34
H_2	C_2H_6 (20), S/N 9100014	F.R. = .45*S -.37
H_2	He (1000), S/N 88CO327	F.R. = 7.76*S + 3.65
H_2	He (200), S/N 9056138	F.R. = 1.55*S - 3.62
N_2	C_2H_6 (20), S/N 9100014	F.R. = .46*S - .45
N_2	CH_4 (200), 9100015)	F.R. = 2.95*S - 6.18
C_2H_4	CH_4 (100), S/N 9702202	F.R. = .89*S + 1.16

A.2 Sample Set of Gas Chromatography (GC) Calibrations

Gas	GC Type	GC Calibration Equations (M = mole percent of gas, W = weight percent of organic oxygneate, T = TCD area count)
CH_4	EG&G Carle Series 400 AGC gas chromatograph	$M = 1.29 * 10^{-4} * T - 3.41$
O_2	EG&G Carle Series 400 AGC gas chromatograph	$M = 1.18 * 10^{-4} * T + .03$
CO_2	EG&G Carle Series 400 AGC gas chromatograph	$M = 9.02 * 10^{-4} * T + .07$
CO	EG&G Carle Series 400 AGC gas chromatograph	$M = 1.08 * 10^{-4} * T + .44$
C_2H_6	EG&G Carle Series 400 AGC gas chromatograph	$M = 8.19 * 10^{-5} * T - .04$
C_2H_4	EG&G Carle Series 400 AGC gas chromatograph	$M = 8.92 * 10^{-5} * T$
C_2H_2	EG&G Carle Series 400 AGC gas chromatograph	$M = 9.80 * 10^{-5} * T + .02$
H_2	EG&G Carle Series 400 AGC gas chromatograph	$M = 5.30 * 10^{-4} * T + .04$
N_2	EG&G Carle Series 400 AGC gas chromatograph	$M = 1.10 * 10^{-4} * T + .41$
CH_3OH	Varian 3300 GC	$W = 3.32 * 10^{-3} * T + .79$
$HCHO$	Varian 3300 GC	$W = 4.41 * 10^{-3} * T + 3.36$
$HCOOCH_3$	Varian 3300 GC	$W = 4.00 * 10^{-3} * T + .64$
$HCOOH$	Varian 3300 GC	$W = 4.68 * 10^{-3} * T + 2.97$
CH_3CH_2OH	Varian 3300 GC	$W = 3.65 * 10^{-3} * T + .55$

APPENDIX B. Methane and Oxygen Conversion as a function of Energy Effieciency

Flow rate (cc/min)	Power (watts)	eV per molecule of methane converted	% Methane conversion	% Oxygen conversion
423	118	51	12	26
222	118	57	21	48
123	118	63	34	81
70	118	86	44	100
39	118	128	53	100
70	26	56	15	36
70	90	73	40	96
70	118	86	44	100
70	178	116	50	100

APPENDIX C. Gap Distance Experiments

2:1 CH₄:O₂ feed ratio, 118 Watts, 1 min. residence time, 15 °C water temperature in water jacket, 688 cm² avg. electrode area						
Gap Distance (cm)	Reaction Volume/electrode surface area (cm)	Moles of CH₄ conv. (moles/min)	eV per molecule of methane converted	% methane converted	% oxygen converted	% hydrogen selectivity
1.9	.2	.0012	61	33	75	13
4.0	.4	.0013	58	17	34	9
6.7	.7	.0014	54	11	26	16
12.0	1.2	.0026	28	13	21	45

2:1 CH₄:O₂ feed ratio, 118 Watts Power Input, 1 min. residence time, 15 °C water temperature in water jacket, 688 cm² avg. electrode area									
Gap Distance (cm)	Selectivity (Carbon Mole Basis)								
	CO₂	CO	Ethane	Ethylene	Acetylene	M	F	MF	FA	Sum
1.9	16	15	2	0	0	15	12	6	19	86
4.0	16	16	2	0	1	14	15	6	18	88
6.7	12	24	4	0	2	12	9	3	14	81
12.0	9	41	7	1	10	5	5	1	12	92
M = Methanol, MF = Methyl Formate, FA = Formic Acid, F = Formaldehyde, Sum = Sum of Carbon Selectivity										

APPENDIX D. Residence Time Experiments

3:1 CH_4:O_2 feed ratio, 118 Watts Power Input, 15 °C water temperature in water jacket, 430 cm² avg. electrode area													
Res. Time (sec)	Moles of CH_4 conv. (moles/min)	eV per molecule of methane converted	% CH_4 conv.	% O_2 conv.	% H_2 select.	Selectivity (Carbon Mole Basis)							
						CO_2	CO	Ethane	M	F	MF	FA	Sum
2.5	.0014	52	3	9	9	11	26	0	31	5	5	6	83
5.0	.0010	71	4	13	12	12	25	1	19	5	4	14	81
10.0	.0009	82	6	25	13	13	22	3	14	6	5	16	80
20.0	.0008	92	11	40	12	12	17	3	14	8	7	19	80
40.0	.0008	94	22	81	16	13	17	4	12	10	12	21	89
M = Methanol, MF = Methyl Formate, FA = Formic Acid, F = Formaldehyde, Sum = Sum of Carbon Selectivity													

APPENDIX E. Energy Deposition Directed Toward a Collision Process

E.1 Energy Deposition Directed Toward a Collision Process for a 5:1 $CH_4:O_2$ System within a DBD Reactor

% eng. = % energy deposition directed toward, 1 = CH_4 attachment collision process, 2 = CH_4 elastic collision process, 3 = CH_4 inelastic collision process, 4 = CH_4 ionization collision process, 5 = O_2 attachment collision process, 6 = O_2 elastic collision process, 7 = O_2 inelastic collision process, 8 = O_2 ionization collision process												
E/P	1	4	7	10	15	20	25	30	35	40	45	50	55
% eng 1	0	0	0	0	0	0	0	0	0	0	0	0	0
% eng 2	0	0	0	0	0	0	0	0	0	0	0	0	0
% eng 3	97	95	93	91	83	74	70	69	69	69	70	71	71
% eng 4	0	0	0	0	0	0	0	0	1	1	2	2	3
% eng 5	0	0	0	0	0	0	0	0	0	0	0	0	0
% eng 6	0	0	0	0	0	0	0	0	0	0	0	0	0
% eng 7	3	5	7	9	17	26	30	31	30	29	28	27	25
% eng 8	0	0	0	0	0	0	0	0	0	0	0	0	0

E.2 Energy Deposition Directed Toward a Collision Process for a 5:1 $CH_4:O_2$ System within a DBD Reactor

% eng. = % energy deposition directed toward, 1 = CH_4 attachment collision process, 2 = CH_4 elastic collision process, 3 = CH_4 inelastic collision process, 4 = CH_4 ionization collision process, 5 = O_2 attachment collision process, 6 = O_2 elastic collision process, 7 = O_2 inelastic collision process, 8 = O_2 ionization collision process								
E/P	60	65	70	75	80	85	90	95	100
% eng 1	0	0	0	0	0	0	0	0	0
% eng 2	0	0	0	0	0	0	0	0	0
% eng 3	71	72	72	72	72	71	71	71	71
% eng 4	4	5	6	7	8	9	10	11	12
% eng 5	0	0	0	0	0	0	0	0	0
% eng 6	0	0	0	0	0	0	0	0	0
% eng 7	24	23	22	21	20	19	18	17	17
% eng 8	0	0	1	1	1	1	1	1	1

E.3 Energy Deposition Directed Toward a Collision Process for a 4:1 $CH_4:O_2$ System within a DBD Reactor

% eng. = % energy deposition directed toward, 1 = CH_4 attachment collision process, 2 = CH_4 elastic collision process, 3 = CH_4 inelastic collision process, 4 = CH_4 ionization collision process, 5 = O_2 attachment collision process, 6 = O_2 elastic collision process, 7 = O_2 inelastic collision process, 8 = O_2 ionization collision process

E/P	1	4	7	10	15	20	25	30	35	40	45	50	55
% eng 1	0	0	0	0	0	0	0	0	0	0	0	0	0
% eng 2	0	0	0	0	0	0	0	0	0	0	0	0	0
% eng 3	96	94	92	89	79	70	66	64	64	65	66	66	67
% eng 4	0	0	0	0	0	0	0	0	1	1	2	2	3
% eng 5	0	0	0	0	0	0	0	0	0	0	0	0	0
% eng 6	0	0	0	0	0	0	0	0	0	0	0	0	0
% eng 7	4	6	8	11	21	30	34	36	35	34	32	31	31
% eng 8	0	0	0	0	0	0	0	0	0	0	0	0	0

E.4 Energy Deposition Directed Toward a Collision Process for a 4:1 $CH_4:O_2$ System within a DBD Reactor

% eng. = % energy deposition directed toward, 1 = CH_4 attachment collision process, 2 = CH_4 elastic collision process, 3 = CH_4 inelastic collision process, 4 = CH_4 ionization collision process, 5 = O_2 attachment collision process, 6 = O_2 elastic collision process, 7 = O_2 inelastic collision process, 8 = O_2 ionization collision process								
E/P	60	65	70	75	80	85	90	95	100
% eng 1	0	0	0	0	0	0	0	0	0
% eng 2	0	0	0	0	0	0	0	0	0
% eng 3	67	68	68	68	68	68	68	68	68
% eng 4	4	5	6	7	8	9	10	10	11
% eng 5	0	0	0	0	0	0	0	0	0
% eng 6	0	0	0	0	0	0	0	0	0
% eng 7	28	27	25	24	23	22	21	21	20
% eng 8	1	1	1	1	1	1	1	1	1

E.5 Energy Deposition Directed Toward a Collision Process for a 3:1 $CH_4:O_2$ System within a DBD Reactor

% eng. = % energy deposition directed toward, 1 = CH_4 attachment collision process, 2 = CH_4 elastic collision process, 3 = CH_4 inelastic collision process, 4 = CH_4 ionization collision process, 5 = O_2 attachment collision process, 6 = O_2 elastic collision process, 7 = O_2 inelastic collision process, 8 = O_2 ionization collision process

E/P	1	4	7	10	15	20	25	30	35	40	45	50	55
% eng 1	0	0	0	0	0	0	0	0	0	0	0	0	0
% eng 2	0	0	0	0	0	0	0	0	0	0	0	0	0
% eng 3	95	91	89	85	73	65	59	57	58	58	59	60	61
% eng 4	0	0	0	0	0	0	0	0	1	1	2	2	3
% eng 5	0	0	0	0	0	0	0	0	0	0	0	0	0
% eng 6	0	0	0	0	0	0	0	0	0	0	0	0	0
% eng 7	5	9	11	15	27	35	41	42	42	40	39	37	35
% eng 8	0	0	0	0	0	0	0	0	0	0	0	0	1

E.6 Energy Deposition Directed Toward a Collision Process for a 3:1 $CH_4:O_2$ System within a DBD Reactor

% eng. = % energy deposition directed toward, 1 = CH_4 attachment collision process, 2 = CH_4 elastic collision process, 3 = CH_4 inelastic collision process, 4 = CH_4 ionization collision process, 5 = O_2 attachment collision process, 6 = O_2 elastic collision process, 7 = O_2 inelastic collision process, 8 = O_2 ionization collision process

E/P	60	65	70	75	80	85	90	95	100
% eng 1	0	0	0	0	0	0	0	0	0
% eng 2	0	0	0	0	0	0	0	0	0
% eng 3	62	62	63	63	63	63	63	63	63
% eng 4	4	5	6	7	7	8	9	10	11
% eng 5	0	0	0	0	0	0	0	0	0
% eng 6	0	0	0	0	0	0	0	0	0
% eng 7	34	32	31	30	28	27	26	25	24
% eng 8	1	1	1	1	1	1	1	1	2

E.7 Energy Deposition Directed Toward a Collision Process for a 2:1 $CH_4:O_2$ System within a DBD Reactor

% eng. = % energy deposition directed toward, 1 = CH_4 attachment collision process, 2 = CH_4 elastic collision process, 3 = CH_4 inelastic collision process, 4 = CH_4 ionization collision process, 5 = O_2 attachment collision process, 6 = O_2 elastic collision process, 7 = O_2 inelastic collision process, 8 = O_2 ionization collision process

E/P	1	4	7	10	15	20	25	30	35	40	45	50	55
% eng 1	0	0	0	0	0	0	0	0	0	0	0	0	0
% eng 2	0	0	0	0	0	0	0	0	0	0	0	0	0
% eng 3	93	89	84	77	64	54	49	48	48	49	50	51	52
% eng 4	0	0	0	0	0	0	0	0	1	1	2	2	3
% eng 5	0	0	0	0	0	0	0	0	0	0	0	0	0
% eng 6	0	0	0	0	0	0	0	0	0	0	0	0	0
% eng 7	7	11	16	23	36	46	51	52	51	50	48	46	44
% eng 8	0	0	0	0	0	0	0	0	0	0	0	1	1

E.8 Energy Deposition Directed Toward a Collision Process for a 2:1 $CH_4:O_2$ System within a DBD Reactor

% eng. = % energy deposition directed toward, 1 = CH_4 attachment collision process, 2 = CH_4 elastic collision process, 3 = CH_4 inelastic collision process, 4 = CH_4 ionization collision process, 5 = O_2 attachment collision process, 6 = O_2 elastic collision process, 7 = O_2 inelastic collision process, 8 = O_2 ionization collision process								
E/P	60	65	70	75	80	85	90	95	100
% eng 1	0	0	0	0	0	0	0	0	0
% eng 2	0	0	0	0	0	0	0	0	0
% eng 3	53	54	54	55	55	56	56	56	56
% eng 4	4	4	5	6	7	8	9	10	10
% eng 5	0	0	0	0	0	0	0	0	0
% eng 6	0	0	0	0	0	0	0	0	0
% eng 7	42	41	39	38	36	35	34	33	31
% eng 8	1	1	1	1	2	2	2	2	2

E.9 Energy Deposition Directed Toward Excitation and Dissociation for CH_4 and O_2 (5:1 $CH_4:O_2$ system within a DBD reactor)

% eng. = % energy deposition directed toward, 9 = CH_4 excitation, 10 = CH_4 dissociation, 11 = O_2 excitation, 12 = O_2 dissociation												
E/P	1	4	7	10	15	20	25	30	35	40	45	50	55
% eng 9	97	95	93	91	81	65	53	42	34	29	25	22	20
% eng 10	0	0	0	0	2	9	18	27	35	40	45	49	51
% eng 11	3	5	6	8	10	10	9	7	6	5	4	4	3
% eng 12	0	0	0	1	7	16	21	24	24	24	24	23	22

E.10 Energy Deposition Directed Toward Excitation and Dissociation for CH_4 and O_2 (5:1 $CH_4:O_2$ system within a DBD reactor)

% eng. = % energy deposition directed toward, 9 = CH_4 excitation, 10 = CH_4 dissociation, 11 = O_2 excitation, 12 = O_2 dissociation									
E/P	60	65	70	75	80	85	90	95	100
% eng 9	18	16	15	14	13	12	11	11	10
% eng 10	54	55	57	58	59	59	60	60	61
% eng 11	3	3	2	2	2	2	2	2	1
% eng 12	21	20	19	19	18	17	16	16	15

E.11 Energy Deposition Directed Toward Excitation and Dissociation for CH_4 and O_2 (4:1 CH_4:O_2 system within a DBD reactor)

% eng. = % energy deposition directed toward, 9 = CH_4 excitation, 10 = CH_4 dissociation, 11 = O_2 excitation, 12 = O_2 dissociation												
E/P	1	4	7	10	15	20	25	30	35	40	45	50	55
% eng 9	96	94	92	89	77	62	49	39	31	27	23	20	19
% eng 10	0	0	0	0	2	8	17	25	33	38	43	46	48
% eng 11	4	6	8	10	12	12	10	8	7	6	5	4	4
% eng 12	0	0	0	1	9	18	24	27	28	28	27	26	26

E.12 Energy Deposition Directed Toward Excitation and Dissociation for CH_4 and O_2 (4:1 CH_4:O_2 system within a DBD reactor)

% eng. = % energy deposition directed toward, 9 = CH_4 excitation, 10 = CH_4 dissociation, 11 = O_2 excitation, 12 = O_2 dissociation								
E/P	60	65	70	75	80	85	90	95	100
% eng 9	16	15	14	13	12	11	11	10	9
% eng 10	51	53	54	55	56	57	57	58	58
% eng 11	3	3	3	3	2	2	2	2	2
% eng 12	24	23	23	22	21	20	19	19	18

E.13 Energy Deposition Directed Toward Excitation and Dissociation for CH_4 and O_2 (3:1 $CH_4:O_2$ system within a DBD reactor)

% eng. = % energy deposition directed toward, 9 = CH_4 excitation, 10 = CH_4 dissociation, 11 = O_2 excitation, 12 = O_2 dissociation												
E/P	1	4	7	10	15	20	25	30	35	40	45	50	55
% eng 9	95	91	89	85	72	58	44	34	28	24	21	19	17
% eng 10	0	0	0	0	2	7	15	23	30	35	38	42	44
% eng 11	5	9	11	13	15	14	12	10	8	7	6	5	5
% eng 12	0	0	0	2	11	21	29	32	33	33	33	32	31

E.14 Energy Deposition Directed Toward Excitation and Dissociation for CH_4 and O_2 (3:1 $CH_4:O_2$ system within a DBD reactor)

% eng. = % energy deposition directed toward, 9 = CH_4 excitation, 10 = CH_4 dissociation, 11 = O_2 excitation, 12 = O_2 dissociation									
E/P	60	65	70	75	80	85	90	95	100
% eng 9	15	14	13	12	11	10	10	9	9
% eng 10	47	48	50	51	52	53	53	54	54
% eng 11	4	4	3	3	3	3	2	2	2
% eng 12	30	28	27	26	25	25	24	23	22

E.15 Energy Deposition Directed Toward Excitation and Dissociation for CH_4 and O_2 (2:1 CH_4:O_2 system within a DBD reactor)

% eng. = % energy deposition directed toward, 9 = CH_4 excitation, 10 = CH_4 dissociation, 11 = O_2 excitation, 12 = O_2 dissociation												
E/P	1	4	7	10	15	20	25	30	35	40	45	50	55
% eng 9	93	89	84	77	62	48	36	29	24	21	18	16	14
% eng 10	0	0	0	0	2	6	13	18	24	29	33	36	38
% eng 11	7	11	15	19	20	18	15	12	10	9	8	7	6
% eng 12	0	0	0	4	16	28	36	39	41	41	40	39	38

E.16 Energy Deposition Directed Toward Excitation and Dissociation for CH_4 and O_2 (2:1 CH_4:O_2 system within a DBD reactor)

% eng. = % energy deposition directed toward, 9 = CH_4 excitation, 10 = CH_4 dissociation, 11 = O_2 excitation, 12 = O_2 dissociation									
E/P	60	65	70	75	80	85	90	95	100
% eng 9	13	12	11	10	9	9	8	8	8
% eng 10	40	42	44	44	46	47	47	48	48
% eng 11	5	5	4	4	4	3	3	3	3
% eng 12	37	36	35	34	32	31	30	30	29

APPENDIX F. Error Propagation Results

2:1 CH₄:O₂ feed ratio, 4 mm Gas Gap, 118 Watt Power Input, Water Jacket Temp. = 15 degrees C, E/P = 30 volt/cm/torr at 1 atmosphere										
% CH₄ conv.	% O₂ conv.	Moles of CH₄ conv. (moles/min)	% CO Select.	% CO₂ Select.	% Ethane Select.	% M Select.	% F Select.	% MF Select.	% FA Select.
9.3 ± .6	22 ± 1	.00152 ± .00009	15.7 ± .8	12.8 ± .8	1.2 ± .1	15 ± 1	14 ± 1	10 ± 2	20 ± 2
M = Methanol, F = Formaldehyde, MF = Methyl Formate, FA = Formic Acid, Selectivity for Carbon Compounds is on a Carbon Mole Basis										

200 cc/min flow rate & 3:1 CH₄:O₂, 200 Hz, 16 kV										
% CH₄ conv.	% O₂ conv.	Moles of CH₄ conv. (moles/min)	% CO Select.	% CO₂ Select.	% Ethane Select.	% M Select.	% F Select.	% MF Select.	% FA Select.
14.0 ± .4	48.0 ± .5	.00091 ± .00009	18.2 ± .7	15.3 ± .6	4.7 ± .1	13.3 ± .8	11.9 ± .4	8.8 ± .6	16 ± 2
M = Methanol, F = Formaldehyde, MF = Methyl Formate, FA = Formic Acid, Selectivity for Carbon Compounds is on a Carbon Mole Basis										